Freeze-Thaw Damage Assessment of Internally Insulated Historic Brick Masonry Walls Under Canada's Future Climates

Sahar Sahyoun

A Thesis

In the Department of

Building, Civil and Environmental Engineering

Presented in Partial Fulfillment of the Requirements

For the Degree of

Doctor of Philosophy (Building, Civil and Environmental Engineering)

at Concordia University

Montreal, Quebec, Canada

May 2024

Évaluation des Dommages Causés par le Gel et le Dégel aux Murs Historiques en Maçonnerie de Briques Isolés par L'intérieur dans les Conditions Climatiques Futures au Canada

Sahar Sahyoun

Thèse

Présentée au Département de

Génie du bâtiment, civil et environnemental

Dans le cadre de l’accomplissement partiel des

Exigences pour le diplôme de

Docteur en philosophie (génie du bâtiment, civil et environnemental)

à l’Université Concordia

Montréal, Québec, Canada

Mai 2024

CONCORDIA UNIVERSITY

SCHOOL OF GRADUATE STUDIES

This is to certify that the thesis prepared

By: Sahar Sahyoun

Entitled: Freeze-Thaw Damage Assessment of Internally Insulated Historic Brick Masonry Walls under Canada's Future Climates.

and submitted in partial fulfillment of the requirements for the degree of

Doctor of Philosophy (Building Engineering)

complies with the regulations of the University and meets the accepted standards with respect to originality and quality.

Signed by the final examining committee:

	Dr. Todd Eavis	Chair
	Dr. Fitsum Tariku	External Examiner
	Dr. Radu Grigore Zmeureanu	Examiner
	Dr. Ahmed Soliman	Examiner
	Dr. Yong Zeng	Thesis Supervisor
	Dr. Hua Ge	Thesis Supervisor
	Dr. Michael A. Lacasse	
Approved by	Dr. Chunjiang An	Graduate Program Director
May 17, 2024	Dr. Mourad Debbabi	Dean of Faculty

— This page purposely left blank —

ABSTRACT

Freeze-Thaw Damage Assessment of Internally Insulated Historic Brick Masonry Walls under Canada's Future Climate

Sahar Sahyoun, Ph.D.
Concordia University, 2024

Canada has taken steps to address climate change and protect heritage buildings by setting energy reduction targets and ensuring occupant comfort. Whereas internal insulation systems have emerged as a potential strategy to address these challenges, the use of such systems may also increase the risk to freeze-thaw (FT) damage of the exterior wall assembly and thereby lead to long-term deterioration of historic brick walls due to reduced drying capacity. Current standards provide general heritage preservation advice, but more specific technical guidance is needed to enhance thermal performance, ensure wall durability with interior insulation, and address climate change impacts on the masonry system. The information provided in this study is to contribute to the existing body of knowledge related to the long-term performance of historic masonry walls, by examining the FT damage of internally insulated historic brick masonry walls under a changing climate. In this study, recommendations are provided for optimal insulation selection to minimize freeze-thaw damage.

Typically, a 30-year period is recommended to evaluate the long-term effects of climate change on building envelopes. However, an alternative approach is to select a single moisture reference year (MRY) that can accurately assess moisture stress over time, reducing the time and costs of simulations with multiple climate parameters. This study assessed the reliability of of presently used climate-based indices for selecting an MRY to evaluate the risk to FT damage in internally insulated brick walls. Finding the existing methods inadequate, the study proposed an alternative approach based on hygrothermal simulations.

A parametric analysis was thereafter conducted to identify the key factors influencing FT damage in brick masonry walls. Simulations were conducted over a continuous 31-year period, as well as for each separate year, demonstrating no cumulative impact on annual FT cycles. The study determined that MRYs at the 93rd percentile severity could be employed for evaluating FT in retrofitting design decision-making.

By examining potential FT damage under different future climatic conditions and considering various factors, this research offers a decision-making process for internal insulation retrofit projects and proposes solutions when significant risk of FT deterioration is expected.

ACKNOWLEDGEMENTS

"*And my success is only through Allah. Upon Him I have relied, and to Him I return*" – The Quran 11:88 (Surat Hud).

I would like to express my sincere gratitude to my supervisors, Dr. Hua Ge and Dr. Michael A. Lacasse, for their unwavering support and invaluable guidance throughout the research process. Their expertise, encouragement, and insightful feedback have been instrumental in shaping this dissertation. I consider myself very fortunate to have had the opportunity to work under their mentorship. In addition to their academic support, they provided me with access to the National Research Council's state-of-the-art research facility, an experience that has greatly enriched my research environment. Special thanks again to Dr. Hua Ge for the opportunity to assist her in teaching her engaging courses and for including me as a member of the team organizing international conferences. Her guidance and support have provided me with valuable networking opportunities.

I would also like to thank the members of my thesis committee for their insightful comments and encouragement. Their input has greatly enhanced the overall quality of this dissertation. I am also deeply grateful to my colleagues for their unwavering support throughout this process, especially Dr. Lin Wang and Dr. Chetan Aggarwal. Our discussions and collaborations have been invaluable in shaping my ideas and improving the quality of this thesis.

My deepest appreciation goes to my father, Mr. Majed Sahyoun, and my mother, Mrs. Souha Koubayter, for their unwavering support, encouragement, and sacrifices throughout my academic journey. Their love, understanding, and belief in my abilities have been a source of strength and motivation without which I would not have been able to reach this milestone. My heartfelt thanks also go to my sister, Dr. Amal Sahyoun, my brother, Mr. Bassem Sahyoun, my brother-in-law, Dr. Modar Kassan, and my loved ones for their unwavering support and empathy. Their confidence in my abilities and their continued motivation have been extremely valuable to me.

I am also deeply grateful to Mr. Mohamed El Salahi for providing me with the emotional support and encouragement I needed while working on my thesis. His constant support and unwavering belief in me have been instrumental in keeping me motivated. I greatly appreciate his presence in my life.

— This page purposely left blank —

Table of Contents

List of Figures

List of Figures, cont'd

List of Figures, cont'd

List of Figures, cont'd

List of Tables

List of Tables, Cont'd

Nomenclature

Symbol	Parameter	Unit
A	Conductive heat flux to the porous material	W/m^2
A_w	Water absorption coefficient	$kg/m^2 \cdot s^5$
D	Hourly mean wind direction from North	°
e	Vapor partial pressure in the air	Pa
e_a	Saturated partial vapor pressure of the air	Pa
E_v	Solar radiation incident on the wall	W/m^2
F_D	Rin deposition factor	-
F_E	Rain exposure factor	-
F_L	Empirical constant	$kg \cdot s/(m^3 \cdot mm)$
h_{ce}	Outdoor convective heat exchange coefficient	$W/m^2 \cdot K$
h_m	Convective vapor transfer coefficient	s/m
I	Latent heat of vaporization	J/kg
I_{cl}	Cloud Index	-
I_{min}	Lowest value of the index	-
I_{max}	Highest value of the index	-
K	Net short-wave radiation	W/m^2
Kl	Liquid water conductivity	s
L	Net long-wave radiation	W/m^2
p_v	Partial vapour pressure	Pa
p_{vs}	Saturation vapour pressure	Pa
R	Hourly rainfall intensity on a horizontal plane	mm
Rse	External surface thermal resistance	$m^2 \cdot K/W$
Rsi	Internal surface thermal resistance	$m^2 \cdot K/W$
r_{bv}	Rain deposition on a vertical wall	$kg/(m^2 \cdot h)$
r_{wd}	Wind-driven rain on the wall	$kg/m^2 \cdot h$
si	Thickness	m
S_{ice}	Saturation degree of ice content	-
T_i	Hourly values of temperature at point of investigation	K

Symbol	Parameter	Unit
T_L	Critical value of temperature	K
U	Hourly average wind velocity at height of 10 m above the ground	m/s
v	Air velocity	m/s
w_i	Hourly values of moisture content at point of investigation	m^3/m^3
w_L	Critical value of moisture content	m^3/m^3

Greek Symbols

β_v	Convective vapour diffusion coefficient	s/m
θ	Angle between wind direction and normal to the wall	°
λ	Thermal conductivity	W/m.K
Δ	Gradient between saturation vapor partial pressure and air temperature	Pa/K
μ	Water vapor diffusion resistance factor	-
ϕ	Relative humidity	-
γ	Psychometric constant	Pa/K

Abbreviations

31Y	31 consecutive years
AFW	Amount of Frozen Water
CaSi	Calcium Silicate
CI	Climatic Index
CBI	Climate-Based Index
CMHC	Canada Mortgage and Housing Corporation
DI	Drying Index
ECCC	Environment and Climate Change Canada
FDEI	Frost Decay Exposure Index
FT	Freeze-Thaw
FTC	Freeze-Thaw Cycle
FTCcrit	Critical Freeze-Thaw Cycle
FTCd	Freeze-Thaw Cycles obtained from DELPHIN
FTDR	Freeze-Thaw Damage Risk Index
HAM	Heat, Air and Moisture

Abbreviations, cont'd

HDD	Heating Degree Days
IFTC	Indicative Freeze-Thaw Cycles
IPCC	Intergovernmental Panel on Climate Change
IVR	Ice Volume Rate
I_{sev}	Severity Index
LD	Likely Damage
MC	Moisture Content
MEWS	Moisture Management of Exterior Wall Systems
MI	Moisture Index
MRY	Moisture Reference Year
MW	Mineral Wool
MWI	Modified Winter Index
ND	No Damage
OD	Observable Damage
ORG	Original wall / non-insulated wall
PD	Possible Damage
PUR	Polyurethane
R^2	Coefficient of determination
RH	Relative Humidity
RH_{crit}	Critical Relative Humidity
RIBuild	Robust Internal Thermal Insulation of Historic Buildings
RMSE	Root Mean Square Error
S_{crit}	Critical degree of moisture saturation
SPF	Spray Foam Polyurethane
SY	Single Year
T	Ambient temperature
TOF	Time of Frost
TZ	Time Zone
WDR	Wind-Driven Rain
WI	Winter Index
XPS	Extruded Polystyrene Insulation

— This page purposely left blank —

Preface

This manuscript-based thesis comprises two published journal papers and one recently submitted journal paper currently under peer review, that together form Chapter 4, Chapter 5, and Chapter 6. To enhance readability, the three manuscripts have been slightly modified from their original versions. The numbering of figures, tables, and equations includes the respective chapter numbers. Additionally, all references from the chapters have been combined and are presented at the end of the thesis.

— This page purposely left blank —

Chapter 1. Introduction

1.1. Background

With the increased concern to the effects of climate change, Canada has made a commitment to reduce greenhouse gases emissions by 30% as of 2030, as compared to emissions levels (Environment and Climate Change Canada (ECCC), 2016) attained in 2005, and achieve carbon neutrality by 2050. The building stock, which contributes up to 22% of Canada's carbon emissions, can be part of the solution (Natural Resources Canada., 2007) as existing buildings can be made more thermally efficient. Whereas new construction relies on improved thermal performance to enhance energy efficiency and as well, attain acceptable levels of comfort for building occupants, the retrofit of existing buildings has now been recognised as a strategic measure to realise carbon reductions, given that existing buildings evidently account for most of the building stock. Given their cultural significance, heritage buildings usually have a long lifespan, hence their adaptability to the future needs is of high importance. Although thermal retrofits were seen as a threat to conservation until recent decades, now they started to be recognised as a measure to help with the protection of heritage, ensuring healthy environments for a longer lifetime. For most historical buildings, energy retrofit actions are more complicated because of architectural and artistic constraints; and therefore, any insulation work has to be done on the interior side of the exterior wall. In Canada, many buildings constructed before the Second World War are designated as heritage properties. And the Canadian Federal Government's basic inventory of built heritage consists of about 1,300 federal heritage buildings – among which are the Parliament Building of Canada (Parks Canada, 2009). Historic buildings are typically comprised of large multi-wythe masonry walls having little or no wall insulation. Due to their inability to control heat loss, heritage buildings currently fail to meet occupant comfort standards and energy requirements. Therefore, adding insulation and taking measures to control air leakage can dramatically improve the energy performance and occupant comfort of a heritage building. However, doing so may also have negative effects on the integrity of masonry units that form the exterior walls. Consideration must be given to the location and amount of insulation added to a masonry wall as the installation of insulation can significantly alter the micro-environment of the brick and thus lead to premature damage to the masonry structure from the effects of freeze-thaw action.

Studies have shown that under a changing climate, more frequent storm events, climate events having greater rainfall, more intense winds, and of longer duration are likely to occur (IPCC, 2022). This may increase the wind-driven rain loads on the building façade and as a consequence, likewise, increase the risks of rain penetration. On the other hand, increases in solar radiation and air temperature may enhance the drying potential of exposed wall components. Such severe climate effects, together with the installation of insulation on the interior of masonry walls, may provide conditions favourable to the occurrence of frost related problems. It is therefore important to assess the effect of climate change on the potential risk of freeze-thaw (FT) damage to masonry wall structures. A review of publications on the conservation, rehabilitation, and restoration of historic buildings in North America has been completed, with specific consideration given to historic buildings of masonry construction (Sahyoun and Ge, 2020). However, there were a very limited number of comprehensive scientific and technical studies that have been published that are pertinent to the Canadian context, and that address improvements in thermal performance of masonry structures with the use of interior insulation and the expected durability of these retrofitted structures. Also, very limited research has been carried out to study the effect of climate change on older building structures. To determine the risk to deterioration of building elements, heat, air, and moisture (HAM) simulation tools are typically used. Another challenge in respect to gaining a better understanding of potential risks to premature degradation, is that simulations need to be completed over a long period of time (e.g., > 30 years); this could necessarily result in excessive computation time when completing simulations. Thus, when undertaking performance evaluations using a single representative weather year, model computation time can be considerably reduced and thus facilitate the decision-making process in design. Existing methods to select a moisture reference year (MRY) are based on the evaluation of the risk to damage arising from mould growth, and no method has yet been developed that is appropriate for assessing the risk to damage of masonry structures resulting from FT action.

1.2. Objectives and scope

Given these motivations, the objectives of this study are to: (1) Review current approaches to the selection of MRYs, evaluate their reliability in assessing FT damage risks, and develop a consistent and reliable method for MRY selection appropriate for the FT risk assessment of exterior masonry walls; (2) Develop a framework for the proper assessment of FT damage of masonry walls; (3)

Understand and assess the FT damage risks of historical masonry walls, having been retrofitted using interior insulation, under historical climatic conditions and predict the FT damage risks under projected future climates; (4) Investigate and develop the most appropriate strategies to safely retrofit historical walls with interior insulation including providing recommendations for optimal wall designs and the use of appropriate types and thickness of insulation to achieve reduced energy usage in historical buildings while maintaining the long term moisture integrity of historic brick masonry structures.

This research is of importance, both on a regional and a national level, since it will fill gaps in knowledge related to strategies to improve the thermal performance of building envelopes of historical masonry buildings without compromising their long-term durability. This will, in turn, help expand existing guidelines for the energy retrofit of heritage buildings and will permit incorporating the use of hygrothermal simulation tools to assess building performance. This work will also provide answers to the questions raised within the industry regarding whether heritage masonry structures could be internally insulated without potential damage to the masonry structure. Additionally, it will help provide a set of best practices on the appropriate level and types of insulation materials and insulating strategies to mitigate the effect of climate change and thereby permit adapting historical masonry structures to future climates.

1.3. Outline of the thesis

In Chapter 2, a thorough examination is provided of existing literature, offering an overview of the: necessity for improving the thermal performance of historic buildings; existing guidelines for conservation, rehabilitation, and restoration of historic buildings in North America; research on the retrofit of historic buildings in North America and Europe; available insulation materials for the thermal retrofit from the interior of the wall assembly; durability criteria and component degradation models, and; existing moisture reference year selection methods for HAM simulations. Based on a review of the existing literature, specific areas have been highlighted in this chapter where further research is needed and as well, key questions for investigation are outlined.

In Chapter 3 the methodology for undertaking hygrothermal simulations is described. It includes information on the climatic data, wall assemblies, different factors as may affect the simulation results, such as wall orientation and moisture sources, and the location of critical areas of the

masonry wall assembly for assessing freeze-thaw response, and as well, settings for the simulation solver.

In Chapter 4, the reliability of existing climate-based indices to assess the risk to freeze-thaw damage of internally insulated masonry walls is evaluated. The assessment relies on various methods of correlation and approaches for ranking the results of analysis. Hence, in this section the findings using existing climate-based indices are provided and these are compared to the results from simulations.

A parametric study is presented in Chapter 5 from which the most influential parameters affecting the occurrence of freeze-thaw damage in masonry wall structures can be identified. A simulation-based approach is described for the selection of a moisture reference year to assess the freeze-thaw damage of masonry structures.

In Chapter 6, the impact of different interior insulation systems on the freeze-thaw damage response of historic masonry walls is investigated in respect to a combination of various different parameters. This chapter concludes with a proposed decision-making procedure for internal insulation retrofit projects and proposes solutions for retrofits where a high degree of caution is required.

Finally, in Chapter 7, a summary of the contributions is provided, and as well, the primary conclusions derived from this thesis work, and on which is based a description of potential future work.

Chapter 2. Literature Review

2.1. Internal insulation retrofits for historic masonry walls

2.1.1. The need for improving the thermal performance of historic buildings

Historic buildings are mainly composed of loadbearing masonry walls, its mass and storage capacity are used to resist moisture loads. However, during wetting events, moisture progressively infiltrates through the mortar and brick pore structure (Straube and Schumacher, 2007). Moisture will then accumulate in the pores until the conditions at the wall surface allow for drying. Moisture is usually removed by the evaporation of water through capillary suction and vapor transport by diffusion through the pores. Both mechanisms occur to the inside and the outside surfaces, as long as the wall assembly is not insulated on its interior. Interior insulation retrofits may reduce the temperature within the masonry and limit its ability to dry to the interior in case the insulation material is not vapor permeable (CMHC, 2011; Straube et al., 2011; Straube and Schumacher, 2007). In general, the outer face of masonry is subject to similar conditions as the outdoor climate before or after retrofit, while main changes happen through the inside face of the masonry wall. Figure 2-1 shows that before any insulation is added, the assembly had moderate temperatures – close to interior conditions. However, the inside face experiences much colder temperatures post-retrofit, therefore, any interior air that contacts this face could condense if the surface temperature is below the dewpoint of the indoor air. In addition, insulating masonry walls on the interior, especially in cold and wet climates may increase the potential risks for performance and durability related problems. Therefore, the design of the internally insulated buildings needs to be done carefully.

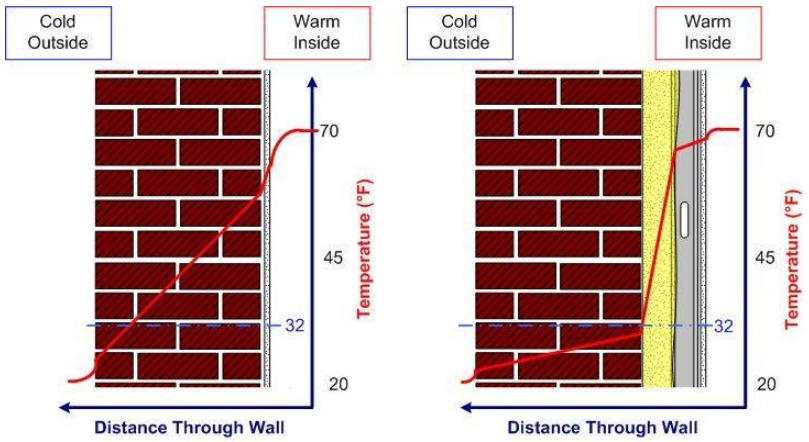

Figure 2-1. Temperature gradient through the wall before and after retrofit (Straube et al., 2012).

Multiple interior insulation retrofits have been carried out in the past; however, findings seem inconsistent. For instance, some research, despite the increase potential for deterioration after the retrofits, have found that the thermal performance of wall assemblies has improved with no noticeable signs of deterioration. Whereas others have reported increased damage risks. This discrepancy can be due to several reasons. A few studies only observed the envelope performance for the first few years following a retrofit, and thus provided evidence of short-term success. Other studies have been evaluated under normal moisture loads, while others counted the effect of highest WDR impinging on the envelope surface. In addition, the location and the amount of insulation added to a masonry wall can significantly alter the micro-environment of the brick. Other influencing factors are the type of masonry and its thickness, the severity of the climate and the investigating region within the wall assembly. Furthermore, most of the reviewed studies were performed under average weather conditions, including Canadian cities. Therefore, further research on the long-term effects of the application of interior insulation under a most severe climate is still required.

2.1.2. Guidelines for conservation, rehabilitation, and restoration of historic buildings in North America

A review of available publications on the conservation, rehabilitation and restoration of historic buildings in North America has been recently completed (Sahyoun and Ge, 2020). The literature reviewed consisted of a range of governmental and non-governmental standards and guidelines, journal papers, conference proceedings and case studies published from January 1998 to the beginning of 2020. The majority of the references retrieved are from (Canada's Historic Places,

2010, 2007, 2003), the City of Vancouver (Fan, 2014; Vancouver Heritage Foundation, 2012), the Region of Waterloo (Region of Waterloo, 2013a, 2013b) the U.S. Department of the Interior National Park Service Technical Preservation Services (Hensley and Aguilar, 2012; Jandl, 1988; Weeks and Grimmer, 1995; Weeks and Jandl, 1996). ASHRAE Standard (ANSI/ASHRAE, 2019), the Canada Mortgage and Housing Corporation (Khudaverdian, 2005; Masson, 2015) and the Building Science Corporation (Musunuru and Pettit, 2015; Ueno, 2015). A number of commonly used scientific databases were searched for the collection of technical and research-based publication, however, the number of journal articles addressing improvements in thermal performance of masonry structures with their retrofit using interior insulation and the resulting durability assessment that is pertinent to North American context is very limited.

Amongst the reports reviewed, the Region of Waterloo guideline (Region of Waterloo, 2013a) recommends three strategies to be applied in a retrofitting work: (1) Incorporating a vented airspace to keep brick units below a critical moisture content during FT seasons; (2) Filling insulation in between studs through openings drilled in the existing walls, and thereafter, blowing in dry cellulose, fiberglass, or spraying in open-cell foam, when there are restrictions to ensure that the existing internal finish remains intact; in this situation, the holes need to then be repaired; (3) Installing insulation systems that are hygroscopic and vapour permeable or adding a vapour control layer for certain types of insulation. In addition, for buildings constructed with cavity or 'hollow' walls before World War II, the guide describes ways to insulate them internally or placing insulation within the cavity. If the latter option is required in order to preserve the interior appearance of the wall, it is suggested to use mineral wool, beads or granules, foam insulation, which are blown in or injected into the cavity. It is not advised to perform such method for cavities thinner than 50mm, since there is a risk that the insulation may allow water to cross the cavity.

Moreover, Canada Mortgage and Housing Corporation (CMHC) carried out a review of the in-service performance of solid masonry buildings retrofitted with interior insulation (Khudaverdian, 2005). This study presents the results of a series of condition assessments on existing retrofitted wall systems, located in Montreal area, based mainly on visual inspection of existing retrofitted buildings. The 2005 project was then followed by another study (Masson, 2015) that consists of a follow-up visual assessment of the same retrofitted massive masonry exterior walls. Buildings investigated varied in terms of the type of masonry used in their construction: solid red clay brick,

limestone, and structural wood and steel elements. The exterior walls were internally insulated using either polyurethane foam or batt insulation. The results of the exterior condition assessment (for both 2005 and 2015 investigations) varied between very good to poor facade conditions. For instance, some degradation indications were still observed for cases with overall very good facade conditions, such as the presence of efflorescence, cracks in mortar joints, and cracked stones.

ASHRAE recently published a new guideline "ASHRAE Guideline 34 – 2019, *Energy Guideline for Historic Buildings*", which provides specific retrofitting and upgrading procedures for historic buildings to achieve greater energy efficiency, while avoiding disruption to the historic character (ANSI/ASHRAE, 2019). This guide recommends removing or replacing existing fiberglass or cellulose insulation materials that show sign of wetness. Because, once wet, these insulations lose much of their thermal resistance value (R-value). In addition, the guide describes the proper application of a few commonly used insulation materials. For instance, fiberglass may not provide a suitable thermal resistance if installed at too low or too high densities or when it is not carefully applied. In cavities, where air movement is to be impeded, cellulose insulation is usually installed; however, if the material contains fire-retardant salts, those salts might migrate to interior or exterior finishes. Also, it is desirable that most insulation materials are reversible; thus, the guideline prohibited the use of spray-applied foam to insulate attic floors or under-roofs because this material fails to be easily removed. Guideline 34 also provides recommendations on how to reduce potential deterioration on exterior and interior materials. For instance, minimizing the risk of damage to exterior materials can be primarily achieved through mitigating exposure and correcting flaws in the façade. However, reducing the risk of damage to interior materials depends on mitigating the indoor exposure. It is thus suggested to follow ASHRAE Standard 160 (ANSI/ASHRAE, 2021) in order to address concerns for mould and moisture damage within the thickness of the wall assembly.

Moreover, Moore et al. (2022) recently developed a method for assessing the potential to improve the thermal efficiency of a historical building's structure while minimizing risk to its long-term durability and heritage features. Their approach involves evaluating the impact of adding insulation to the interior surface of the heritage structure on freeze-thaw resistance of masonry components, aligning with three main project stages outlined in the Standards and Guidelines for Historic Places in Canada (Parks Canada, 2010): Understanding, Planning, and Intervening.

2.1.3. Review of research on retrofit of historic buildings in North America and Europe

It has been agreed that internally insulating historical buildings may pose a risk to reduced performance and the onset of durability problems. For masonry wall assemblies, such interventions may reduce the temperature within the masonry and limit its ability to dry to the interior (CMHC, 2011; Straube and Schumacher, 2007). This possibly increases moisture levels and reduces the temperature in the masonry, leading to FT damage of the facing brickwork. As well, the outer face of masonry is subject to similar conditions as the outdoor climate before or after retrofit, whereas the primary changes occur through the inside face of the masonry wall. However, post-retrofit, the inside face experiences much colder temperatures and therefore, any moisture within the indoor air that contacts this face could condense if the surface temperature is below the indoor air dewpoint temperature. Therefore, the design of internally insulated buildings must be undertaken with these considerations in mind.

Different experimental measurements and HAM modeling have been carried out with the use of different types of insulation materials as a means of evaluating the hygrothermal performance of building envelopes of masonry construction. (Maurenbrecher et al., 1998) have conducted a field measurement study for a 4-story masonry warehouse located in Winnipeg and retrofitted on the interior side using insulation with integrated aluminum foil. It was found that the temperature at the interface of the insulation layer and masonry dropped below freezing point for several months in the winter. However, the moisture levels did not seem to exceed the critical level.

Straube and Schumacher (Straube and Schumacher, 2006) led a comparative study of two interior retrofit options on a masonry wall assembly, using 50 mm extruded polystyrene insulation (XPS) and 90 mm batt insulation; adding about similar insulation level when thermal bridging through the studs is considered. It was concluded that both insulation systems were safe for the five Canadian cities considered, and no significant changes to the FT and corrosion indices were recorded.

Scheffler and Grunewald (Scheffler and Grunewald, 2003) suggested using capillary-active insulation materials to reduce the initiation of moisture problems. Measurements and numerical simulation methods were used to investigate the application of capillary-active materials as an interior retrofit strategy. This application proved advantageous for the drying process of potential built-in moisture as well as for limiting the presence of condensation during the winter period; this

study was patient to building located in cold climates, as may occur in Eastern Europe (Haupl et al., 2004, 2003; Stopp et al., 2001) and Central Europe (Toman et al., 2009).

Wilkinson *et al*. (Wilkinson et al., 2009), evaluated the effect of applying closed-cell spray foam insulation at a school building in Toronto through measurements and HAM modeling. The results from both the measurements and HAM modeling indicated that the moisture content of the brick and mortar increased after retrofit, but it did not reach to levels favorable for FT damage (i.e. the maximum monitored and modelled moisture content were found below the 12 % threshold where freeze-thaw damage is expected to occur. This 12 % threshold corresponds to 85 % of the free water saturation). Further study to verify selected freeze-thaw thresholds is recommended.

Scheffler (Scheffler, 2011) introduced a new internal insulation technology based on lightweight autoclaved aerated concrete. This insulation technique was applied for an old school in Germany, and was investigated through 1D and 2D simulations, using DELPHIN[1]. The outcome of the study proved that the moisture content inside the masonry increased, though the overall moisture level was kept below critical value, even for sensitive materials such as wooden floor beams.

Furthermore, (Kočí et al., 2017) compared the hygrothermal performance of a masonry wall located in the Czech Republic, retrofitted using three types of capillary-active thermal insulation materials. The computational analysis showed that all three hydrophilic insulation materials did not cause any accumulation of moisture within the wall. Likewise, a recent study by (Bottino-Leone et al., 2019) on a heritage residential building situated in the city of Bamberg, Germany, concluded that vegetal and mineral based insulation systems are appropriate for interior retrofits.

Nevertheless, Morelli *et al.* (Morelli et al., 2010) examined the impact of internal insulation on masonry walls with wooden floor beams in the northern and humid climate of Denmark through 2D and 3D numerical simulations. The computational analysis showed that the retrofit not only reduced the heat loss through the wall but also the drying potential of that wall, putting the structure at risk to moisture-induced problems.

Vereecken and Roels (Vereecken and Roels, 2011) compared the efficiency of capillary-active and traditional vapor-tight interior insulation systems; and concluded that although capillary-active

[1] www.bauklimatik-dresden.de; Simulation program for coupled HAM and salt transport in porous materials; developed at the Institute of Building Climatology, Dresden University of Technology, Germany.

systems performed better, they were, however, more sensitive to many climate parameters, such as wind-driven rain load and orientation, and wall thickness.

A large number of uncertainties concerning the use of internal insulation in masonry structures has been found in the literature (Nielsen et al., 2012; Zhao et al., 2011). Johansson *et al.* (Johansson et al., 2013b) conducted an experimental and numerical (WUFI 2D) study to analyse the hygrothermal performance of masonry envelopes with vacuum insulated panels as interior insulation. The study was done under the climates of the west-coast of Norway and Sweden, where high levels of WDR are expected. Results showed that embedded wooden beams experienced risky conditions after retrofit.

As well, Klõšeiko *et al.* (Klõšeiko et al., 2015), measured the hygrothermal performance of four different internal insulation materials (diffusion open, capillary-active and vapor-tight) for a historic school building in Estonia under high moisture load. Both measurements and 1D computer simulations showed moisture accumulation within the wall, as well as favorable conditions of temperature and relative humidity for the onset of mould during nine months of monitoring period.

Williams and Richman (Williams and Richman, 2017) examined the long-term risk of internally insulating a historic solid brick masonry house in Toronto. They used in-situ moisture content measurement and 3D laboratory frost dilatometry methods to permit a comparison of the hygrothermal performance between a base-case of a clay brick load-bearing wall and the retrofit-case, for which a medium density closed-cell polyurethane spray foam insulation was used. Results showed an increase in the number of FT cycles (FTCs). It was also recorded that the number of FTCs increased when the wall was exposed to solar radiation.

Odgaard *et al.* (Odgaard et al., 2018) observed the performance of a historic masonry wall (with and without diffusion open insulation) under a normal moisture load and low WDR impact in Copenhagen. Both experimental and visual investigations indicated that the relative humidity of the insulated wall increased by 20 – 30%; however, none of the evaluated damage criteria showed an actual damage post-retrofitting damage. The authors expected that should outdoor conditions worsen, the risk of moisture induced damage could likewise increase.

The European project on Robust Internal Thermal Insulation of Historic Buildings (RIBuild, 2015-2019) provides information on the most recent research on the use of internal insulation in historic

buildings. Several historic buildings constructed before the World War II were inspected for this project; these were primarily buildings having massive external walls, largely constructed of brick masonry. The RIBuild project has been on-going since 2015 and has permitted the integration of the work of ten research institutions and companies from several European countries. As such, this project has been able to consider building located in various climates and of different building practice. The principal outcome from this project is to convert research work into guidelines applicable to all of Europe. To date, more than 20 deliverables have resulted from the research, which has been undertaken in the areas of, for example: pre-renovation assessment, characterisation of materials, laboratory measurements, case studies, and solutions for assessing the use of internal insulation products using a probabilistic approach.

One of the deliverables focused on the variety of historic building materials and the lack of complete knowledge of material properties (Möller et al., 2018). A compilation of material properties for both historic building materials and insulation materials has been made; a clustering-based approach was implemented to permit estimating the properties of any missing materials, based on the work done by (Fraley et al., 2012; Fraley and Raftery, 2002). Another deliverable was a review of results obtained from a number of case studies developed within the RIBuild project (Freudenberg et al., 2019). An assessment was done regarding the recorded damages, as well as influencing conditions for damage to occur, such as, weather conditions, indoor environment, historic and retrofit construction, as well as specific aspects of construction problems (e.g. as occur at joist ends, and air tightness). This helped identify the most relevant risk factors for diminished hygrothermal performance for the installation of internal insulation in building retrofit projects. The risk factors depended on a number of conditions and properties related to the existing masonry wall (e.g. initial conditions, material properties), the insulation system (e.g. type, thickness, robustness) and the exterior climatic and indoor environmental conditions. Moreover, a probabilistic approach was implemented to evaluate the hygrothermal performance of interior insulated historical buildings, in respect to mould growth, rot fungi, frost damage and the presence of algae and discolouring effects (Janssen et al., 2019). The set of practical guidelines (Blumberga et al., 2020) as were developed consists of those valuable for: Establishing goals for applying internal insulation to the retrofit of historic buildings; deciding whether a building is suitable for the installation of internal insulation; selecting an internal insulation system, and; evaluating the potential for energy savings and environmental impact.

2.1.4. Insulation materials for interior insulation retrofit

Numerous internal insulation options and products are currently offered in the market. These options vary based on their material characteristics, installation techniques, environmental effects, longevity, and expenses. The hygrothermal properties of the insulation material determine the classification of internal insulation systems into two primary categories: vapor-tight and vapor-open systems.

- **A vapour-tight internal insulation system:**

A vapor-tight internal insulation system hinders the infiltration of warm and moist indoor air into the insulation. This can be achieved by utilizing a vapor-tight insulating material such as Polyurethane (PUR), XPS, or cellular glass. Alternatively, it can be accomplished by combining a vapor barrier (a non-permeable foil) with a vapor-open material like mineral wool. Special care is essential when using a vapor barrier to prevent any breaks or punctures that could lead to moisture penetration and reduced system effectiveness (RIBuild, n.d.).

- **A vapour-open internal insulation system:**

A vapor-permeable insulation system is typically achieved by utilizing a vapor-permeable insulation material that also facilitates capillary action (capillary-active insulation material). The capillary activity of the material enables moisture to be transported through the insulation towards indoor air if the inner surface of the current wall becomes moist, such as from interstitial condensation (RIBuild, n.d.).

Selecting the appropriate insulation solution requires an understanding of the hygrothermal characteristics of both the materials within the current wall and potential insulation systems. Key factors to consider include: the thermal conductivity λ [W/(m K)], the capillary action, and the water vapor diffusion resistance factor μ [-] (Blumberga et al., 2019).

The *thermal conductivity* λ [W/(m K)] represents the speed at which heat is conducted through a unit cross-sectional area of the material in the presence of a temperature difference. Knowledge of all λ-values of the materials within the insulated wall is necessary to compute the intended air-to-air U-value (thermal transmittance, [W/(m^2.K)]) of the wall, typically indicated in building regulations. It is calculated based on Equation (2.1):

$$U = \frac{1}{R_{si} + \sum_{i=1}^{N} \frac{S_i}{\lambda_i} + R_{se}} \quad \textbf{(2.1)}$$

Where, *Rsi* and *Rse* are the internal and external surface thermal resistances [m^2.K/W], respectively. And *si* and λi are the thickness (m) and the thermal conductivity [W/(m.K)] respectively, of the i-th layer of the retrofitted wall.

The *capillary action* is the capability of some materials to absorb liquid water through capillary suction and then spread it throughout the material. The pore size in these materials allows for absorption and redistribution of liquid water and vapor towards the surrounding room, driven by an inward capillary pressure gradient (Vereecken and Roels, 2016).

The *water vapor diffusion resistance factor* μ (-) represents the material's resistance to allowing water vapor to pass through. It is determined by dividing the water vapor permeability of air by that of the specific material. This characteristic is commonly utilized for categorizing insulation materials into either vapor-open insulation systems (with low μ values) or vapor-tight insulation systems (with high μ values).

Vapour-tight insulation systems are achieved by using a vapour-impermeable insulating material or, alternatively, by combining a vapour-open insulating material with a vapour barrier. Only three different insulation systems were selected for evaluation through this thesis: Polyurethane, Mineral Wool and Calcium Silicate.

2.1.4.1. SPRAY POLYURETHANE FOAM (SPF)

Polyurethane insulation is produced through a chemical reaction between isocyanate and polyols. This reaction creates a rigid foam that has excellent thermal insulation properties (Liu, 2013). Additionally, polyurethane insulation materials are known for their versatility and ability to be molded into various shapes and sizes (Bharadwaj-Somaskandan et al., 2003). This makes them ideal for a wide range of applications, including building insulation, refrigeration, and packaging (Berezkin and Urick, 2013). Polyurethane insulation materials have become increasingly popular in the construction industry due to their exceptional thermal performance and versatility. The usual end result consists of PUR boards or loose-fill material used to fill small cavities. (Jelle, 2011) provided an extensive review on the PUR material properties and information on its installation, advantages, and disadvantages. Furthermore, polyurethane

insulation has a closed-cell structure, which helps to minimize heat transfer through convection and conduction (Jelle, 2011).

2.1.4.2. MINERAL WOOL (MW)

Mineral wool (MW) is produced using sand and basalt rocks as its primary raw materials. (Jelle, 2011) has also described the production procedure, the installation and material properties of mineral wool. Mineral wool has versatile applications for filling frames, cavities, floors, and roofs. Similarly to polyurethane, perforation and cutting can be carried out on-site during construction without compromising the material's thermal properties.

2.1.4.3. CALCIUM SILICATE (CASI)

Calcium silicate (CaSi) is an insulating material made up of hydrated calcium silicate, typically strengthened by the addition of fibers. It is commonly used as calcium silicate boards as the end product. Perforation and cutting can be carried out at the construction location without compromising the material's thermal characteristics. Calcium silicate is a commonly utilized insulation material for historic structures due to its capillary-active nature, which helps prevent the accumulation of moisture within the building's components (Walker and Pavía, 2015). Other benefits include its ability to withstand high pressure, non-flammability, and resistance to frost. Additionally, due to its high bulk density, the material exhibits sound-absorbing qualities.

2.1.5. Comparison of insulation materials

The classification, characteristics and hygrothermal properties of the selected insulation systems are presented in Table 2-1, Table 2-2, Figure 2-2 and Figure 2-3.

Table 2-1. Internal insulation system examples – classified based on water vapour diffusion resistance of the composing materials.

Vapour-open (capillary active) internal insulation systems	**Vapour-tight internal insulation systems**	
	Vapour tight materials	**Vapour-open materials coupled with a vapour barrier**
Calcium Silicate (CaSi)	Polyurethane (PUR)	Mineral Wool (MW) + PE foil

Table 2-2. Advantages & disadvantages of insulation materials used for internal insulation, adapted from (RIBuild, 2015-2019).

	Parameter	MW	SPF	CaSi
Adv	Cheap compared to other materials	x		
	Easy to customize on the construction site	x	x	
	Low thermal conductivity compared to other materials		x	
	Low density compared to other materials		x	
	Wide range of insulation thicknesses is available	x	x	
	Fire resistant	x		x
	Improved sound blocking	x	x	
Dis	Expensive compared to other materials			
	Requires flat surface to apply the material	x	x	x
	High thermal conductivity compared to other materials	x		x
	High density compared to other materials			x
	Contains fibers that can be potentially harmful when inhaled	x		
	Suffers from loss of heat conductivity during the lifespan		x	
	Can change the dimensions due to shrinkage over time		x	

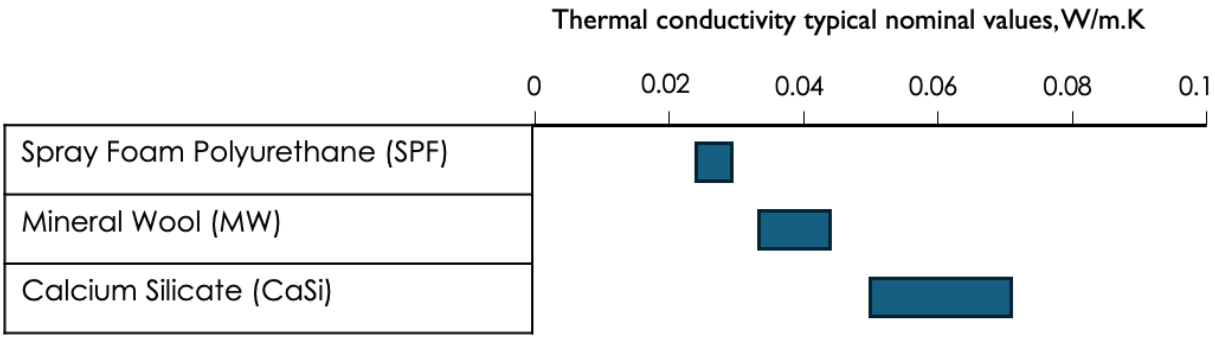

Figure 2-2. Comparison of insulation materials based on their thermal conductivity, adapted from (RIBuild, 2015-2019).

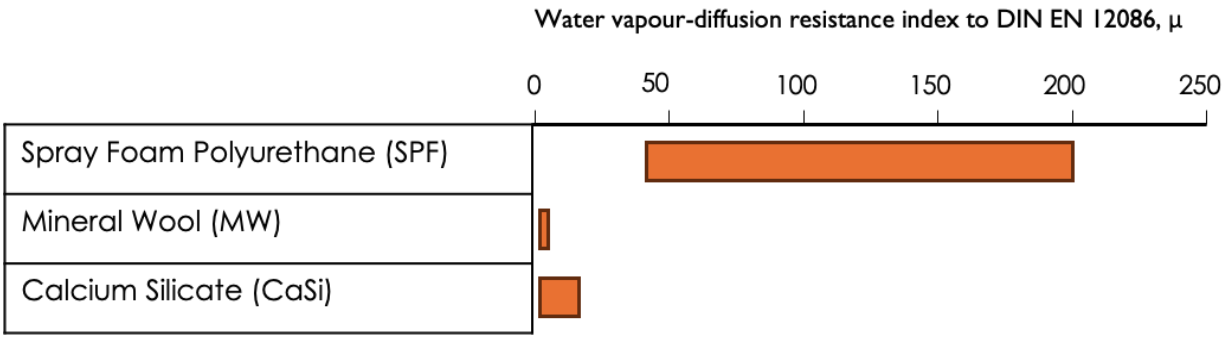

Figure 2-3. Comparison of insulation materials based on vapour diffusion resistance, adapted from (RIBuild, 2015-2019).

2.2. Review of the durability criteria and component degradation models

Moisture is known as the major source of materials deterioration. After a wetting event, if moisture is accumulated within the pores of the material and is stored for a duration at which the capacity of moisture storage is exceeded, moisture-related damage may happen. The hygrothermal response of an exterior wall is affected by several parameters including the wall configuration, the materials selection, the wall design and the outdoor climate (Kočí et al., 2017). In order to assess the type of damage that might occur under different climatic conditions, specific damage functions have been developed. This section covers the most pertinent damage mechanisms to masonry buildings, such as frost damage to masonry elements, corrosion of metal and damage as arises from the formation of mold.

2.2.1. Frost damage

Frost damage is considered one of the most important damage mechanisms in porous materials (e.g. stone and brick masonry) that threatens the durability of masonry buildings in cold climates. The damage is primarily affected by the action of freezing and thawing inside the porous materials and is the result of multiple critical freeze-thaw-cycles (FTC_{crit}) (Lisø et al., 2007; Wardeh and Perrin, 2008). Nonetheless, freezing temperature is not the only factor to provoke damage. According to Fagerlund (1973), the onset of damage in porous materials is a function of exceeding the moisture saturation concurrently with the occurrence of freezing temperatures. For instance, regardless of the number of fluctuations around the freezing point, no damage occurs if the saturation in a material remains below its critical degree of moisture saturation (S_{crit}). This critical saturation level is a function of the material properties and is defined as a constant that indicates

the moisture content at which frost damage can occur in proportion to the fully saturated moisture content. The value of the critical moisture content can be experimentally defined using laboratory freezing test at different moisture contents. And since material properties can substantially change between different types of masonry, so does the S_{crit} (Straube and Schumacher, 2006). The value of the S_{crit} for three different brick materials obtained from Canada was measured by non-destructive laboratory testing – using frost dilatometry. Of the bricks tested, the range of values for S_{crit} varied widely: values of 0.25, 0.30 and 0.87 were obtained (Straube et al., 2010a).

Fagerlund (1977) considered a hypothetical critical saturation of 66% determined from the *x*-axis intercept of the strain of the damaged specimens. Whereas an average range of 70%-80% was obtained by Williams and Richman (Williams and Richman, 2017) for the specimens tested. These values were in line with data collected by Van Straaten (Van Straaten, 2014) on existing North American brick masonry units of a number of buildings constructed between 1830 and 1950 and tested by Building Science Laboratories, where critical saturation values varied between 30% and 90%.

Aldabibi et al. (2022, 2020) have also examined the value of S_{crit} of five different types of bricks obtained from vendors in Montreal. They have found that the value of S_{crit} varies between 30% and 75%, with values for average exterior brick between 45% and 55%.

Based on these findings, it can therefore be suggested that the range of values for S_{crit} can be considered between 25% and 90%.

For frost damage to occur, three conditions must be fulfilled: (1) Material must be sufficiently wet; (2) Temperature must be sufficiently low, so that water in the material can freeze; and (3) Material must be sensitive to frost. From the perspective of the initiation of mechanical strain and stresses arising from the freezing action, the principal mechanism for the occurrence of frost damage is the volume expansion of freezing water by nine percent (Kralj et al., 1991; Powers and Helmuth, 1953). Damage occurs once the material is no longer able to withstand the tensile forces as arise from the formation of ice in the pore system, and fine cracks start to appear. These cracks can gradually develop under successive frost events and induce scaling at the material surface, and therefore may cause complete disintegration of the masonry unit (Lisø et al., 2007). In addition, Wardeh and Perrin (Wardeh and Perrin, 2008) described two other frost damage mechanisms that occur simultaneously: (1) hydraulic pressure, and (2) ice lens formation. Hydraulic pressure is

triggered by friction at the pore surface due to moisture transport upon freezing. For instance, since the vapour pressure in small pores is relatively higher compared to larger pores, water freezes in the largest pores first. When the volume of ice increases and larger pores fill up, water migrates to smaller pores resulting in hydraulic pressure. The friction resulting from the moisture transport induces tensile stresses to the pore surface, causing damage.

Information on the critical saturation degree of brick masonry materials would be very helpful for the design of new buildings as well as for retrofit purposes. For instance, for a conservative retrofit strategy, the moisture content of walls post-retrofit would have to be compared to the S_{crit} of the existing brick. In situations where the interior insulation does not increase the moisture content above the S_{crit} threshold, the strategy could be safely applied. However, the retrofit plan should be modified if the moisture content increases above S_{crit} (Mensinga, 2009). A considerable amount of research has been previously completed to investigate the risk of degradation due to FT effects on masonry buildings using critical saturation threshold measurements. These studies utilized expensive specialized equipment and labor (Ueno et al., 2013a; Van Straaten, 2014; Wilkinson et al., 2009). As is often the case for masonry buildings retrofit projects, time and budget limitations preclude the use of specialized methods and the use of representative material properties is more often preferred rather than sample measurements.

2.2.1.1. FREEZE-THAW MODELS

To quantify the risk of frost induced damage to masonry structures, FT damage functions are often used; a portfolio of several of these models were examined.

One definition used in the FT cycle analysis is a day with a positive average temperature, followed by a day with a negative average temperature (Grossi et al., 2007). According to the information provided in the NOAH's ARK project, the average temperature was taken below -3°C, while the previous or following day should have an average temperature above 1°C to consider a FT cycle. However, the accepted way of quantifying the risk of FT damage is through counting the number of possible freeze-thaw cycles (FTC) on an hourly basis.

The FT index is described as the number of cycles when temperatures fluctuate between the freezing and thawing point of envelope materials, and simultaneously the material exceeds its critical degree of saturation (S_{crit}) (Mukhopadhyaya et al., 2005). Therefore, the larger the number

of FTC exceeding the critical moisture content, the larger the potential freeze- thaw damage. According to Straube and Schumacher (Straube and Schumacher, 2006), freezing occurs when the temperature within the material falls below -5°C and thawing starts at temperatures above zero. The authors mentioned that between 0°C and -5°C, no significant frost damage develops.

Walder and Hallet (Walder and Hallet, 1985) determined that crack growth is more representative at temperatures between -4°C and -15°C, because at very low temperatures, the water migration necessary for withstanding crack growth was inhibited. And at higher temperatures, the thermodynamic limitation meant pressure was not enough to cause crack growth. It is thus important to note that for masonry materials, the process of freezing water begins in the largest pores and as the temperature drops it affects pores with smaller diameter. Therefore, the freezing temperature is influenced by the size and distribution of small diameter pores (Maage, 1984).

In some studies, the time of freezing and thawing were considered as important factors for the onset of damage. For instance, the CSN EN 12371 (CSN EN 12371, 2010) requires that one FTC be considered as 6 hours of freezing be followed by 6 hours of thawing. However, both *CSA Standard A82-06 (CSA, 2006)* and *ASTM Standard C67-07a (ASTM, 2007)* require that the brick samples are soaked for approximately 4 hours in a thawing tank and then placed in a cold chamber for approximately 20 hours.

Koči et al. (Kočí et al., 2017) has introduced the concept of the number of indicative freeze-thaw cycles (IFTC), where freezing must take at least 2 hours, separated by at least 2 hours of thawing. Another damage function developed by Koči et al. (Kočí et al., 2014) is the winter index (WI), in which the risk of frost damage is evaluated based on calculating the level of severity in the instance where the RH is above the critical level and concurrently, temperature falls below its freezing value.

Similarly, the Time-of-Frost (TOF) function permits evaluating the risk of frost damage based on calculating the number of hours during the year when conditions are favorable for ice formation. According to Straube and Schumacher (Straube and Schumacher, 2006), the RH is not a good measure for FT damage, because the sorption isotherm of brick materials is very steep in the region in which FT damage is possible, and therefore the RH would typically be above 99% regardless of which critical MC is selected.

Koci et al. (Kočí et al., 2017) proposed modified versions of the winter index (MWI) and (TOF), which utilise hourly values of MC instead of RH, and calculates the level of severity in the case that the MC is higher than the critical level. The Modified Winter Index (MWI) and Time-of-Frost (TOF) are given, respectively, in Equations (2.2) and (2.3):

$$MWI = \sum_{i=1}^{8760} (T_L - T_i)(w_i - w_L) \qquad for\ [T_i < T_L \cap\ w_i > w_L] \tag{2.2}$$

$$TOF = \sum_{i=1}^{8760} [T_i < T_L \cap\ w_i > w_L] \tag{2.3}$$

The same authors developed the amount of frozen water (AFW), which assumes that the entire amount of moisture found in the material at a temperature below its critical level is vulnerable to ice formation (Kočí et al., 2017). The (AFW) function is presented in Equation (2.4).

$$AFW = \sum_{i=1}^{8760} w_i\ \ [T_i < T_L \cap\ w_i > w_L] \tag{2.4}$$

Where,

T_L and w_L are the critical values of temperature (K) and moisture content (m^3/m^3), respectively.

T_i and w_i are the hourly values of temperature (K) and moisture content (m^3/m^3) at the investigation point; respectively.

Moreover, Zhou *et al.* (2017) further developed a freeze-thaw damage risk index (FTDR), presented in Equation (2.5). Their study proved that incomplete FTC would potentially increase the risk to FT damage. This index is defined as the accumulation of the difference between highest and lowest value for the saturation degree of ice content in each complete or incomplete FTC.

$$FTDR\ index = \sum_{cycle} \left(S_{ice,max} - S_{ice,min}\right); \quad for\ \left(S_{ice,max} - S_{ice,min}\right) > 0.05 \tag{2.5}$$

Where,

$S_{ice,max}$ – the saturation degree of ice content (which is the ratio between the ice mass density and the total moisture content).

The literature comprises a few more indexes to assess the risk of frost damage; including but not limited to the length of propagated crack (Walder and Hallet, 1985), the surface frost intensity (Nelson and Outcalt, 1987) and the frost decay exposure index (FDEI) developed by (Lisø et al., 2007).

Several indexes were developed to evaluate the potential risk to frost damage using results from HAM simulations. Whereas some indexes are based on the climate severity, others depend on the frost resistance of a specific material; however, no model exists that permits translating the development of mechanical stresses and strains to be weighed against the frost damage sensitivity of the material. This implies that the actual FT indicators do not provide information on damage evolution, as is provided for wood rot from the VTT model (Johansson et al., 2019). Besides, Janssens et al. (2024) concluded that the severity of a freeze-thaw cycle has a greater impact on the damage than the frequency of cycles. Therefore, it is crucial to examine the conditions during the most extreme freeze-thaw cycles rather than counting low threshold FTCs.

2.2.2. Mould Growth

Mould fungi are part of our natural environment which are known to be dangerous – depending on the type of mold – if they ever grow in our buildings. When moisture accumulates substantially, mould can develop on numerous material surfaces, thus adversely affecting the indoor environment and air quality, putting human health at risk. Health Canada (Health Canada, 2011) considered mold growth a major problem since it can be toxic for the building's occupants, causing allergies, diseases or infections. In addition to the occupants' comfort, mold growth might affect the appearance of surfaces and lead to structural damages. Thus, in order to prevent mould development, it would be necessary to limit the excess in moisture. However, managing moisture penetration and protecting the building materials from mold spores' contaminations seems very challenging (Li, 2005). Masonry materials are non-organic in nature, and thus are able to withstand mould decay. Though, sometimes historical masonry buildings include wooden elements, vulnerable to mould growth and decay.

Significant differences exist among the various mould species, thus the appropriate conditions for their development and propagation vary as well. It has been demonstrated that mould growth in building structures is primarily affected by humidity and temperature (Hukka and Viitanen, 1999;

Viitanen and Ojanen, 2007; Viitanen and Ritschkoff, 1991). Fungi are usually vulnerable to a relative humidity (RH = 75% - 80%) to germinate. Besides, the minimum temperature required for mold onset is 0 ºC. Faster spores' germination occurs at higher temperatures (at a maximum of 50 ºC). However, some species are found susceptible to lower temperatures. For instance, Nielsen (Nielsen et al., 2012) concluded that both Cladosporium and Penicillium are able to develop at -5 °C on wood surfaces. Nonetheless, the critical relative humidity (RH_{crit}) for mould germination is function of temperature (Hukka and Viitanen, 1999; Viitanen and Ojanen, 2007). Moreover, mould onset requires that former conditions are attained for a sufficient amount of time. Exposure time is determined by RH_{crit} and temperature. In addition to relative humidity, temperature and the time of exposure, mold growth is influenced by other variables; such as substrate properties and the characteristics of mould fungi. In order to prevent growth in buildings, these variables must be considered during the design, construction, and maintenance of a building. The literature offers a great deal of knowledge concerning mold growth risk and ways to avoiding it (Hukka and Viitanen, 1999; Johansson, 2014; Johansson et al., 2013a). However, the following section focuses on previously developed mathematical models to estimate the risk of mould growth.

2.3. Review of climate change effect on durability: Existing research

A major challenge at present is to compile trustworthy technical information on sustainability criteria and practices as a means of quantifying the environmental effects on the long-term performance of our buildings. Considering the expected effects of future climate on the existing infrastructure, this task is becoming more important (Lacasse, 2019). A general observation from the historical weather data for the past 130 years shows that the average temperature has increased by 0.85°C (IPCC, 2014). For Canada, the temperature increase was double and in the arctic latitudes the increase was triple (IPCC, 2014). Similar trends have also been observed for precipitation events and average wind speeds. Significant changes are anticipated in temperature and precipitation in future years: at least an increase of 20-25% in precipitation, and temperature increase relative to the baseline of 2-3°C are anticipated. Studies are anticipating that even the smallest rise in weather and climate extremes can significantly increase the risk of existing infrastructure deterioration. Existing buildings are designed based on the past climate, which might no longer be able to truthfully account for the future projected weather conditions. It is therefore

necessary to identify if this change in climate would in turn increase the risk of durability of historical masonry building envelopes; particularly those undergone interior refurbishment.

Very few studies have been conducted on the durability of energy efficient building envelopes under climate change compared to the thermal performance of these buildings. Van Aarle *et al.* (van Aarle et al., 2015) reported that the risk of frost damage might increase under severe rainfall events. However, this damage risk might be reduced with the increase in air temperature. Hence, following a series of simulations using a hygrothermal model of a building envelope with calcium silicate brick, the risk for frost damage significantly decreased under anticipated future climate in the Netherlands. Similarly, a study led by Grossi *et al.* (Grossi et al., 2007) on the long-term freeze-thaw risk of porous materials for European cities concluded that the risk of frost damage on the masonry in monumental buildings would tremendously decrease under future climate. On the contrary, Nijland *et al.* (Nijland et al., 2009) stated that the expected decrease in the number of freeze-thaw cycles (FTCs) is small; whereas materials may be wetter at onset of frost, due to higher precipitation with a possible increase in freeze-thaw damage. In 2016, Sehizadeh and Ge analysed the impact of the anticipated future climate in Montreal on the durability performance of conventional masonry residential wall assemblies retrofitted to meet the PassiveHaus requirements. The outcome of this study denoted an increased frost damage risk of bricks over the years 2020 and 2050, however, under 2080 climate this risk seemed to be reduced. Furthermore, the plywood sheathing layer was found at risk of mold growth; especially when rain leakage was assumed to penetrate through the wall assembly. On the contrary, the decay index indicated a reduction of potential risk (Sehizadeh and Ge, 2016). In an attempt to compare the hygrothermal performance of residential building envelopes typically built in New York, Cabrera *et al.* (Cabrera et al., 2019) verified a procedure combining hygrothermal and mold-growth simulation tools with future weather files. The study demonstrated unfavorable conditions for mold growth at present weather conditions, whereas mold development seemed to be more serious under future climate and for a more prolonged period. Vandemeulebroucke *et al.* (Vandemeulebroucke et al., 2019) were concerned about the effect of global warming and the urban heat island on the durability of retrofitted historical solid masonry walls in the city of Ghent. HAM simulations revealed that the urban heat island effect and climate warming mutually help mitigate the freeze-thaw damage risk to historical masonry in the city, in comparison with the surrounding rural areas.

From the studies conducted on the impact of climate change, few were concerned for the durability of retrofitted buildings. It is obvious from the reviewed work that the future climate would impact the resilience of building envelopes differently. In addition, most of the studies done were for European cities, therefore, more work should be focused on North America and especially Canada. Thus, understanding the existing and the anticipated risk to moisture-induced damage risks across Canada is of a high importance.

2.4. Review of moisture reference year (MRY) selection for HAM simulations

Many expert practitioners and researchers who are engaged in the retrofit of masonry buildings and practical field problems rely on HAM simulation tools to determine the risk to deterioration of building elements. It is common to carry out one-dimensional (1D) hygrothermal simulations of building envelopes to assess their long-term performance; a period of 30 years is usually recommended to evaluate the impact of climate change (WMO, 2017). However, having to deal with many climate parameters over a long period incurs high computation time and cost. One way to reduce such expenses is to develop a method to select a "moisture reference year" (MRY) that can accurately represent a climate over the long term and as such, potentially allow a correct assessment of the moisture stress to which the building envelope is subjected over time (Djebbar et al., 2001). An MRY is usually selected from existing long-term climate data to represent a climate that allows a correct evaluation of the moisture stress to which the building envelope is subjected (Delgado et al., 2012; Zhou et al., 2016a). Several methods for the selection of MRYs have been developed in the past – they can be summarized into two types: (i) construction-independent methods, relying only on weather data analysis, which is referred to climate-based (Cornick et al., 2003; Geving, 1997; Hagentoft and Harderup, 1996; Kalamees and Vinha, 2004; Salonvaara et al., 2010; Zhou et al., 2016a, 2016b) and; (ii) construction-dependent methods based on the hygrothermal response, which is referred to simulation-based (Rode, 1993; Sanders, 1996). However, there is still no agreement on how MRYs should be selected. A review of the literature suggests a few general methods that have been proposed. An MRY should: (i) Be location-specific because climate conditions will vary between geographic locations; (ii) Reflect the location's climate variability; and therefore, it should be based on 30 years of weather data; (iii) Allow evaluation of the performance of the building envelope under critical moisture stress, and therefore; (iv) Represent the most severe year, or the 93rd percentile (P93) year – which is the year

having the second highest severity index in a 30-year period according to ASHRAE Standard (ANSI/ASHRAE, 2021). The most commonly used climate-based indices are presented below.

2.4.1. The Moisture Index (MI)

The Moisture Index (MI) approach developed as part of the IRC-led research consortium MEWS (Moisture Management of Exterior Wall Systems) which includes wetting and drying indices (Cornick et al., 2003), and then further categorizes the year as dry, average and wet based on lowest, average and highest MI value. From a dataset of years, the years having a MI value in the range of more than one standard deviation (+/-) from the mean MI value are considered as dry and wet years, while those years having a value within (+/-) one standard deviation are referred to as average years. This method attempts to combine the wetting and drying functions. The wetting index (WI) can be represented by the mean annual total horizontal rainfall or the annual wind-driven rain load. The drying index (DI) is based on the yearly evaporation potential – meaning the total hourly difference between the saturation vapor ratio and actual vapor ratio of the ambient air. The saturation vapor pressure, p_{vs}, was calculated as suggested by (ASHRAE, 2009). The magnitude of Δp_v is calculated using Equation (2.6):

$$\Delta p_v = p_{vs} - p_v \quad \textbf{(2.6)}$$

Normalized values of Δp_v and accumulated hourly rainfall were used as DI_h and WI_h magnitudes respectively and equal weights are assigned for both the indices. Then, both the wetting and drying indices are normalized using Equation (2.7):

$$I_{normalized} = (I - I_{min})/(I_{max} - I_{min}) \quad \textbf{(2.7)}$$

where,

I — the index of interest

I_{min}—the minimum values of the annual sums for each year

I_{max}—the maximum values of the annual sums for each year.

Wetting and drying were assumed to be of equal importance and thus they were given equal weight in the determination of the hourly moisture index (MI) (Equation (2.8)).

$$MI_h = \sqrt{(1 - DI_{h,norm})^2 + WI_{h,norm}{}^2} \quad (2.8)$$

The MI was calculated for 31 years in each historical and future time period. The moisture index (MI) was thus obtained by a yearly averaging of the MI (1 value for each year).

2.4.2. The Severity Index (Isev)

ASHRAE (ASHRAE, 2010) has further developed MRY selection measures, combining climate loads and durability criteria to select more "severe" weather years, thus providing a more representative ranking of the weather data. This new approach – the Severity Index (Isev), consists of a simple equation that would be used to calculate the predicted damage function value for each year. Salonvaara *et al.* (Salonvaara et al., 2010) have considered that Isev is the most reliable and the most accurate among all available methods in selecting the most severe years. A regression equation used for computing RHT as the damage function considers different input climate parameters (Equation (2.9)). The yearly average value of each climate parameter is used in the equation and years are ranked in the ascending order of the RHT values. The year corresponding to the 97th percentile (second out of the 31 years) in each time-period is chosen as the MRY.

$$I_{sev} = 108307 - 241.E_v - 1391.I_{cl} - 312326.\phi + 183308.r_{wd} + 15.2.p_v + 27.3.T^2 + 261079.\phi^2 - 0.00972.p_v^2 \quad (2.9)$$

where,

E_v—the solar radiation incident on the wall, (W/m^2)

I_{cl}—the cloud index, (0–8)

ϕ—the relative humidity, (0 < RH < 1)

r_{wd}—the wind-driven rain on the wall, (kg/m^2·h)

p_v—the vapor pressure, (Pa)

T is the ambient temperature, (°C)

As specified by the method, Isev was calculated for the orientation receiving the least solar radiation (North). All the weather parameters were calculated in terms of annual average values for each year using the number of hours during that year.

Note that Equation (2.9) was developed based on the simulation results at the OSB-layer within wood-framed walls of stucco cladding facing North and located in a number of cities in the United States. This equation was then verified and found suitable for a number of cities in Canadian and European countries and for other types of walls (Salonvaara et al., 2010).

2.4.3. The Climatic Index (CI)

Zhou *et al.* (Zhou et al., 2016a) introduced the Climatic Index (CI) as a fraction between annual wetting and drying components (Equation (2.10)). The wetting component depends on the annual WDR, and the drying component depends on the annual potential evaporation; calculated based on Penman equation (Equation (2.11)).

$$CI = \frac{Annual\ WDR\ load\ (r_{bv})}{Annual\ potential\ evaporation\ (E)} \tag{2.10}$$

$$E = \frac{\Delta}{\Delta+\gamma}\frac{K+L-A}{I} + \frac{\gamma}{\Delta+\gamma}h_m(e_a - e) \tag{2.11}$$

where,

$\frac{\Delta}{\Delta+\gamma}\frac{K+L-A}{I}$ — the radiation term

$\frac{\gamma}{\Delta+\gamma}h_m(e_a - e)$ — the turbulence term

E — the drying index

K — the net short-wave radiation, (W/m^2)

L — the net long-wave radiation, (W/m^2)

A — the conductive heat flux to the porous material, (W/m^2)

I — the latent heat of vaporization, (J/kg)

γ — the psychometric constant, (Pa/K)

Δ — the gradient between saturation vapor partial pressure and air temperature, (Pa/K)

e_a — the saturated partial vapor pressure of the air, (Pa)

e — the vapor partial pressure in the air, (Pa)

h_m — the convective vapor transfer coefficient, (s/m).

In the calculation of drying index, the conduction heat flux and long wave radiation is neglected since the values are much smaller in comparison to short wave radiation.

2.4.4. Wind-Driven Rain (WDR)

WDR is the quantity of rain that has a horizontal velocity component due to wind that falls obliquely on vertical surfaces such as facades, and inclined surfaces such as roofs. In this study, the semi-empirical WDR model by ASHRAE (ANSI/ASHRAE, 2016) was used (Equation (2.12)).

$$r_{bv} = F_E \times F_D \times F_L \times U \times cos\theta \times R \quad (2.12)$$

where,

r_{bv} — the rain deposition on a vertical wall, [kg/(m2·h)]

F_E — the rain exposure factor

F_D — the rain deposition factor

F_L — an empirical constant of 0.2 kg·s/(m^3·mm)

U — the hourly average wind velocity at height of 10 m above the ground measured at airport weather station [m/s]

θ — the angle between wind direction and normal to the wall [°]

R — the hourly rainfall intensity on a horizontal plane [mm].

Climatic data including temperature, RH, wind speed and direction, solar radiation and precipitation have become an essential part of current hygrothermal simulation models. The selection of reference years is often made with the intention to test wall assemblies to the most severe/representative hygro-climatic conditions. There are several criteria that can be considered when selecting the reference years. However, existing methods are mostly based on the evaluation of mold growth damage risk. And to the author's knowledge, no weather representative year selection method was developed specifically for FT risk assessment.

2.5. Summary

Today, there is a need to retrofit historical buildings in order to meet contemporary and anticipated changes to the energy code requirements for buildings and to mitigate the effects of climate change. In respect to the preservation of cultural and heritage buildings, the only way to retrofit these buildings is through interior insulation, albeit knowing there is a potential risk of reducing the durability of the exterior wall. Most of the Canadian guidelines focus on cultural preservation in general. As for upgrades to the envelope thermal performance, most guides do not suggest or are very cautious about insulating the historical masonry walls from the interior. On the other hand, a number of interior insulation retrofits have been carried out in the past; these findings seem, however, inconsistent. For instance, some of the research has shown that despite the increase potential for deterioration after the retrofits the thermal performance of wall assemblies has improved with no noticeable signs of deterioration. Whereas others have reported increased frost damage risks. This discrepancy can be due to several reasons. In some studies envelope performance was only observed for the first few years following a retrofit, and thus only provided evidence of apparent success over the short-term. Other studies have been evaluated under normal moisture loads, whereas others considered the effect of the highest WDR loads impinging on the envelope surface.

2.5.1. Literature main findings / Knowledge gaps

- A variety of insulation materials and installation methods were suggested by practical guides and standards. However, guidance from Canada and the United States tend to favor materials such as spray foam and a few projects used cellulose and fiberglass.
- The location and the amount of insulation added to a masonry wall can significantly alter the hygrothermal state of the brick. Other influencing factors are the type of masonry and its thickness, the severity of the climate and the zone of investigation within the wall assembly.
- No method for the selection of a representative weather year has been developed specifically for FT risk assessment.

- No comprehensive study to evaluate the FT damage risks of historic masonry brick walls under future climates

2.5.2. Research questions

Given the limited number of scientific publications, it is clear that there is a lack of research in systematically investigating the strategies and a need for developing design guideline to improve thermal performance of building envelopes in historical buildings without compromising their long-term durability. Therefore, the intent of this thesis is to answer the following questions:

1) Is it safe to internally insulate historic masonry walls?
2) How would masonry walls of buildings of historical significance perform under projected future climate loads of Canada when retrofitted with insulation to the interior?
3) Are existing methods for the selection of MRY adequate to accurately assess frost damage risk?
4) What would be the best strategies to safely retrofit historical solid masonry walls with interior insulation that are appropriate for their intended indoor climatic conditions, and environmental loads?
    - What type of insulation system should be used?
    - What is the safe and optimal insulation thickness?

Chapter 3. Methodology

One of the most challenging retrofitting procedures to investigate in respect to historic buildings are measures taken to improve the thermal efficiency of such buildings using “interior insulation”, where interior insulation refers to the installation of insulation products on the interior surface of the wall assembly. The selection of insulation materials for internal applications of historic masonry buildings should be approached with caution, as certain modern insulating materials may not be compatible with the unique properties of historic brick masonry walls. An improper choice of insulation product can lead to accelerated deterioration and irreversible damage to the masonry wall, undermining the very preservation efforts intended to protect these buildings having cultural and architectural significance. Thus, the aim of this research is to investigate strategies as may be used to retrofit historic walls with interior insulation by determining the optimal types of insulation of appropriate thickness for their intended environment without risk of damage to the exterior masonry wall. Consequently, it is imperative that an accurate method of evaluation be determined in respect to the influence of interior insulation on the risk of freeze-thaw damage to historic masonry walls in response to climate change. This could be achieved through a proper modelling of the wall assembly over the long-term using hygrothermal simulations tools. The results derived from simulations can provide a comprehensive understanding of how the use of internal insulation affects the moisture and thermal performance of historic masonry walls, such results ultimately guiding the development of effective preservation strategies that prioritize the resilience and long-term sustainability of historic brick masonry structures. It must, however, also be considered that undertaking simulations having many climate parameters, and thus, of high computational complexity, over an extended period of time, e.g., 30-year, necessarily incurs high computation time and as well, potentially elevated costs. Typically, a moisture reference year (MRY) is established that can accurately represent a climate over the long term and that, at the same time, allows for a correct evaluation of the moisture stress to which the building envelope is subjected over time. In consideration of this approach, the objective in this study was to assess the reliability of existing methods for the selection of an MRY. This included a comparison between the use of climate-based indices to that of simulation-based indices (regarded as the actual moisture performance of the masonry wall assembly) on the basis of the respective results from simulations. Thereafter, a parametric study was conducted, the results from which were used to develop a

framework for an accurate selection of a MRY, and that was considered to provide reliable results in respect to analyzing freeze-thaw damage of masonry walls.

To take into consideration the uncertainty in climate change effects and the variability of factors having the most influence on the FT damage response of masonry walls, in this study different climate realizations or climate runs, were included, each run comprised of 31 years of hourly historical and future climate data. As well, two wall geometries were adapted in this study: (1) a brick masonry wall, deemed to be an example of a historic masonry wall assembly, in its original state (ORG) – considered as the reference wall – and (2) an internally insulated brick masonry wall having three different types of internal insulation. The reference wall consisted of a typical 300mm historic brick masonry (corresponding to one full and a half brick) and 15 mm of gypsum plaster, as interior finish, as was commonly used in Canadian construction and typically found in the literature (CMHC, 2004; Ritchie, 1960; Sehizadeh and Ge, 2016). Retrofitted wall assemblies differed in regard to the type and thickness of insulation products, and generally comprised a layer of insulation, followed by steel studs and a gypsum board. A description of the common elements of the wall assemblies is given in Section 3.3. Simulations were performed using the hygrothermal simulation program DELPHIN 5, version 5.9.4. No sources were assumed, for either air leakage or rain leakage. Only a one-dimensional cross-section of both the reference wall and the retrofit walls were simulated. In the following sections, details are provided for the various different parameters required to undertake the simulations and assess the risk of freeze-thaw damage to the wall assemblies.

A concise overview is provided in Figure 3-1 of the methodology employed in this study. Some input and output parameters were different for each chapter of this thesis. Information on specific factors and assumptions used in the simulations is provided in the sections below.

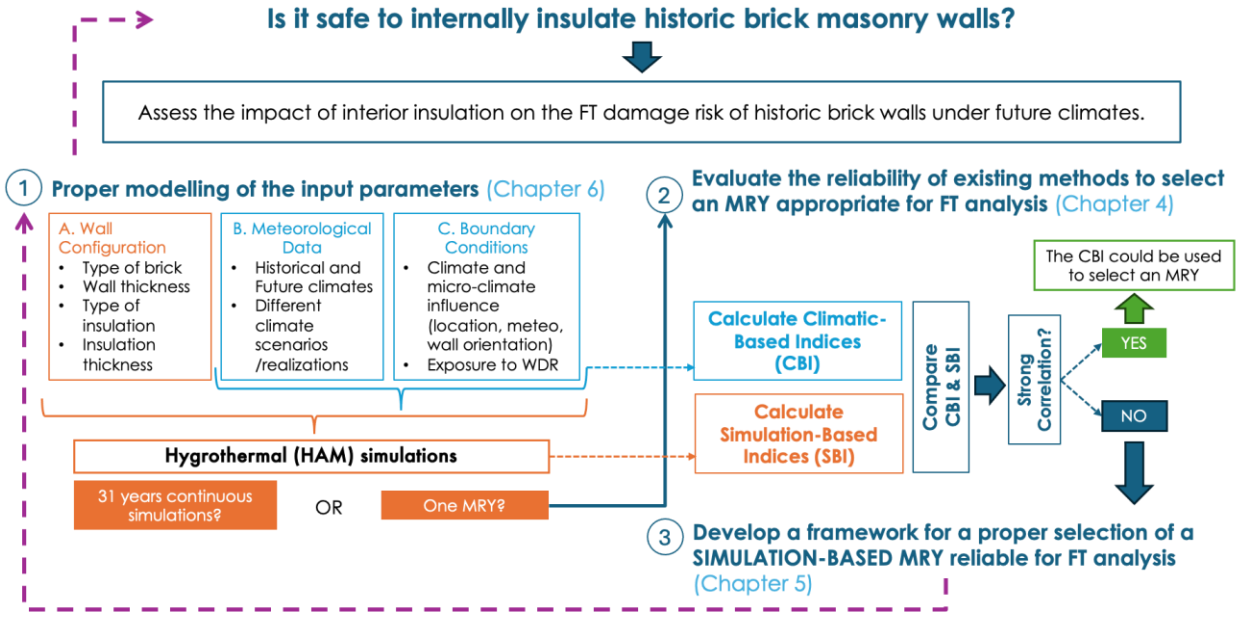

Figure 3-1. Proposed methodology to investigate the impact of internally insulating historic masonry walls.

3.1. City selection

In Chapter 4, two Canadian cities, belonging to two different climate zones, were selected to assess the freeze-thaw damage to historical masonry walls: Ottawa (ON) and Vancouver (BC). Their geographical locations, weather data (Figure 3-2) and respective climate characteristics are presented in Table 3-1. The Heating Degree-Days (HDD) and Moisture Index (MI) for Ottawa and Vancouver, respectively, are 4500 and 0.84, and 3100 and 1.93 (National Building Code of Canada (NBC)., 2020). It is to be noted that, only Ottawa was selected as an example, as described in Chapter 5 and Chapter 6, to develop and test the approach on whether it is safe to internally insulate historic brick under representative future MRY specific to freeze thaw damage.

Table 3-1. Characteristics of the selected cities (National Building Code of Canada, 2020).

City (Province)	Latitude	Longitude	Climate zone	TZ*	HDDD18*	MI*	Annual rain [mm]
Ottawa (ON)	45.25°	75.42°	6	-5	4500	0.84	750
Vancouver	49.28°	123.12°	5	-8	3100	1.93	1850

*HDD18: heating degree days below 18°C, TZ: time zone, MI: moisture index

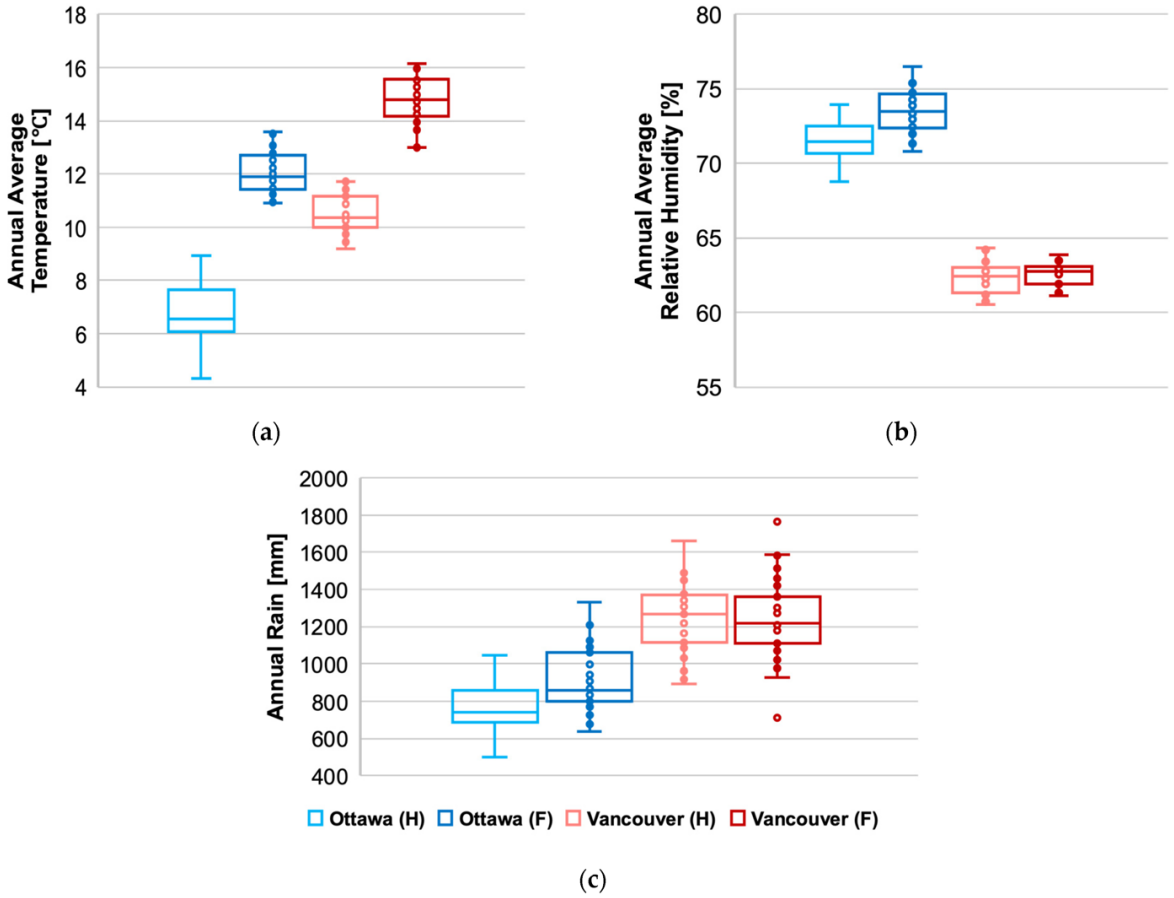

Figure 3-2. Comparison of (a) annual average temperature, (b) annual average relative humidity, and (c) annual rainfall, during the time periods of 1989–2016 (H) and 2062–2092 (F) in Ottawa and Vancouver.

3.2. Climate data

The meteorological, or weather data, was comprised of hourly climatic data for temperature, relative humidity, solar radiation, rain, wind velocity, and other pertinent climate parameters. They were provided by the National Research Council of Canada (NRC). Further, given the anticipated changing climate and the possible vulnerability of historical masonry buildings to such changes, it was essential to consider the resilience of these walls when exposed to loads as may occur in the future. The dataset was generated by dynamically downscaling future projections from the CanESM2 global climate model and thereafter bias-corrected (Gaur et al., 2019). The dataset comprised 15 realizations with variations in respect to their initial conditions, each of which included a continuous hourly time-series[2] of climate parameters for a baseline time-period spanning from 1986 to 2016 and 31-years of future time-periods, when a global warming of 2°C

[2] The full dataset can be accessed from: 10.17605/OSF.IO/UPFXJ.

and 3.5°C is expected to be reached in the future (Gaur et al., 2019). In this study, the RCP8.5 warming scenario was considered, which supposes that the temperature is expected to increase by 3.5°C, and assumed to occur between 2062 and 2092 (Environment and Climate Change Canada (ECCC), 2018). Information on the selection of the specific climate data (realizations/runs) used in the simulations will be provided in each chapter.

3.3. Wall assemblies

The hygrothermal simulation of a reference wall in its original state (ORG) and internally insulated retrofit wall assemblies (Figure 3-3) are described in this section. Chapter 4 emphasized the importance of initially assessing the reliability of existing climate indices to evaluate the risk to FT damage. Once a suitable indicator was determined, it formed the basis for carrying out further simulations to evaluate different retrofit strategies. And therefore, to represent a wall assembly that meets energy code requirements, simulations were undertaken, as described in Chapter 4 (Reliability of Existing Climate Indices in Assessing the Freeze-Thaw Damage Risk of Internally Insulated Masonry Walls), of a retrofitted wall having 100mm of Spray Foam Polyurethane (SPF) insulation (Straube et al., 2012). Thereafter, simulations were performed for three (3) different insulation systems: Spray Foam Polyurethane (SPF), Calcium Silicate (CaSi) adhered to the brick wall with 4mm glue mortar, and Mineral Wool (MW) with a vapour barrier. For each insulation system, three thicknesses were considered: 50, 100 and 200 mm. The total thermal resistance of the wall assemblies based on the insulation types and thicknesses is presented in Table 3-2. Also, for the retrofitted walls, empty steel studs were installed after the insulation material, because according to (Straube and Schumacher, 2007) the empty stud space is ideal for services distribution and allows the easy application of a drywall finish. This series of simulations were used in Chapter 5 and Chapter 6.

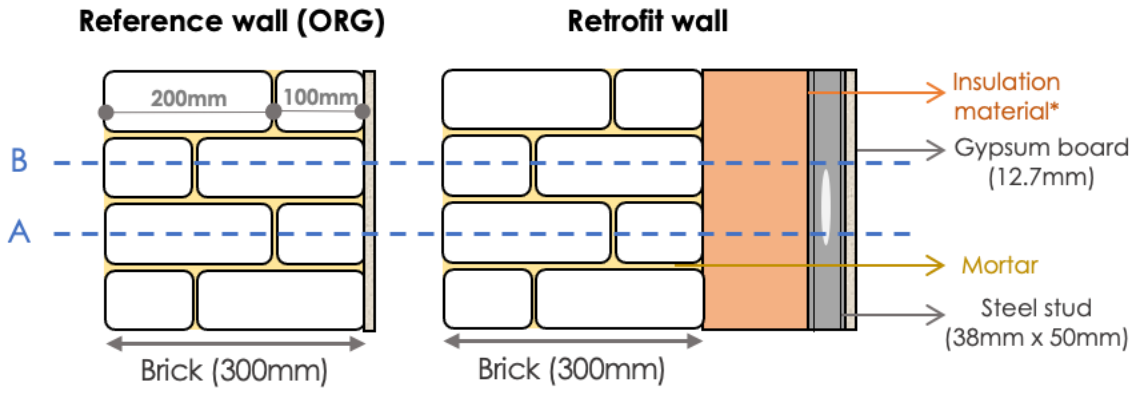

Figure 3-3. Configuration of typical brick masonry wall assemblies: reference wall (ORG) (top left), and internally insulated wall (top right).

Table 3-2. The total thermal resistance of the wall assemblies based on the insulation types and thicknesses.

Insulation material	Insulation thickness	Total R-value of the wall (m^2.K/W)
No insulation	0 mm	0.50
SPF	50 mm	2.50
	100 mm	4.20
	200 mm	7.65
MW	50 mm	2.00
	100 mm	3.25
	200 mm	5.75
CaSi	50 mm	1.60
	100 mm	2.40
	200 mm	4.00

3.4. Settings in HAM simulations

3.4.1. Overview of the simulation tool - DELPHIN

In this study, simulations were performed using DELPHIN 5, v5.9.4. The DELPHIN 5 (Coupled Heat, Air, Moisture and Pollutant Simulation in Building Envelope Systems) was first developed at Dresden Technical University by John Grunewald in 1997 (Grunewald, 1997). It has been expanded to include air flow (Grunewald and Nicolai, 2006; Langmans et al., 2011), pollutant transport (Xu et al., 2009), and salt transport (Nicolai, 2007). Scheffler utilized it as a platform for developing material and transport models related to moisture transfer (Scheffler, 2008), while Ochs employed it for non-linear thermal storage and transportation purposes (Ochs, 2010). The development of this simulation software was possible given the financial support obtained from various research grants including those from the U.S. Environmental Protection Agency, U.S. Department of Energy, Syracuse Center of Excellence in Energy and Environmental Systems, EQS-STAR Center/New York State Office of Science, Technology and Academic Research as well

as Syracuse University. The maintenance responsibility for this software lies with the Institute for Building Climatology at Faculty of Architecture, Technical University Dresden located in Germany. Its purpose is to simulate the simultaneous transport processes involving heat, air, and matter (e.g., water, vapour, salts and pollutants) within porous building materials. The model is capable of solving one- or two-dimensional problems. It has been successfully verified using the HAMSTAD Benchmarks, numbered 1 to 5 (Nicolai et al., 2013a; Sontag et al., 2013a). The model utilizes either the complete sorption isotherm or the water retention function to characterize the drying behavior of a material. Material properties are determined based on volumetric moisture content and temperature. Climate data is inputted as a separate file for each climate variable. A notable aspect of DELPHIN is its capacity to manage the deposition of wind-driven rain on building exterior surfaces, solar radiation, air leakage, as well as sources of heat and moisture within its boundary conditions. Additionally, it can account for cavity walls; in cases having wall assemblies with ventilated cavities, the effect of airflow on heat and moisture transfer can be addressed through the use of an air exchange rate through, or an air flow rate in the cavity. DELPHIN can be used in a variety of different applications, such as: the evaluation of thermal bridging, including assessment of potential hygrothermal issues like surface condensation and interstitial condensation; the evaluation of external and internal insulation; the assessment of drying problems and mould growth risks, as well as the evaluation of ventilated roofs and ventilated facades.

3.4.2. Material properties

The following material properties were defined for each of the wall assembly components:

- Density
- Specific heat capacity
- Thermal conductivity
- Open porosity
- Water absorption coefficient
- Vapor resistance factor
- Liquid water conductivity

All material properties are listed in Table 3-3. The selection of the historic brick material differed through the chapters of this thesis, i.e. the Old Building Brick (outer brick 1) was selected in Chapter 4. In Chapter 5, the Old Building Brick Persiusspeicher was selected from the DELPHIN materials database given that it has similar properties to that of the exterior reclaimed brick "ERUL" found in Canada and measured by Aldabibi (Aldabibi et al., 2022). This brick material is considered typical of that used in Canada, and has average FT resistance properties, with a critical degree of saturation (S_{crit}) of 55% (measured experimentally). In Chapter 6, both "the Old Building Brick Persiusspeicher" and "Old Building Brick Dresden ZH" were selected from the DELPHIN material database for comparison, as they both have similar properties to the exterior reclaimed bricks "ERUL" and "ERUH", respectively, found in Canada and also measured by Aldabibi (Aldabibi et al., 2022).

Table 3-3. Material properties of the historic brick (DELPHIN material database)

Material	Density (kg/m^3)	Specific heat (J/kg.K)	Thermal conductivity (W/mK)	Open porosity (m^3/m^3)	A_w ($kg/m^2.s^5$)	μ (-)	Kl (s)	S_{crit} (%)
Old Building Brick (outer brick 1)	1842.5	772.2	0.7975	0.3047	0.0669	37.56	2×10^{-8}	25%
Old Building Brick Persiusspeicher	2014.9	775.2	0.8682	0.2396	0.0457	139.5	4.92×10^{-9}	55%
Old Building Brick Dresden ZH	1972	794	0.30	0.659	0.258	12.031	2.81×10^{-9}	45%
Plaster *	840	1380	0.588	0.0890	-	73.33	10^{-16}	
Mortar (historic)	1568	488	0.5815	0.4083	0.175	11.37	9.65×10^{-9}	
Closed-cell Spray Foam Polyurethane (SPF)	45	1500	0.029	0.92	0.0001	104		
Calcium Silicate (CaSi)	225	1129	0.063	0.913	0.726	4.234		
Mineral Wool (MW) + VB**	67	840	0.04	0.92	-	1	-	

A: Water absorption coefficient; μ: Vapor resistance factor; Kl: Liquid water conductivity
*** Plaster was only used inboard in the case of the original wall (reference wall).**
**** VB: Vapour barrier.**

3.4.3. Boundary conditions

3.4.3.1. INDOOR BOUNDARY CONDITIONS

The indoor temperature and relative humidity conditions were set to 21°C and 50%, respectively, assuming that the buildings were equipped with air conditioning and dehumidification. The indoor vapour diffusion and the heat conduction coefficient were set to 1.52×10^{-8} s/m and

8 W/m^{2}K (convective heat transfer coefficient: 2.5 W/m^{2}K and radiative heat transfer coefficient: 5.5 W/m^{2}K) respectively, and in accordance to that provided in EN ISO 6946 (2017).

3.4.3.2. OUTDOOR BOUNDARY CONDITIONS

Outdoor boundary conditions included heat conduction, vapour diffusion, wind driven rain, shortwave and longwave radiation. To compute the transfer coefficient, the boundary layer method was selected in DELPHIN. The exterior building surface long-wave emission coefficient was set to 0.9. The outdoor convective heat exchange coefficient (h_{ce}) and convective vapour diffusion coefficient (β_v) were calculated using Equations (3.1) and (3.2) (EN ISO 6946, 2017). In Equation (3.2), the value of (β_v) was computed using the convective heat exchange coefficient (h_{ce}) and the Lewis relation (Incropera et al., 2015).

$$h_{ce} = 4 + 4 \cdot v \quad \textbf{(3.1)}$$

$$\beta_v = 2.44 \cdot 10^{-8} + 2.44 \cdot 10^{-8} \cdot v \quad \textbf{(3.2)}$$

where, v – the wind speed, (m/s)

The reflection coefficient of the surrounding ground (albedo) was set to 0.2 and the value for the short-wave absorptance coefficient of the masonry cladding surface was 0.6.

3.4.3.3. INITIAL CONDITIONS

For all components of the wall assembly, the initial conditions in respect to relative humidity and temperature were set, respectively, to 50% RH and 21°C.

3.4.3.4. CRITICAL LOCATION IN WALL ASSEMBLY AT RISK OF FT DAMAGE

The assessment of freeze-thaw damage risk in masonry walls is crucial for ensuring the durability and longevity of building envelopes, especially in cold climates. It has been observed that the risk of FT damage is higher on the outer layer of the masonry walls due to exposure to varying temperatures and moisture levels. Therefore, to avoid the direct effect of climatic parameters, a point located at 5mm from the exterior surface of brick is commonly considered in the literature as the critical investigation point for FT related problems (Zhou et al., 2017).

3.4.3.5. FREEZE-THAW DAMAGE PERFORMANCE INDICATORS

In Chapter 4, different FT performance indicators were used to assess the risk to FT damage: the Modified Winter Index (MWI), the number of Indicative Freeze-Thaw Cycles (IFTC), the Freeze-

Thaw Damage Risk index (FTDR), as well as the number of freeze-thaw cycles outputted from Delphin (FTCd). More details about the indicators can be found in Section 4.2.1. In Chapter 5 and Chapter 6, the risk to freeze-thaw damage was computed using the number of critical freeze-thaw cycles obtained from DELPHIN (FTCd) as well as the number of critical freeze-thaw cycles (FTCcrit) calculated manually. DELPHIN takes ice formation into account by assuming the instantaneous equilibrium between the three phases (vapor, liquid, and ice), and by applying a freezing point depression whilst assuming that the pore space fills from the smallest to the largest pore and that ice crystalizes outside of the liquid phase (Nicolai et al., 2013b; Sontag et al., 2013b). The use of this model permits investigating whether the moisture content is sufficiently high to fill pores where water could freeze. One FT cycle was counted when the ice volume rate (IVR), the ratio of the volume of ice formed, to that of the pore volume. is lower than a minimum value. In this study, the minimum IVR value is assumed to be equal to the S_{crit} of the masonry material. The value for the critical number of freeze-thaw cycles, FTCcrit, is calculated when two conditions exist concurrently: 1) the moisture content of the material exceeds a critical threshold corresponding to the material's critical saturation degree (S_{crit}), and; 2) the temperature of the material is below freezing point of water, assumed to be 0°C (Sedlbauer and Künzel, 2000; van Aarle et al., 2015).

3.5. Assumptions for undertaking hygrothermal simulations

The hygrothermal simulations are based on the following assumptions:

- There is no transfer of mass or energy through the upper and lower boundaries of the geometry.
- No sources were assumed for either air leakage or rain leakage.
- All materials layers are presumed to be in ideal contact with each other.
- Throughout the simulation period, it is assumed that the material properties of different layers in the wall assembly remain consistent regardless of their thickness.

Chapter 4. Reliability of Existing Climate Indices in Assessing the Freeze-Thaw Damage Risk of Internally Insulated Masonry Walls[3]

4.1. Introduction

To evaluate the moisture risks of building components, HAM simulation tools are frequently utilized. However, conducting simulations and managing numerous climate parameters for an extended period results in significant computational time and expenses. One approach to mitigate these costs is to choose a year that can effectively depict long-term climate conditions, enabling accurate assessment of the moisture stress experienced by the building envelope over time. This specified year is referred to as a moisture reference year. Several methods have been developed and utilized in the past to define moisture reference years. The most common ones include the Moisture Index, Severity Index, and Climatic Index - introduced in Chapter 3. These approaches rank the years based on their moisture severity, helping in the selection of MRYs.

Some studies have explored the impact of climate change on the durability of building envelopes, but few focus on retrofitted buildings in Canadian cold climates. It is evident from a review of literature that the effect of future climate varies across different climates and building envelope constructions. While several methods for selecting an MRY exist, they mainly assess the risk of damage from mold growth, and no specific method has been developed to evaluate freeze-thaw damage risk. The reliability of these methods in assessing freeze-thaw damage remains uninvestigated.

The primary objective of this chapter is to evaluate the reliability of the currently used climate-based indices in selecting a moisture reference year to assess the freeze-thaw damage risk of an internally insulated solid brick wall. This would be achieved by comparing the ranking of the years

[3] The content of this chapter is published in the journal paper "*Sahyoun, S., Ge, H., Lacasse, M.A., and Defo, M. (2021). Reliability of Existing Climate Indices in Assessing the Freeze-Thaw Damage Risk of Internally Insulated Masonry Walls*". Buildings, 11 (10), 482. https://doi.org/10.3390/buildings11100482. The abstract from the original paper is excluded in this chapter to avoid duplication. Additionally, details such as wall assemblies, climate-based index, model settings that were included in the original paper can be found in Chapter 3 – Methodology.

determined using climatic indices with that ranking based on results of HAM simulations, regarded as the reference performance. This section also intends to investigate the effect of climate change on the freeze-thaw damage risk of internally insulated brick masonry walls of buildings located in different Canadian cities.

4.2. Methodology

To address the objectives of this study, the methodology employed includes the use of hygrothermal simulations of an old brick masonry wall assembly configured: (1) in its original configuration (base wall); and (2) when insulation is added to the interior wythe of its masonry (retrofitted wall). The walls are assumed to be located in two Canadian cities (i.e., Ottawa and Vancouver), and simulations are carried out under historical and projected future climates when global warming of 3.5 °C is expected to be reached at the end of the century. Moreover, two wall orientations were considered in this study: (1) the orientation with the least solar radiation – North; (2) the orientation with the highest amount of wind-driven rain. In total, 496 simulations were carried out. The methodology followed in this chapter is illustrated in Figure 4-1.

Four different climate-based indices, commonly used in the literature, were used for the selection of MRYs and included: the amount of Wind-Driven Rain (WDR), the Moisture Index (MI), the Climatic Index (CI), and the Severity Index (Isev). The computation procedure of these indices can be found in Section 2.4. Part of these climate-based indices were introduced in (Sahyoun et al., 2020). Four freeze-thaw performance indicators were calculated based on output from hygrothermal simulations, i.e., response-based indices were used to evaluate the potential risk of freeze-thaw damage. These are comprised of the Modified Winter Index (MWI), Indicative Freeze-Thaw Cycles (IFTC), Freeze-Thaw Damage Risk (FTDR) and, the number of Freeze-Thaw cycles output from Delphin (FTCd). These indices were calculated for each simulated case, and MRYs were then chosen based on these four indicators. Three methods of comparison amongst MRYs were used in the analysis to evaluate the reliability of climate-based indices in selecting MRYs and were selected based on values obtained for climate-based indices and response-based indices derived from simulations. These included: matching year method, scatter plots method, and the Salonvara et al. method (Salonvaara et al., 2010).

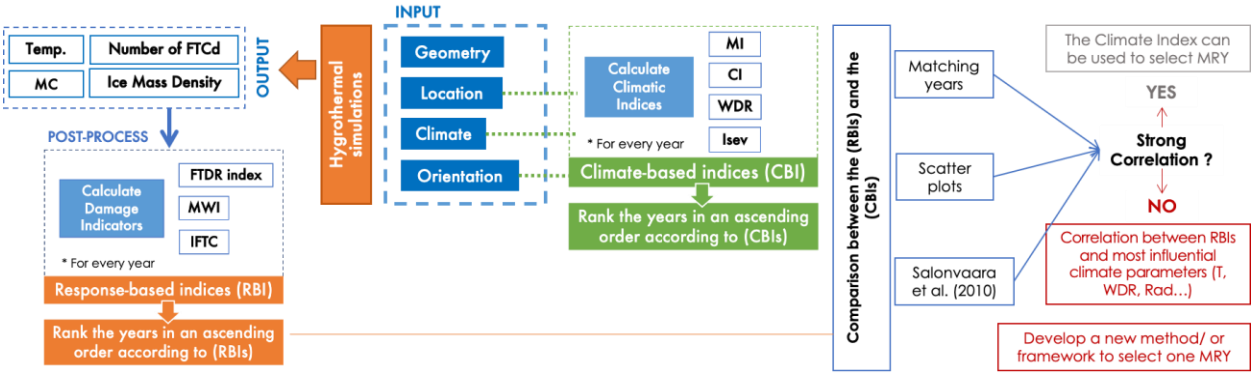

Figure 4-1. Methodology to assess the reliability of existing climate-based indices.

4.2.1. Simulation-based indices

The FT performance indicators used in this study are the Modified Winter Index (MWI), the number of Indicative Freeze-Thaw Cycles (IFTC), the Freeze-Thaw Damage Risk index (FTDR), as well as the number of freeze-thaw cycles outputted from Delphin (FTCd).

4.2.1.1. THE MODIFIED WINTER INDEX (MWI)

The Modified Winter Index (MWI) (Kočí et al., 2017) utilizes hourly values of MC instead of RH and calculates the level of severity for that instance where the MC is higher than the critical level (Equation (4.1)).

$$MWI = \sum_{i=1}^{8760} (T_L - T_i)(w_i - w_L) \qquad for\ [T_i < T_L \cap\ w_i > w_L] \tag{4.1}$$

where,

T_L—the critical value of temperature, (K)

w_L—the critical value of moisture content, (% m^3/m^3)

T_i—the hourly values of temperature at the investigation point, (K)

w_i—the hourly values of moisture content at the investigation point (% m^3/m^3)

Values of (S_{crit}) equal to 0.25, 0.45, 0.55 and 0.8 were considered throughout the chapters of this thesis. Each chapter will have a description of the S_{crit} selection made. Moreover, freezing is assumed to occur at 0 °C within the material to allow comparison between different FT performance indicators.

4.2.1.2. INDICATIVE FREEZE-THAW CYCLES (IFTC) NUMBER

The number of indicative freeze-thaw cycles (IFTC) is another performance indicator developed by Koci et al. (Kočí et al., 2017), where, in addition to meeting the previous conditions of temperature and moisture content, a freeze-thaw cycle is counted when the freezing lasts at least 2 hours and is followed by at least 2 hours of thawing. The same parameters set in the previous index (MWI) were also used here.

4.2.1.3. FREEZE-THAW DAMAGE RISK (FTDR) INDEX

The freeze-thaw damage risk index (FTDR) (Pachauri and Meyer, 2013) is described as "the accumulation of the difference between the maximum and the minimum saturation degree of ice content in each complete or incomplete freeze-thaw cycle", and it can be calculated using Equation (4.2).

$$FTDR\ index = \sum_{cycle} \left(S_{ice,max} - S_{ice,min}\right); \quad for\ \left(S_{ice,max} - S_{ice,min}\right) > 0.05 \tag{4.2}$$

where,

S_{ice} — the saturation degree of ice content (which is the ratio between the ice mass density and the total moisture content).

One complete FTC is the process of ice formation in the porous material and then its total melting. Whereas an incomplete FTC occurs when the freezing activity re-starts prior to the termination of the thawing process. This means that an incomplete FTC is counted after the ice is formed, and the ice content starts decreasing—but before it reaches zero—the ice content increases again. Zhou et al. (Zhou et al., 2017) concluded that incomplete FTC would potentially increase the risk of freeze-thaw damage. The FTDR index is calculated for each complete FTC and incomplete FTC. A value of 0.05 is introduced as a threshold neglecting the effect of FTCs having a small variation in ice content. The greater the value of the FTDR Index, the greater is the risk of freeze-thaw damage.

4.2.1.4. NUMBER OF CRITICAL FREEZE-THAW CYCLES – DELPHIN OUTPUT (FTCd)

Similar to the IFTC, DELPHIN has an integrated model that counts the number of critical FT cycles. DELPHIN takes ice formation into account by assuming the instantaneous equilibrium between the three phases (vapor, liquid, and ice), and by applying a freezing point depression whilst assuming that the pore space fills from the smallest to the largest pore and that ice crystalizes

outside of the liquid phase (Sontag et al., 2013b). The use of this model permits investigating whether the moisture content is sufficiently high to fill pores where water could freeze.

4.2.2. Setting in HAM simulations

Two wall assemblies were evaluated in this study: a solid masonry wall assembly in its original state and a retrofit of the same solid masonry wall assembly with 100 mm (4 inches) of spray polyurethane foam (SPF) (Straube et al., 2012). The simulations were performed for a one-dimensional cross-section of the base wall and the retrofit wall. The material properties of historical brick (Old Building Brick – outer brick 1) were taken from the database in Delphin as listed in Table 3-3.

The wall orientation facing North and the one receiving the highest amount of annual wind-driven rain calculated according to ASHRAE (ANSI/ASHRAE, 2021) were both selected for simulations. To determine this critical orientation, an analysis of the prevailing wind direction (during all hours and rain hours only) and the driven-rain index was performed for historical and future data periods. Using the airfield WDR index (I_A) (Equation (4.3)) (EN ISO 15927-3, 2009), the wall orientation with the most severe WDR intensity was 202.5° and 157.5° from the North for Ottawa and Vancouver, respectively (Table 3-1 and Figure 4-2).

$$I_A = \frac{2}{9} \sum v \times r^{8/9} \times \cos(D - \theta) \quad \textbf{(4.3)}$$

where,

v—the hourly mean wind speed, (m/s)

r—the hourly rainfall, (mm)

D—the hourly mean wind direction from North, (°)

θ—the wall orientation relative to the north.

The summation is calculated for all hours during which $cos\ (D - \theta)$ is positive.

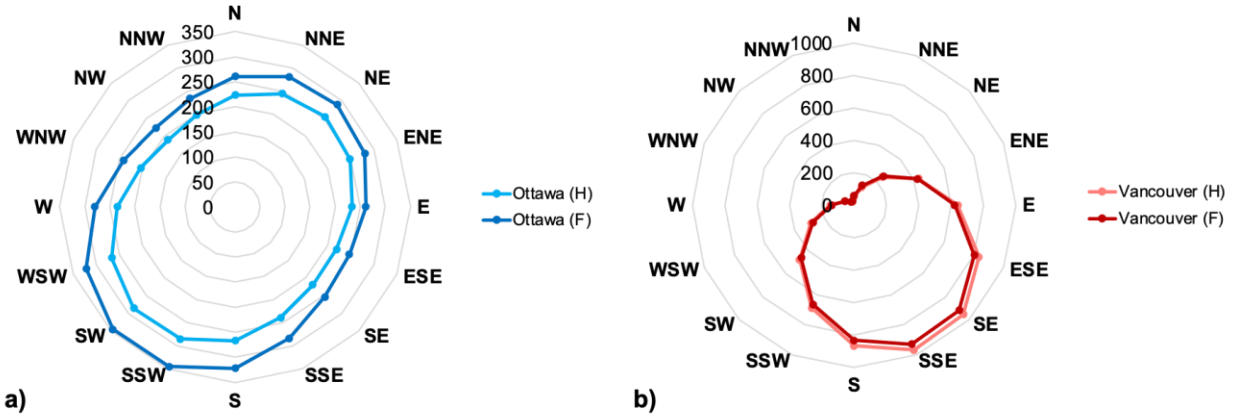

Figure 4-2. Annual average driven-rain index for (a) Ottawa and (b) Vancouver over historical and future time periods.

4.3. Results and discussion

4.3.1. Comparison between Climate-Based Indices and Response-Based Indices

A moisture reference year can be selected amongst the most severe years ranked according to climate-based indices. However, for an MRY to be representative and reliable, it should deliver consistent performance evaluations as that obtained from the actual hygrothermal performance. Using scatter plots, the capability of the climate-based indices in predicting the response of an internally retrofitted solid masonry wall was first evaluated. The values of climate-based indices were calculated for different cities, orientations, and climates and were compared to response-based indices. Besides, the coefficient of determination R^2 was computed for comparison.

In general, results in Table 4-1 show that the correlation between the climate-based indices and the response-based indices is very weak (R^2 is found less than 5% for most of the cases). This indicates that climate-based indices alone do not represent the actual performance of the walls, and therefore mis-assess the potential risk to freeze-thaw. However, for walls-oriented North under a historical climate in Ottawa, the climate-based indices are found to have a better correlation with the FTDR index. For a solid masonry wall in its original condition, R^2 varied between 46% and 58% and was highest for Isev. As for the retrofitted wall, the correlation between the indices was less: R^2 varied between 28% and 45% and was highest for MI.

Table 4-1. Correlation between climate-based and response-based indices for the two orientations N and WDR of each wall: original solid masonry wall (Base wall) and internally retrofitted wall (Retrofit) located in Ottawa and Vancouver. The highest values per index and climate are marked in bold.

City	Wall	Orientation	Indicator	Historical				Future			
				MWI	FTCd	IFTC	FTDR	MWI	FTCd	IFTC	FTDR
Ottawa	Base	North	CI	0.0458	0.1416	0.0687	**0.5181**	0.0221	0.0188	0.0769	0.067
			WDR	0.0321	0.1353	0.0621	**0.5276**	0.1207	0.1034	0.0688	**0.2776**
			MI	0.0486	0.0927	0.1414	**0.4629**	0.0316	0.0001	0.0076	**0.1479**
			Isev	0.0969	0.1144	0.1462	**0.5877**	0.1419	0.0619	0.0331	**0.2823**
		Prevailing WDR orientation	CI	0.0341	0.0248	0.1407	**0.3393**	**0.2573**	0.1953	0.1712	0.2343
			WDR	0.0272	0.0435	0.2148	**0.3511**	**0.2225**	0.1804	0.2192	0.2157
			MI	0.0005	0.004	0.0436	0.0513	**0.1918**	0.1433	0.0343	0.1831
			Isev	0.0009	0.0023	0.0441	0.0164	0.0581	0.0329	0.0001	0.0014
	Retrofit	North	CI	0.0546	0.121	0.0738	**0.3674**	0.0056	0.0226	0.0072	0.0635
			WDR	0.0394	0.1069	0.0612	**0.3602**	0.1307	**0.2164**	0.1861	0.0336
			MI	0.0395	0.1945	0.2241	**0.4569**	0.0246	0.081	0.0589	0.0826
			Isev	0.0719	0.1039	0.1085	**0.2866**	0.1421	**0.2159**	0.1827	0.0462
		Prevailing WDR orientation	CI	0.0593	0.1474	**0.3075**	0.001	0.0898	0.0013	0.0393	0.0434
			WDR	0.0456	0.1719	**0.3485**	0.002	0.0723	0.004	0.039	0.0346
			MI	0.003	0	0.0056	0.0334	0.0842	0.0003	0.0563	0.0635
			Isev	0.0005	0.0075	0.0126	0	0.0255	0.0295	0.0068	0.0164
Vancouver	Base	Prevailing WDR orientation	CI	0.0699	0.1235	0.1231	0.0015	0.0028	0.0396	0.02	0.0652
			WDR	0.0568	0.1122	0.1139	0.0009	0.0009	0.0153	0.0036	0.0963
			MI	0.026	0.1514	0.1301	0.0051	0.0054	**0.1213**	0.0746	0.0052
			Isev	0.1324	0.1547	**0.1998**	0.0377	0.2233	0.335	**0.2041**	0.0696
	Retrofit		CI	0.0909	0.0287	0.0372	0.0012	0.01	0.0531	0.0497	0.0251
			WDR	0.0536	0.0241	0.0275	0.0013	0.0038	0.024	0.0212	0.0532
			MI	**0.1934**	0.0501	0.0806	0.0075	0.0224	0.0989	0.0938	0.0012
			Isev	0.1653	0.1958	**0.2154**	0.1119	**0.2795**	0.1407	0.1387	0.038

Since in the majority of the cases the climate-based indices have failed to represent the actual performance of the walls, although the correlation between the climate-based indices and FTDR

was found relatively good in a few cases compared to other indices, further investigation was carried out based on the indices' ability in properly ranking years according to their severity. The climate-based indices calculated for 31 years in each time period were first ranked from highest to lowest. To verify whether the ranking of these years was indeed representative of the actual severity of the risk of frost damage, these years were also ranked using response-based indices. Three methods were used to evaluate whether the climate-based indices and the response-based indices lead to a similar ranking: i.e., the number of matching year method, scatter plots (where the R^2 of the average per index is computed), and the Salonvaara et al. method (Salonvaara et al., 2010). This would indicate the reliability of a climate-based method in ranking and selecting MRYs for freeze-thaw risk assessment. In addition, for the selected MRY to be representative, it should be applicable to a series of different situations—and not only for a few particular cases. Thus, the years' ranking during historical and future periods was studied for different indices and orientations.

4.3.1.1. NUMBER OF MATCHING YEARS

This method of comparison was first applied in an attempt to count the number of matchings between the years ranked using the response-based indices (response-based being regarded as providing the correct value of actual performance) and those ranked according to climate-based indices. The higher the number of matching years between climate-based and response-based indices, the more reliable the climate-based indices are in representing the actual order (ranking) of the years; and therefore, the higher possibility for a more accurate selection of an MRY, depending on the selection criteria of MRY.

At first, this method was applied to the entire duration of the time period (i.e., 31 years) for both historical and future climates. The same method was then used only for the three most severe years, i.e., the first three years with the highest index ranked according to the values obtained for the climate-based and response-based indices. Results for Vancouver were provided only for a wall facing the direction of highest wind-driven rain because a north-facing wall showed almost no risk to freeze-thaw damage (because the North orientation receives almost no WDR, refer to Figure 4-2), and therefore, values of indicators were zero, or close to zero, for most of the cases.

In general, the number of matching years between the climate-based indices and the response-based indices was found to be relatively small for all compared scenarios under both historical and

future climates. For instance, the matching number was found, for the most part, between zero and two (2) and reached a maximum of four (4) years for a few scenarios in Ottawa—a base wall facing prevailing WDR direction under historical climate (Figure 4-3a) and future climate, and a retrofit wall facing North under future (Figure 4-3b) and historical climate. In these cases, it is not possible to draw a general conclusion on which climate-based index provides a better ranking with the response-based indices as each scenario leads to different results. For instance, the best match (4 out of 31 years) was ranked according to the moisture index (MI) and the IFTC—for a base wall facing prevailing WDR direction under historical climate (Figure 4-3a). However, the same number of matching years was achieved by the ranking of WDR and MWI indices—for a retrofit wall facing North under future climate (Figure 4-3b) and the ranking of the severity index (Isev) and FTDR for a retrofit wall facing North under historical climate.

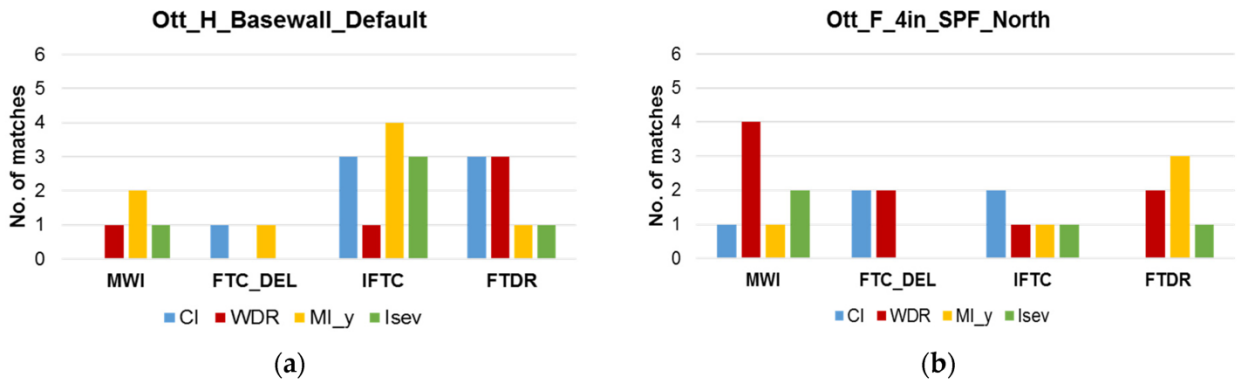

Figure 4-3. Number of matching years between climate-based indices (legend) and the response-based indices (x-axis) for (a) a base wall facing prevailing WDR orientation under historical climate, and (b) a retrofit wall facing North under future climate, in Ottawa.

A similar comparison was completed for the ranking of different indices for the three most severe years only (the first three years ranked based on each index). Results showed that in most of the cases the number of matching years was found to be zero or one (1) out of three.

For Vancouver, the number of matching years was also very low; with a maximum of four years (4) out of 31 when comparing within the entire time period, and only one (1) matching year when comparing the ranking of the three most severe years.

This method of the comparison showed that the ranking of years based on climate-based indices does not represent the same ranking as that based on the walls' performance; meaning that the years selected based on climate-based indices alone do not represent the actual frost damage risk

to masonry wall assemblies. The ranking using neither different climate-based indices nor response-based indices is consistent amongst different scenarios, i.e., orientation, location, and time periods. Therefore, relying on counting the number of matching years between the different indices alone is not likely sufficient to provide a consistent evaluation of the correlation between the climate-based indices and freeze-thaw performance indicators.

4.3.1.2. SCATTER PLOTS

The method using scatter plots is intended to permit comparison of the correlation between the actual performance indicator, which is the response-based indices of ranked years, and the corresponding response-based indices of the ranked years based on the climate-based indices ranking. This method allows evaluating the ranking performance of climate-based indices, which provides an indication of how reliable climate-based indices represent the risk to FT damage, i.e., the risk as determined by response-based indices of the wall assemblies. As such, the response-based indices values are given in ascending order on the *x*-axis of the plot, and on the *y*-axis, are the values of the response-based index corresponding to the year ranked in ascending order according to the climate-based indices. The coefficient of determination R^2 is also computed for comparison.

Figure 4-4 and Table 4-2 show the correlation between the actual performance of the walls, using an FTDR index, and the corresponding FTDR values based on the ranking of climate-based indices for a masonry building located in Ottawa. If climate-based indices rank the years accurately, all dots should fall on a straight line and R^2 should be 1. Results showed that the ranking performance of climate-based indices is generally poor and varies with the wall types, orientation, and climate scenarios and that the FTDR index is a better indicator of risk to FT damage compared to other response-based indices. For walls facing the prevailing WDR orientation in Ottawa, the highest R^2 of 0.39 was achieved using WDR for the reference wall under historical climate. In general, WDR and CI indices provided better ranking performance as compared to the other indices, which have R^2 close to zero for all cases. The ranking performance of climate-based indices was found better for the reference wall than the retrofit wall, in which all climate-based indices have R^2 close to zero. For a north-facing wall in Ottawa (Figure 4-4), the ranking performance of climate-based indices is slightly better than walls facing the prevailing WDR orientation, however, the results are not consistent. The correlation between the actual performance using the FTDR index and its

corresponding index based on climate-based indices' ranking varied between different scenarios: under a historical climate, the FTDR index had a better correlation with the CI, WDR, and Isev indices, having the highest R^2 value of 0.49 for CI. However, under a future climate, an improved correlation for WDR (R^2 of 0.38) and Isev (R^2 of 0.35) indices was found. Similar to walls facing the prevailing WDR direction, under future climate for the retrofitted walls, all climate-based indices fail to rank the years reliably, with R^2 less than 0.1. As shown in Table 4-2, the ranking performance of climate-based indices is very poor when other response-based indices are used, with $R^2 < 10\%$.

The analysis for Vancouver showed the ranking performance of climate-based indices is very poor for all cases with $R^2 < 0.01$ and therefore, the results were not provided in this study.

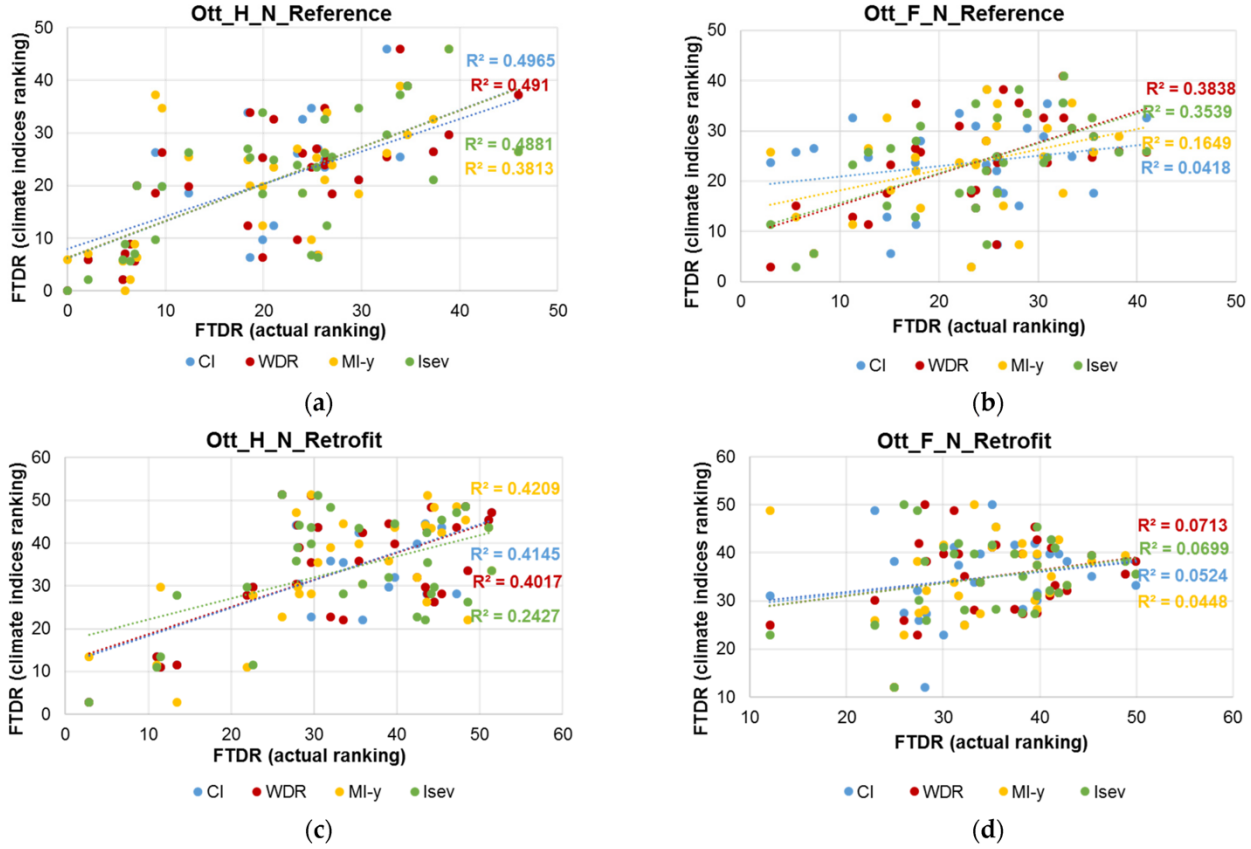

Figure 4-4. Correlation between FTDR values based on the actual ranking and FTDR values based on the climatic indices ranking—for (a) a reference wall under historical period, (b) a reference wall under future period, (c) a retrofit wall under historical period, (c) a retrofit wall under historical period, and (d) a retrofit wall under future period, all facing North orientation in Ottawa.

Table 4-2. The correlation coefficient (R2) between response-based indices values based on their actual ranking, and their corresponding values based on climate-based indices ranking—for a North and WDR oriented reference wall and retrofit wall under historical and future periods in Ottawa. The highest values per index and climate are marked in bold.

Wall	Orientation	Indicator	Historical				Future			
			MWI	FTCd	IFTC	FTDR	MWI	FTCd	IFTC	FTDR
Base	North	CI	0.0004	0.0646	0.0012	**0.4965**	0.1069	0.0095	0.026	0.0418
		WDR	0.0013	0.0609	0.0012	**0.491**	0.0554	0.0694	0.0278	**0.3838**
		MI	0.0251	0.0936	0.0535	**0.3813**	0.01	0	0.001	**0.1649**
		Isev	0.0398	0.1226	0.0455	**0.4881**	0.0671	0.0531	0.035	**0.3539**
	Prevailing WDR orientation	CI	0	0.011	0.1609	**0.3325**	**0.3678**	0.2198	0.1502	0.2326
		WDR	0	0.0208	0.1471	**0.3907**	**0.3561**	0.1553	0.1585	0.2239
		MI	0.0018	0	0.021	0.0536	**0.2754**	0.1168	0.0241	0.1051
		Isev	0.0014	0.0045	0.0055	0.015	0.1873	0.0493	0	0.0031
Retrofit	North	CI	0.0056	0.0764	0.0139	**0.4145**	0.0929	0.0359	0.0205	0.0524
		WDR	0.0019	0.0711	0.016	**0.4017**	0.0287	0.224	0.2024	0.0713
		MI	0.0119	0.1257	0.1249	**0.4209**	0.0076	0.0768	0.0546	0.0448
		Isev	0.0067	0.061	0.045	**0.2427**	0.0443	0.2394	0.195	0.0699
	Prevailing WDR orientation	CI	0.0074	0.1665	**0.3484**	0.0031	0.1138	0	0.0395	0.0416
		WDR	0.0052	0.1168	**0.3209**	0.0021	0.1124	0.002	0.0336	0.0314
		MI	0.0074	0.0002	0.0056	0.035	0.1005	0.0003	0.0497	0.0416
		Isev	0.0018	0.0071	0.004	0.0123	0.0503	0.0157	0.0102	0.0343

Seasonal Analysis

Since it is more likely for frost damage to occur during the winter season, the same scatter plot method has been applied to the months experiencing freeze-thaw cycles (November to April) to investigate whether this will result in a better correlation. The climate-based indices (Isev and WDR) and the response-based indices were calculated only for this period, and results are plotted in Figure 4-5. Comparing the coefficient of determination (R^2) shown in Figure 4-4 and Figure 4-5, it was noticed that the seasonal calculation did not improve the correlation between the indices. For instance, when WDR was used to rank the years, R^2 dropped from 49% to 32%, and from 38% to 35%, for a reference wall under historical and future climate, respectively. Besides,

the decrease in the correlation between FTDR and Isev was even more significant; with R^2 decreasing from 49% to 10% under a historical climate, and from 35% to 10% under a future climate.

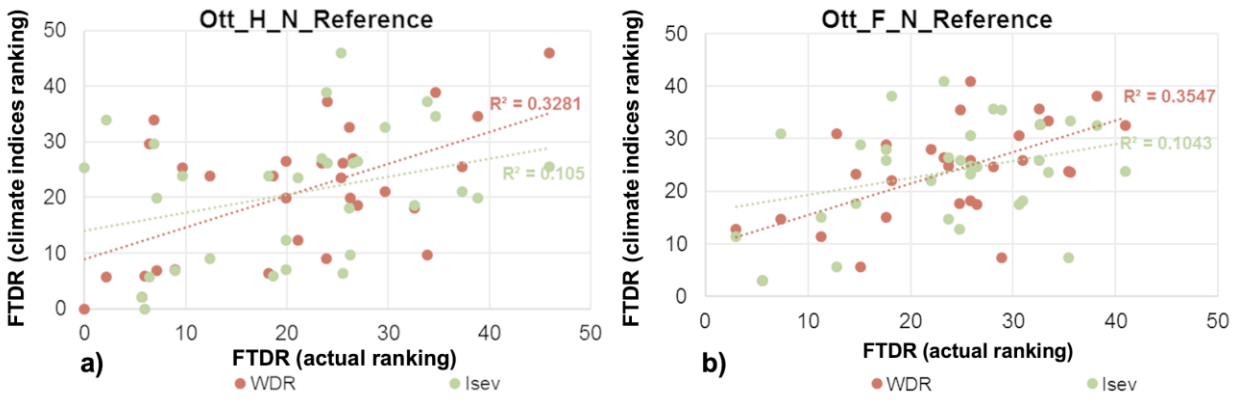

Figure 4-5. Correlation between FTDR values based on the actual ranking and the climate-based indices ranking of the seasonal period—for a reference wall under (a) historical period, and (b) future period, facing North orientation in Ottawa.

4.3.1.3. SALONVAARA ET AL. METHOD

Salonvaara et al. (Salonvaara et al., 2010) developed a method to numerically evaluate the conformity of different MRY selection methods. To apply this method, the weather years are first ranked in decreasing order of risk based on the performance indicator obtained from simulations. The performance indicator is then normalized to attain a range in values between 0% and 100%. Thereafter, the top three years are selected using each MRY selection method to determine the corresponding normalized performance indicator for each year for which the average over the three years for each MRY selection method is subsequently calculated. Finally, a comparison can be completed to establish which method for the selection of MRY permits determining the three years with the highest value for the performance indicator.

The above-mentioned approach was slightly modified by dividing the average normalized performance indicator value of the top three years, ranked using climate-based indices, by the average value of normalized performance indicator over the top three years ranked using simulation results (actual value); this value yields to a ratio. The higher the value of the ratio, the better the ranking performance (i.e., more accurate) of the climate-based index as compared to the actual ranking. As shown in Table 4-3, all climate-based indices have better ranking performance when the FTDR index is used as the performance indicator—with the ratio varying in the range of

41 to 92%. These values indicate a better correlation between FTDR and climate-based indices in selecting an MRY among the most severe years. The ratio for MWI, FTCd, and IFTC, respectively vary between 2–65%, 23–83%, and 14–76%. Although the average normalized MWI values based on climate-based indices ranking were on average low for all cases (i.e., <0.65), a better ranking performance was found for MI when MWI is used as the performance indicator for the historical period, and CI for the projected future period. Results for the FTCd and IFTC indicators were found relatively similar, having a better correlation with MI for North oriented walls under historical climate and CI and WDR for walls facing the prevailing WDR direction. However, when the FTDR index is used as the performance indicator, the correlation with the climate-based indices was inconsistent for different scenarios. For instance, the ratio of the normalized values was highest for MI and Isev for the North-oriented base wall, and the North-oriented retrofit wall under future climate. These values were highest for CI and WDR for walls under future climate and a base wall facing prevailing WDR direction under historical climatic loads.

Table 4-3. Ratio of the average normalized values of the top three years ranked based on the climate-based indices and simulated results for Ottawa.

Wall	Orientation	Climate	Climate-Based Indices	Response-Based Indices			
				MWI	FTCd	IFTC	FTDR
Base	North	H	CI	0.02	0.23	0.15	0.41
			WDR	0.02	0.23	0.15	0.41
			MI	0.54	0.55	0.62	0.70
			Isev	0.4	0.46	0.54	0.58
		F	CI	0.58	0.30	0.14	0.64
			WDR	0.08	0.23	0.14	0.68
			MI	0.08	0.23	0.14	0.68
			Isev	0.08	0.23	0.14	0.68
	Prevailing WDR orientation	H	CI	0.1	0.37	0.64	0.92
			WDR	0.1	0.37	0.64	0.92
			MI	0.17	0.26	0.21	0.77
			Isev	0.17	0.33	0.5	0.78
		F	CI	0.65	0.65	0.53	0.74
			WDR	0.65	0.65	0.53	0.74
			MI	0.51	0.65	0.35	0.44
			Isev	0.51	0.65	0.35	0.44

Wall	Orientation	Climate	Climate-Based Indices	Response-Based Indices			
				MWI	FTCd	IFTC	FTDR
Retrofit	North	H	CI	0.02	0.28	0.19	0.83
			WDR	0.02	0.28	0.19	0.83
			MI	0.45	0.63	0.69	0.64
			Isev	0.27	0.41	0.46	0.67
		F	CI	0.53	0.49	0.56	0.63
			WDR	0.10	0.38	0.41	0.71
			MI	0.10	0.38	0.41	0.71
			Isev	0.10	0.38	0.41	0.71
	Prevailing WDR orientation	H	CI	0.22	0.83	0.76	0.57
			WDR	0.22	0.83	0.76	0.57
			MI	0.24	0.51	0.24	0.48
			Isev	0.23	0.43	0.56	0.41
		F	CI	0.49	0.31	0.63	0.54
			WDR	0.49	0.31	0.63	0.54
			MI	0.41	0.28	0.47	0.57
			Isev	0.41	0.28	0.47	0.57

For Vancouver, the average normalized values ranged between 0% and 66% among all indices, and it was obvious that the Moisture Index (MI) has the best correlation with the response-based indices (Table 4-4). Moreover, the ratio for Isev is found much higher for Ottawa than obtained for Vancouver. This could be explained that Isev was developed based on structures facing North; however, it was only possible to obtain results for a wall facing the prevailing wind-driven rain direction in Vancouver, since a north-facing wall showed almost no risk to freeze-thaw damage.

Table 4-4. Ratio of the average normalized values of the top three years based on climate-based indices and the simulation results for Vancouver for a wall facing the prevailing WDR orientation.

Wall	Climate	Climate-Based Indices	Response-Based Indices			
			MWI	FTCd	IFTC	FTDR
Base	H	CI	0.45	0.49	0.46	0.33
		WDR	0.27	0.49	0.46	0.33
		MI	0.39	0.50	0.48	0.44
		Isev	0.31	0.39	0.36	0.66

	Climate	Climate-Based Indices	Response-Based Indices			
			MWI	FTCd	IFTC	FTDR
Retrofit	F	CI	0.02	0.45	0.38	0.18
		WDR	0.08	0.27	0.23	0.09
		MI	0.15	0.64	0.58	0.25
		Isev	0	0.05	0.04	0.08
	H	CI	0.52	0.37	0.42	0.32
		WDR	0.52	0.37	0.42	0.32
		MI	0.41	0.53	0.64	0.48
		Isev	0.35	0.25	0.24	0.53
	F	CI	0.12	0.24	0.27	0.29
		WDR	0.11	0.23	0.25	0.23
		MI	0.28	0.36	0.49	0.43
		Isev	0	0	0.01	0.08

In summary, all three methods indicate that the ranking performance of climate-based indices is generally poor compared to the ranking based on response-based indices (i.e., the actual performance) from simulations, and inconsistent for different scenarios. Relying on counting the number of matching years between the climate-based indices and the response-based indices based on their ranking alone is not sufficient to draw conclusions, given the results were not consistent. Both the scatter plots and the method developed by Salonvaara et al. provided a more quantitative evaluation of the ranking performance of the climate-based indices, which varies with different scenarios. The scatter plot method compared the correlation between climate-based and response-based indices ranking for all years in each time period, while the Salonvaara et al. method applies to ranking the three most severe years only through the normalization of the performance indicator. Both methods indicated that, in general, the FTDR has a better correlation with the climate-based indices, and particularly with CI and MI in Ottawa and MI in Vancouver.

4.3.2. Effects of the Response-Based Indices on the selection of MRY

To evaluate the consistency of using the response-based indices in selecting an MRY for freeze-thaw damage, correlations amongst the four different response-based indices were analyzed using the scatter plot method. The coefficient of determination R^2 is also computed for comparison (Table 4-5).

Table 4-5. Coefficient of determination (R^2) among different response-based indices for all the simulated cases for a solid brick in its original state and after being retrofitted, in Ottawa and Vancouver.

City	Wall	Orientation	Indicator	Historical				Future			
				MWI	FTCd	IFTC	FTDR	MWI	FTCd	IFTC	FTDR
Ottawa	Base	North	MWI	1.00	0.44	0.25	0.20	1.00	0.60	0.32	0.38
			FTCd		1.00	0.62	0.37		1.00	0.74	0.45
			IFTC			1.00	0.36			1.00	0.40
			FTDR				1.00				1.00
		Prevailing WDR orientation	MWI	1.00	0.48	0.23	0.06	1.00	0.65	0.52	0.10
			FTCd		1.00	0.3	0.09		1.00	0.62	0.13
			IFTC			1.00	0.01			1.00	0.11
			FTDR				1.00				1.00
	Retrofit	North	MWI	1.00	0.47	0.35	0.08	1.00	0.55	0.56	0.06
			FTCd		1.00	0.73	0.27		1.00	0.73	0.04
			IFTC			1.00	0.27			1.00	0.07
			FTDR				1.00				1.00
		Prevailing WDR orientation	MWI	1.00	0.54	0.32	0.03	1.00	0.58	0.25	---
			FTCd		1.00	0.53	0.02		1.00	0.44	0.03
			IFTC			1.00	0.04			1.00	0.01
			FTDR				1.00				1.00
Vancouver	Base	Prevailing WDR orientation	MWI	1.00	0.47	0.51	0.13	1.00	0.53	0.43	0.07
			FTCd		1.00	0.92	0.50		1.00	0.54	0.04
			IFTC			1.00	0.48			1.00	0.26
			FTDR				1.00				1.00
	Retrofit		MWI	1.00	0.47	0.48	0.25	1.00	0.33	0.41	0.10
			FTCd		1.00	0.92	0.69		1.00	0.90	0.51
			IFTC			1.00	0.63			1.00	0.51
			FTDR				1.00				1.00

A general observation of the results shows that different response-based indices may lead to a different ranking of the years in each time period, therefore a different selection of MRY. The overall best correlation was found between IFTC and FTCd, with $0.3 < R^2 < 0.92$. This may be explained by the nature of these two indicators as they both count the number of critical FT cycles. The difference between the two is that the IFTC index considers the freezing and thawing period, whereas the FTCd considers a minimum ice volume rate for thawing to occur. Although the correlation between the FTDR index and other indices is generally poor, it correlates better with the FTCd and IFTC than the MWI.

Moreover, although the MWI and the FTDR indices consist of numerical equations, they have however provided different results in ranking the years to predict the severity of FT damage. This difference may be explained because the MWI is a product of temperature below its critical freezing value and MC above its critical value; thus, for events where the temperature is well below the freezing value, or MC is well above the critical saturation value, the product of the two parameters may indicate a very high index value. However, the FTDR is calculated based on the formation and melting of ice. To verify which index is closer to reality, measurements are needed for comparison and validation, however, these types of measurements have not been reported in the literature.

4.3.3. Influence of adding interior insulation

To assess the influence of interior insulation on the risk to frost damage of historical brick masonry walls under a changing climate, the risks to frost damage as calculated from simulation results were compared. The results obtained for a base wall and a retrofitted wall, both facing the prevailing WDR orientation, located in Ottawa and Vancouver, are respectively shown in Figure 4-6 and Figure 4-7. The *x*-axis represents the years in their chronological order for both historical (1986–2016) and future (2062–2092) time periods.

In general, adding interior insulation will increase the risks of freeze-thaw damage as indicated by the values given for all four response-based indices. In Ottawa, the MWI increased in certain years and the difference between a base wall and the retrofit reached a maximum of 60 during the year 1996. In addition, the number of freeze-thaw cycles, as derived from the results of Delphin simulations (FTCd), increased by a maximum of 10 cycles during 2013, and the number of

indicative freeze-thaw cycles (IFTC) increased by a maximum of five cycles during 2015. As for the FTDR index, it increased by a maximum value of 23 during 2012. Besides, the effect of adding interior insulation was even more significant in the future. For instance, an increase of 86 (in 2065), 19 (in 2076), 13 (in 2063), and 21 (in 2068) was observed for MWI, FTCd, IFTC, and FTDR, respectively.

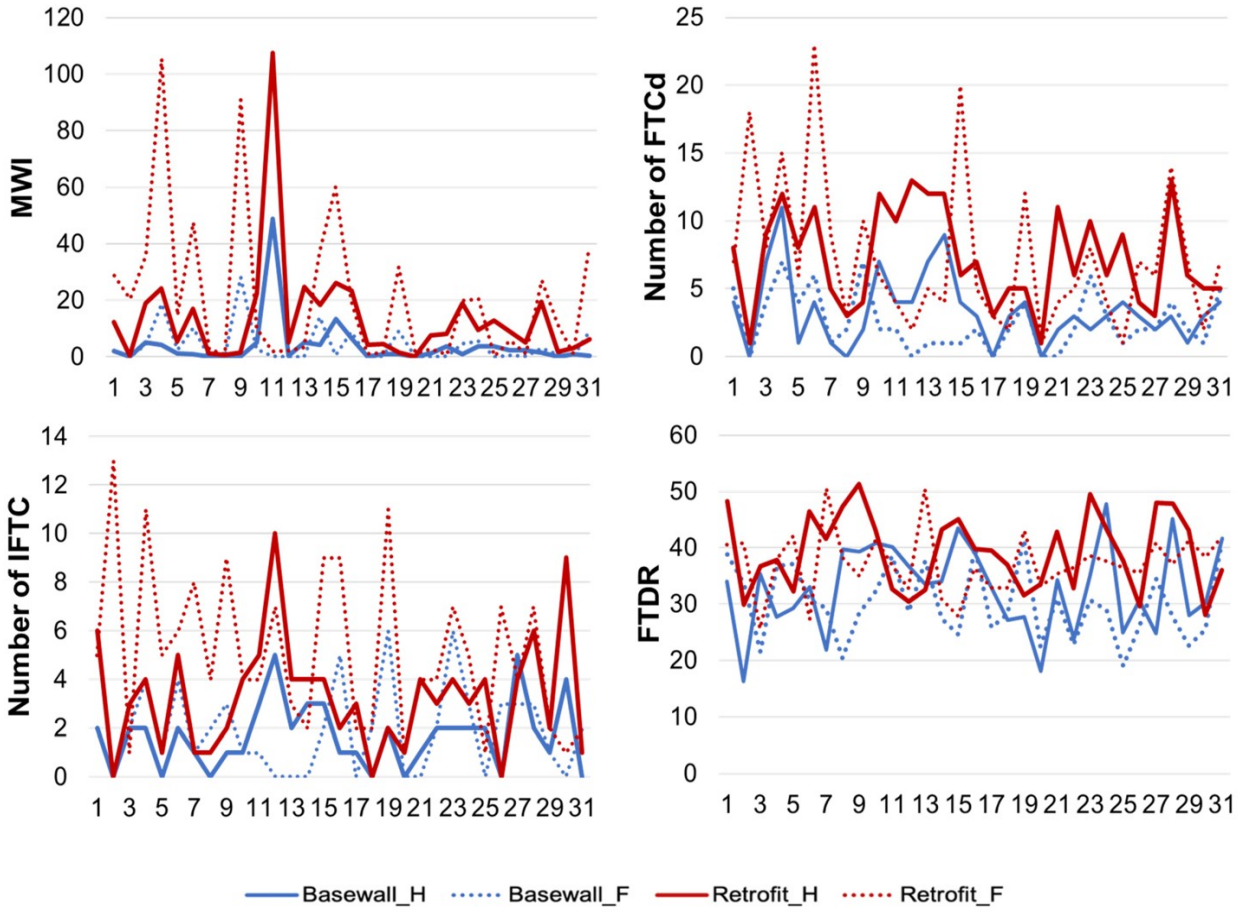

Figure 4-6. Freeze-thaw performance indicators calculated for a base wall and a retrofitted wall (100 mm spray foam and Scrit of 0.25) facing the prevailing WDR orientation in Ottawa under historical and future climates.

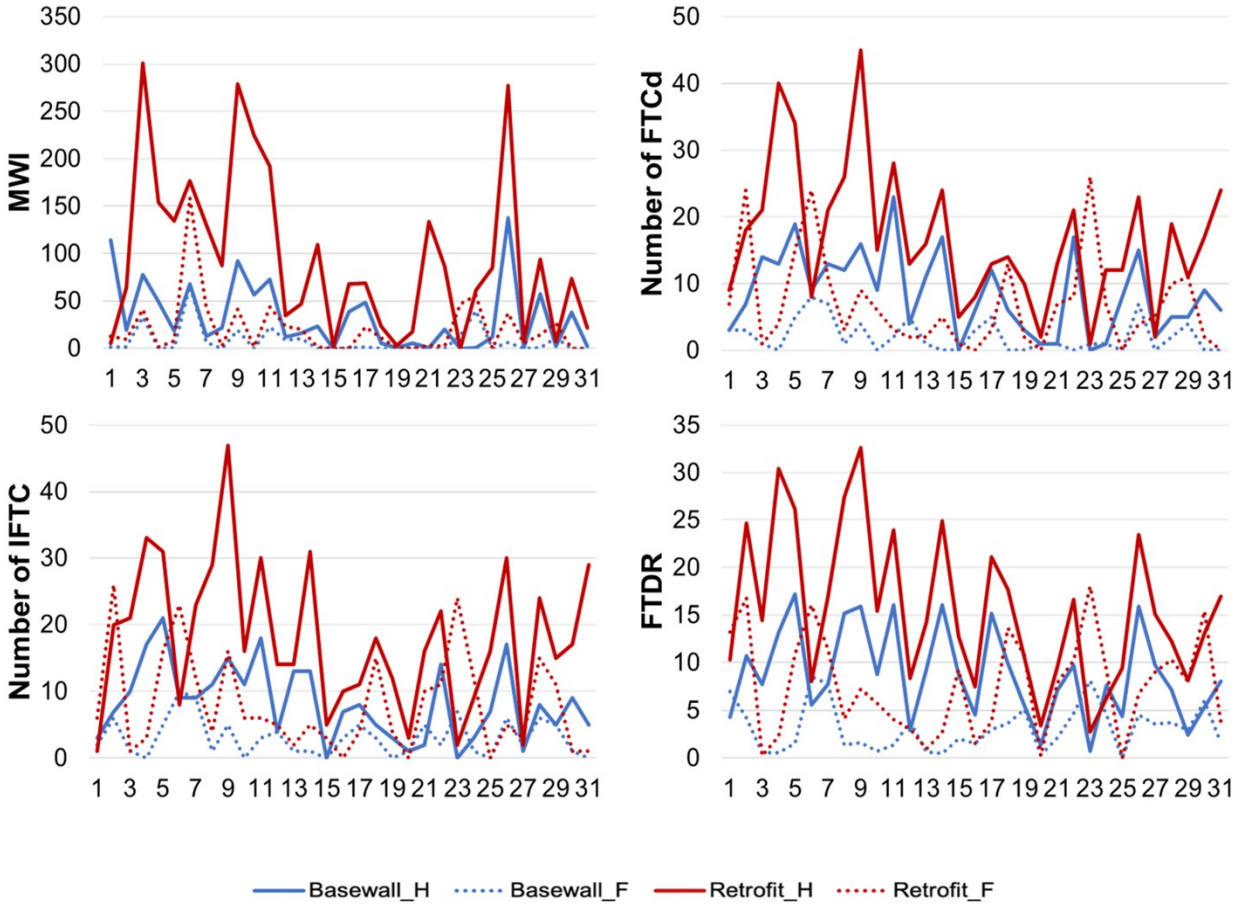

Figure 4-7. Freeze-thaw performance indicators calculated for a base wall and a retrofitted wall (100 mm spray foam and Scrit of 0.25) facing the prevailing WDR orientation in Vancouver under historical (1986–2016) and future climates (2062–2092).

As shown in Figure 4-6, adding interior insulation will also increase the frost damage risk of a masonry wall; however, the impact is more significant in Vancouver than in Ottawa. For instance, the MWI increased for almost all the years and the difference between a base wall and the retrofit reached a maximum of 220 (in 1998), whereas the values for the FTCd and IFTC indices showed an increase of freeze-thaw cycles by a maximum of 29 and 32, respectively during the year 1994. The FTDR index has also increased by a maximum value of 17 (in 1989). Masonry solid walls in Vancouver would still have frost damage risk in the future, but unlike Ottawa, the impact of adding interior insulation would be less significant: an increase of 92 (in 2067), 25 (in 2084), 20 (in 2063) and 12 (in 2063) was observed for MWI, FTCd, IFTC, and FTDR, respectively (Figure 4-7).

As for the impact of climate change, when using MWI, the FTCd, and the IFTC as indicators, in general, the risk of freeze-thaw damage for Ottawa remains constant for some years and increases over other years in the future. However, the FTDR index value has shown a slight increase for a

few years, but also a decrease in the risk of FT damage (Figure 4-6). One explanation for that may be because the FTDR index was developed using a threshold value of 0.05, thus, freeze-cycles having a very small variation in ice content are disregarded and hence the reduction in risk to FT damage. For Vancouver, all response-based indices have predicted a decrease in the risk of freeze-thaw damage (Figure 4-7).

For Vancouver, the increased risk of frost damage is more significant due to the addition of interior insulation, whereas for Ottawa the increased risk of frost damage is more significant due to climate change.

4.4. Conclusions

The objective of this study was primarily to evaluate the reliability of commonly used approaches for the selection of a moisture reference year (MRY) to assess the freeze-thaw damage risk of solid brick masonry walls. This was achieved by comparing the ranking based on the climate-based indices to that based on response-based indices obtained from HAM simulations. Hygrothermal simulations were carried out for a brick masonry wall assembly prior and post-retrofit in two Canadian cities (Ottawa and Vancouver) under historical and projected future climates and for two wall orientations: a North-facing wall and a wall facing the prevailing wind-driven rain direction. Four freeze-thaw performance indicators were used to assess the potential risk to the occurrence of freeze-thaw damage. Four commonly used climate-based indices were calculated for different cities, orientations, and climates and were compared to response-based indices.

The principal conclusions are summarized as follows:

1. The direct correlation between the climate-based indices and the response-based indices is poor, which means that climate-based indices alone do not represent the actual freeze-thaw performance of the walls.

2. The rankings based on climate-based indices are found to have a better correlation with the FTDR index ranking; however, results were not consistent and varied amongst the different scenarios.

3. The correlation between response-based indices: different response-based indices may lead to different rankings of years in each time period and given this, a different selection of

MRY. As well, the best overall correlation was found between IFTC and FTCd. The correlation between FTDR index and other response-based indices was generally poor; however, it had a better correlation with the FTCd and IFTC than MWI.

4. The risk of freeze-thaw increased considerably for a masonry wall after interior insulation was added for buildings located in both Ottawa and Vancouver; however, this was more significant in the case of Vancouver. The risk of FT damage would increase for Ottawa but decrease for Vancouver under a warming climate projected in the future, based on the climate scenario used in this study.

Given the advantage of moisture reference years (MRYs), however, the poor reliability of commonly used climate-based indices in ranking and selecting MRYs for frost damage risk assessment, further research is needed to develop a more reliable and robust method for the ranking and selection of MRYs based on climate-based indices that is suitable for freeze-thaw damage risk assessment. Additionally, the uncertainty due to future climate will be further investigated taking into consideration both additional city locations and climate scenarios.

Chapter 5. Selection of Moisture Reference Year for Freeze-Thaw Damage Assessment of Historic Masonry Walls under Future Climate: A Simulation-based Approach[4]

5.1. Introduction

Based on the findings of the previous chapter (Chapter 4), when assessing the reliability of selecting an MRY based on commonly used climate-based indices for freeze-thaw damage evaluation of solid brick masonry walls, a comparison was made between the ranking of years using these climate-based indices and the results from hygrothermal simulations, which serve as the reference. The comparison revealed a poor correlation between the two sets of indices. This suggests that relying solely on climate-based indices does not accurately represent the freeze-thaw performance of masonry walls, rendering none of these methods reliable for selecting MRYs.

To address the poor reliability of climate-based indices in selecting MRY for FT damage risk assessment, this chapter explores the potential of choosing simulation-based MRYs to assess FT damage in masonry walls. Considering that numerous factors influence the hygrothermal response of historic masonry walls, the selection of MRYs through a simulation-based approach necessitates a substantial number of simulations with various combinations of these parameters. This chapter thus presents a parametric analysis to develop a methodology for the selection of MRYs based on hygrothermal simulations' results of multiple scenarios with a variation of parameters including material properties, moisture loads and climate conditions. The application of those simulation-based MRYs is verified among different constructions. The studied wall assemblies are historic masonry walls in their original state (prior to retrofit) and after being internally insulated using three different types of insulations. The analysis also includes different brick

[4] The content of this chapter is published in the journal paper "*Sahyoun, S., Ge, H., and Lacasse, M.A. (2024). Selection of Moisture Reference Year for Freeze-Thaw Damage Assessment of Historic Masonry Walls under Future Climate: A Simulation-based Approach.*" Building and Environment, 111308. https://doi.org/10.1016/j.buildenv.2024.111308.

The abstract from the original paper is excluded in this chapter to avoid duplication. Additionally, details such as wall assemblies, climate-based index, model settings that were included in the original paper can be found in Chapter 3 – Methodology.

configurations/geometries, different wall orientations and rain deposition factors. Hygrothermal simulations are performed to predict the risk of freeze-thaw damage, which is evaluated by counting the number of freeze-thaw cycles using two damage indicators: FTCd (the number of freeze-thaw cycles outputted from Delphin) and FTCcrit (the number of critical freeze-thaw cycles). Ottawa is chosen as the studied location and hourly climatic parameters were used for the simulations over both historical and future periods.

5.2. Methodology

5.2.1. Methods and materials

Simulation-based MRYs are location, construction, orientation, exposure, and material dependent. One important question to answer is whether one MRY can cover all of these variables? Therefore, we attempt to test this hypothesis and develop an approach to select MRY to be as general as possible for a particular geographical location. Therefore, we have used a typical historic masonry wall construction. We carried out parametric analysis to investigate the impact of orientation, rain deposition factor and climatic realization, and identified the most critical wall orientation, rain deposition factor, and climatic realization to represent a worst-case scenario. The methodology proposed in this paper for the selection of an MRY is presented in (Figure 5-1). It includes the following steps:

1) From a wide selection of input parameters, select typical wall constructions, then investigate and identify the most critical wall orientation and rain deposition factor that have the most significant influence on the FT damage risk.
2) Perform simulations over a) 31 consecutive years (31Y), representing the actual performance, and for b) each single year (SY) recurring for 3 times (the first two years are conditioning years, and the third year is the evaluation year), for each time-period.
3) Rank the single years (SY) according to their FT damage severity and compare the results with the continuous 31Y simulations.
4) Select the most severe common year found for the wall assemblies (according to (Geving, 1997; Rode, 1993; Sanders, 1996), or the year corresponding to 93rd percentile of the FT damage, according to ASHRAE Standard 160.

5) Verify the selection of MRYs for additional brick wall assemblies (with different insulation material and thickness) for the same location.

More details on the hygrothermal simulations settings can be found in the sections below.

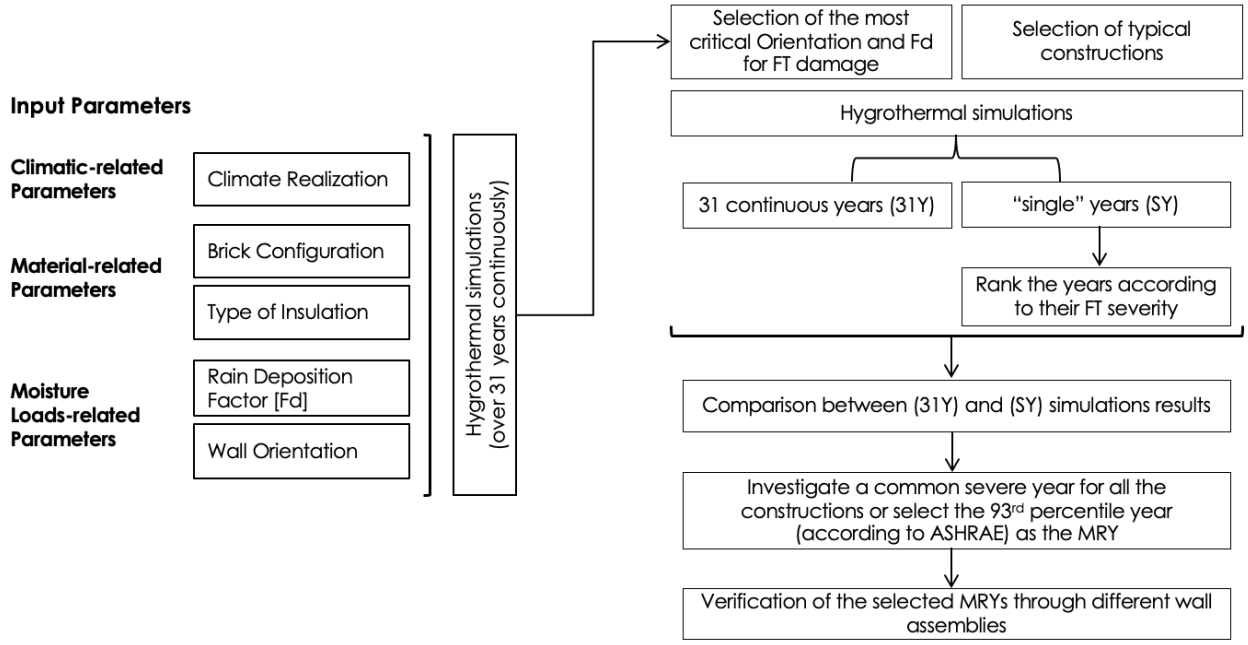

Figure 5-1. The methodology for the selection of simulation-based MRYs for FT damage assessment of masonry walls.

Brick modeling configuration

To evaluate the potential freeze-thaw risk of historic masonry walls under current and projected future climate loads, HAM simulation tools are often used. However, most studies have simplified the configuration of the exterior cladding of brick material into a single isotropic brick layer, without modelling the effect of mortar joints. Given that this simplification may affect the response of the wall to climate loads, in this paper, the results from two different modelling configurations (i.e., isotropic brick and brick with mortar joints) are first compared in respect to how they affect the potential risk of FT damage to historic masonry walls.

Climatic realization

A fundamental part in assessing the building envelope performance and their resistance against freeze-thaw related damages is associated with the environmental load of the present and the future climates. It is expected that buildings in Canada will be exposed to radically different annual and

seasonal climatic conditions and more frequent extreme events. However, due to the uncertainty of the occurrence of these events, different combinations of climate scenarios were generated by the National Research Council (NRC) in Canada, from where the complete climate dataset was retrieved. This paper investigates the impact of different climate realizations on the resultant FT damage risk of historic solid brick masonry walls, and therefore select the climate realization with the greatest FT damage risk.

NRC has generated 15 hourly realizations (namely "run" in this paper) that are part of the datasets derived from the large ensemble of climates simulated by the Canadian Regional Climate Model—version 4 (CanRCM4), each initialized under a different set of initial conditions in the CanESM2 global climate model. The climate realizations are ensemble members which were bias corrected based on observational data (Gaur et al., 2019). Assessing the FT damage risk of building envelopes using all the 15 climate realizations is a complex task. It will, not only, significantly increase the computation time and resource costs when undertaking simulations with many different climate parameters over an extended period, but also may lead to the selection of different MRYs given any alteration of climate parameters (temperature, rainfall, etc.) or of the succession of the extreme events. In addition, one year might provide a high risk to the number of freeze-thaw cycles according to one climate realization, but for other realizations, the same year might be less severe. For example, if in the year 2000 the highest number of FTCs for Run #2 had been estimated, the same year might be less risky for other realizations. Therefore, it is important to select the climate realization from which the greatest FT damage risk for historic masonry walls can be estimated.

Ideally, for the purposes of conducting a probabilistic analysis, investigating the impact of all 15 climate realizations on the FT damage risk of historic masonry walls is recommended. However, since the city of Ottawa has been selected as an example, the climate realizations having the lowest error to the 90^{th} percentile (P90) according to a study done by Vandemeulebroucke et al., 2021, were selected in this paper for further analysis. Those climate realizations are Run2, Run4, Run9 and Run10. In their study the application of a "reduced" ensemble was evaluated that was composed of three (3) climate realizations (those with the lowest error to the 10th, median and 90th percentile based on the least square method) out of 15 and an assessment was conducted on whether the ensemble was robust and reliable for different situations.

Wall orientation

The outer surface layers of historic masonry walls are normally exposed to the highest risk for FT damage, mainly manifested through scaling of the outer surfaces. Both the moisture and temperature levels of porous building materials are influenced by the wall orientation. One major source of moisture is wind-driven rain (WDR). WDR is influenced by the wind speed, the rainfall intensity, environmental topology and the building geometry and orientation. Most deterministic studies consider the prevailing wind direction during all hours as the most critical for the occurrence of moisture damage, given that freeze-thaw damage is the concurrence of wetting and sub-zero temperature. As such, the most critical orientation in respect to the risk of occurrence of FT damage to masonry walls must be the direction facing the highest amount WDR in combination with sub-zero temperature and is not necessarily the prevailing WDR orientation. Thus, in this paper the most severe orientation is determined based on the response of wall assemblies to eight (8) wall orientations assessed.

For example, the prevailing direction for WDR in Ottawa is South-South-West (SSW) whereas the lowest facade temperatures occur in North-facing facades. A further analysis of the wind direction (Figure 5-2) has revealed that the prevailing wind direction is South-South-West (SSW) during all hours as well as during the freezing season (i.e., November to April), whereas during rain hours of the freezing season the orientation is East-North-East (ENE) for the projected future climate.

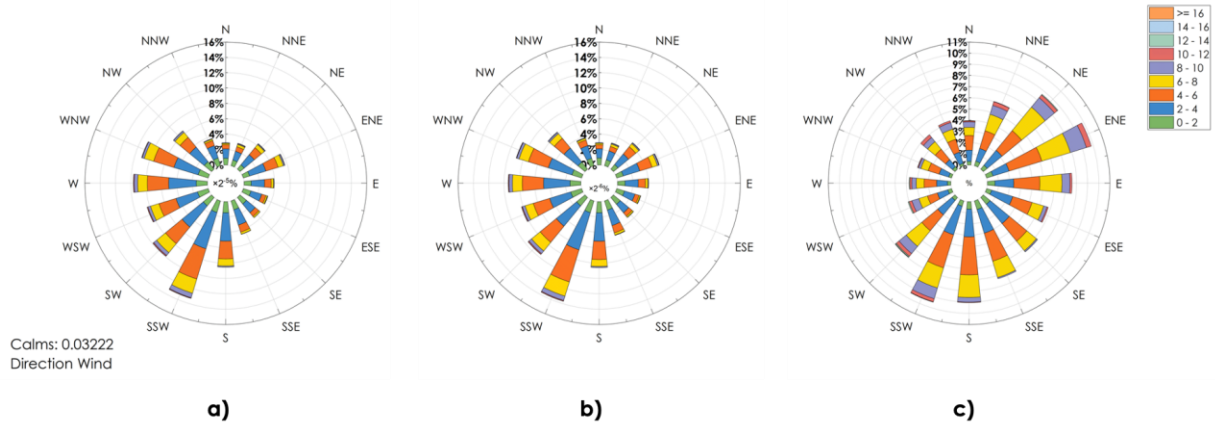

Figure 5-2. The prevailing wind direction for a) all hours, b) all hours during the freezing period, and c) rain hours during the freezing period, based on future climate (2062-2092) of Ottawa.

Rain deposition factor [Fd]

Whereas the wind speed and rainfall intensity are climatic data that are location-dependent, building geometry can affect the rain deposition factor (Fd), which accounts for the spatial distribution of WDR on the façade. In other words, the response of the façade will be strongly influenced by the amount of absorbed rain, which is determined by the amount of rain that impinges the exterior wall surface, a parameter influenced by the value of Fd. Accordingly, different values of deposition factor (Fd) were evaluated, corresponding to three (3) scenarios, according to ASHRAE standard (ANSI/ASHRAE, 2021): 0.3 when walls were assumed to be located below a steep-slope roof; 0.5 when walls were below a low-slope roof; 1.0 when walls were exposed to rain runoff (which in this case is considered the worse-case scenario).

Interior insulation materials

The application of internal insulation increases the risk of moisture accumulation and moisture damage as internal insulation reduces the drying potential of the existing wall as well as the temperature. The severity of the potential damage is affected by the type of internal insulation used, and thus, three different insulation systems were evaluated: Closed-cell spray polyurethane foam or SPF (vapour-tight insulation material), Calcium Silicate or CaSi (Vapour-open/capillary-active insulation material) and Mineral Wool with vapour barrier (vapour-tight insulation material).

5.2.2. Settings in HAM simulations

Simulations were performed for a reference wall in its original state (ORG) and internally insulated retrofit wall assemblies using three different internal insulation systems: Spray Foam Polyurethane (SPF), Calcium Silicate (CaSi) adhered to the brick wall with 4mm glue mortar, and Mineral Wool (MW) with a vapour barrier. The reference wall consists of a typical 300mm historic brick (corresponding to one full and a half brick) and 15 mm of gypsum plaster as commonly found in Canada and typically used in the literature. The sensitivity analysis has shown that different thicknesses of the masonry walls have negligible impact on the freeze thaw cycles. A retrofit wall with 100mm SPF insulation is first evaluated as a reference to other insulation strategies, and also to represent a wall assembly meeting the energy code requirement. As an interior finishing layer, a 12mm gypsum board was used; only the capillary active CaSi was rendered with a 10mm plaster

layer. Also, for the retrofitted walls, empty steel studs were installed after the insulation material, because according to (Straube and Schumacher, 2007) the empty stud space is ideal for services distribution and allows the easy application of a drywall finish. For the different wall assemblies, parameters' variation are presented in Table 5-1 for the continuous 31-year (31Y) simulations, and in Table 5-2 for the single years' (SY) simulations.

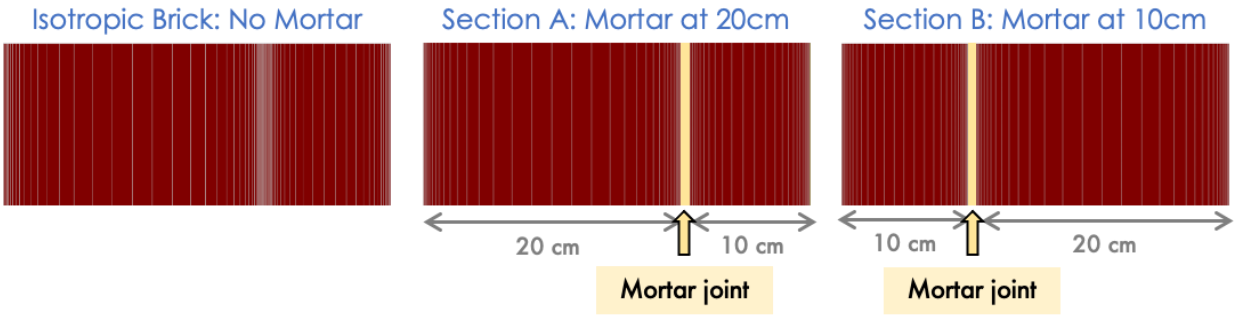

Figure 5-3. Configuration of typical brick masonry wall assemblies: reference wall (ORG) (top left), and internally insulated wall (top right). The brick material was modelled with different configurations: a) isotropic/ or homogenous brick, b) brick with mortar joints applied at 20cm from the exterior wythe, and c) brick with mortar joints applied at 10cm from the exterior wythe.

Previous hygrothermal studies have simplified the brick material into a single isotropic brick layer, ignoring the presence of mortar joints. In this study, the effect of two different brick configurations (i.e., isotropic brick and brick with mortar) on the potential risk to FT damage was investigated. Also, since brick masonry walls were composed of one full brick unit of 200mm, and one half unit of 100mm, two scenarios were compared: i) when mortar was applied at 20 cm from the exterior surface of the brick (Section A) and; ii) when mortar was applied at 10 cm (Section B) from the exterior surface of the brick (shown in Figure 5-3).

Table 5-1. 31 – year continuous (31Y) simulations input parameters and their variations.

Input Parameter	Variation	Description
Location	1	Ottawa
Climate realizations	4	Run2, Run4, Run9 and Run10
Time period	2	Historical (1986-2016) Future (2062-2092)
Wall orientation	8	North (N), North-East (NE), East (E), South-East (SE), South (S), South-West (SW), West (W) and North-West (NW)
Rain deposition factor	3	0.35, 0.5 and 1.0
Brick modelling configuration	3	Isotropic brick, brick with mortar at 20cm and brick with mortar at 10cm
Brick property	1	$S_{crit} = 0.55$
Internal insulation type	3	No insulation (ORG), Spray Foam Polyurethane (SPF) and Calcium Silicate (CaSi)

Table 5-2. Single year's (SY) simulations input parameters and their variations.

Input Parameter	Variation	Description
Location	1	Ottawa
Climate realizations	1	Run4
Time period	2 x 31	Historical (1986-2016) Future (2062-2092)
Wall orientation	1	East (E)
Rain deposition factor	1	1.0
Brick modelling configuration	1	Brick with mortar at 20cm
Brick property	1	S_{crit} = 0.55
Internal insulation type	4	No insulation (ORG), Spray Foam Polyurethane (SPF), Calcium Silicate (CaSi) and Mineral Wool (MW)
Internal insulation thickness	3	50mm, 100mm and 200mm

Simulations were performed under historical and future climatic conditions, using the hygrothermal simulation program DELPHIN 5, v5.9.4. No sources of either air leakage or rain leakage were assumed. The simulations were performed for a one-dimensional cross-section of the reference wall and the retrofit walls. The historic brick material i.e. Old Building Brick Persiusspeicher was selected from the DELPHIN materials database (which has similar properties to that of the exterior reclaimed brick "ERUL" found in Canada and measured by Aldabibi (Aldabibi et al., 2022). This brick material is considered typical and has average FT resistant properties, with a critical degree of saturation (S_{crit}) of 55% (which was measured experimentally). As for the mortar, a historical mortar was selected from DELPHIN's material database. All materials' properties are listed in Table 5-3.

Table 5-3. Material properties of the historic brick (DELPHIN material database)

Material	Density (kg/m^3)	Specific heat (J/kg.K)	Thermal conductivity (W/mK)	Open porosity (m^3/m^3)	A ($kg/m^2.s^5$)	μ (-)	Kl (s)
Old Building Brick Persiusspeicher	2014.9	775.2	0.8682	0.2396	0.0457	139.5	4.92×10^{-9}
Plaster *	840	1380	0.588	0.0890	-	73.33	10^{-16}
Mortar (historic)	1568	488	0.5815	0.4083	0.175	11.37	9.65×10^{-9}
Closed-cell Spray Foam Polyurethane (SPF)	45	1500	0.029	0.92	0.0001	104	
Calcium Silicate (CaSi)	225	1129	0.063	0.913	0.726	4.234	
Mineral Wool (MW) + VB**	67	840	0.04	0.92	-	1	-

A: Water absorption coefficient; μ: Vapor resistance factor;
*** Plaster was only used inboard in the case of the original wall (reference wall).**
**** VB: Vapour barrier.**

The risk of freeze-thaw damage was computed using the number of critical freeze-thaw cycles obtained from DELPHIN (FTCd) and the number of critical freeze-thaw cycles (FTCcrit) calculated manually. DELPHIN takes ice formation into account by assuming the instantaneous equilibrium between the three phases (vapor, liquid, and ice), and by applying a freezing point depression whilst assuming that the pore space fills from the smallest to the largest pore and that ice crystalizes outside of the liquid phase (Nicolai et al., 2013b; Sontag et al., 2013b). The use of this model permits investigating whether the moisture content is sufficiently high to fill pores where water could freeze. In this paper, one FT cycle was counted when the ice volume rate (IVR) is lower than the minimum value of 0.55. The ice volume rate or IVR is the ratio of the ice volume to the pore volume. The number of FTCcrit is calculated when two conditions exist concurrently: 1) the material's moisture content exceeds a critical threshold corresponding to S_{crit} of 0.55, and 2) the material's temperature fluctuates below and above the freezing point assumed to be 0°C (Sedlbauer and Künzel, 2000; van Aarle et al., 2015).

5.2.3. Selection of simulation-based MRYs

The MRY is defined as a single year representing typical long-term climatic conditions, under which the hygrothermal performance of building envelope can be assessed for decision making. The procedure is to use single year's simulation results to represent the long-term simulations results – typically within 10 years or to select the 93rd percentile single year in severity for hygrothermal performance, as recommended by ASHRAE 160. We carried out both 31-year consecutive and single-year simulations. The effect of serval influencing parameters on FT damage risks was investigated and critical parameters were identified through 31 years consecutive simulations. Thereafter, each time-period, i.e., historical and future, is divided into 31 single years and simulations are repeated three times for each of those years (two years are simulated prior to the evaluation year were sufficient to reach a heat and moisture balance in the building components in this study, and the third year is the evaluation year). The results from the 3rd year are used for analysis. The process is summarized as follows:

i. Simulations are set to run over 31 consecutive years (31Y) (from October 1st, 1986, to September 30th, 2016);

ii. Climate data are split into 31 individual years (also referred to as single years or SY);

iii. Simulations are set to run for each SY, recurring for three times;

iv. Once the simulations are complete, the values for FTCcrit and FTCd are computed annually for each individual year for 1) results obtained over 31-year consecutive simulations, and 2) results obtained from single-year simulations;

v. Single years are then ranked in a descending order of the estimated FT damage, and the top four years are compared to investigate the existence of any common worst year among different scenarios;

vi. Results obtained from long-term simulations (31Y) are compared to those obtained from a single-year simulation. The comparison indicated that annual FT cycles obtained from 31-year consecutive simulation is very similar to single-year simulation. Therefore, we conclude that yearly weather variation has little accumulative effect on annual FT cycles, and we can use single-year simulation to represent long-term performance for the MRY selection.

vii. The single year with the severity index corresponding to the 93rd percentile is selected as moisture design reference year i.e. the MRY.

viii. The selected MRY is verified for masonry wall assemblies with different insulation material and thicknesses. The selection of MRY procedure is based on simulation results from reference masonry walls: the original (ORG) wall and the retrofit wall with 100mm of SPF facing East in Ottawa. After MRYs are selected for each time-period, they are verified for the other internally retrofitted walls with different insulation materials (CaSi and MW) and thicknesses (50mm and 200mm).

5.3. Results and discussion

In the field of building retrofit, it is crucial to understand and analyze the various factors that can affect the performance of masonry walls. These factors include the orientation of the wall, the level of exposure to rain and other weather elements, the specific materials used in construction, and the geographical location of the building. By conducting a parametric analysis, we can systematically

study the impact of each variable and identify the most critical factors that affect the FT damage response of masonry walls.

This section provides results on the impact of the modelling configuration of the masonry unit, the impact of different climatic realizations, the impact of different wall orientations, as well as the impact of rain deposition factor and that of different interior insulation materials on the FT damage response of historic masonry wall assemblies. And given that the focus of this chapter is to investigate whether it is safe to internally insulate historic brick under representative future MRY specific to freeze thaw damage, these results allow to select the worst case for FT damage for Ottawa by identifying the worst climate run for future climates, worst orientation, highest wind-driven rain deposition factor for a typical historic brick wall with representative brick property.

5.3.1. Impact of different brick modeling configurations

The potential risk of freeze-thaw damage was assessed by counting the total number of freeze-thaw cycles after 31 years of continuous simulations, using two indicators: FTCd and FTCcrit.

Figure 5-4 presents the sum of the FTCd number obtained at several locations within the brick material. In general, both geometries showed similar results at points (locations) close to the exterior surface of the brick. However, the difference between the two geometries was more significant deeper inside the brick layer (Figure 5-4). For instance, starting at 8 cm from the outer brick layer up to 170 cm, numbers of FTCd were much higher when isotropic brick was modelled (brick without mortar). This difference was also more important for retrofit walls with SPF and CaSi. One explanation is that mortar has a higher vapour permeability, water uptake coefficient and liquid water conductivity than brick (the mortar's water vapour diffusion resistance factor is much lower than that of brick: $\mu(\text{mortar}) = 11.37 < \mu(\text{brick}) = 139.5$, while $A_w(\text{mortar}) = 0.175$ kg/m^2.s^5 > $A_w(\text{brick}) = 0.0457$ kg/m^2.s^5 and $Kl(\text{mortar}) = 9.65 \times 10^{-9}$ s > $Kl(\text{brick}) = 4.92 \times 10^{-9}$ s) which means that when mortar was included, moisture in the form of vapour and liquid water could easily diffuse through the wall and find its way out to dry. This might have resulted in a significantly lower moisture content, and thus lower FT damage risk. The isotropic brick configuration seemed to overestimate the severity of FT damage inside the walls, which highlights the importance of a more accurate representation of masonry wall construction in modeling.

Similar results were found when using the number of FTCcrit as FT damage indicator, however the difference between the two geometries was more important.

However, a closer look at the results obtained at 5mm depth from the exterior surface of brick - usually used in the literature as the critical investigation point for FT related problems (Zhou et al., 2017) - showed no difference in the number of FTCd between a brick wall with mortar joints and without over both historical and future periods (Figure 5-5). The FTCd trendline over 31 years was matching for different wall assemblies; i.e., ORG and retrofit cases with SPF and Casi. Similar results were also found when comparing the impact of mortar joint using the number of FTCcrit; however, with an increased FT risk in the future.

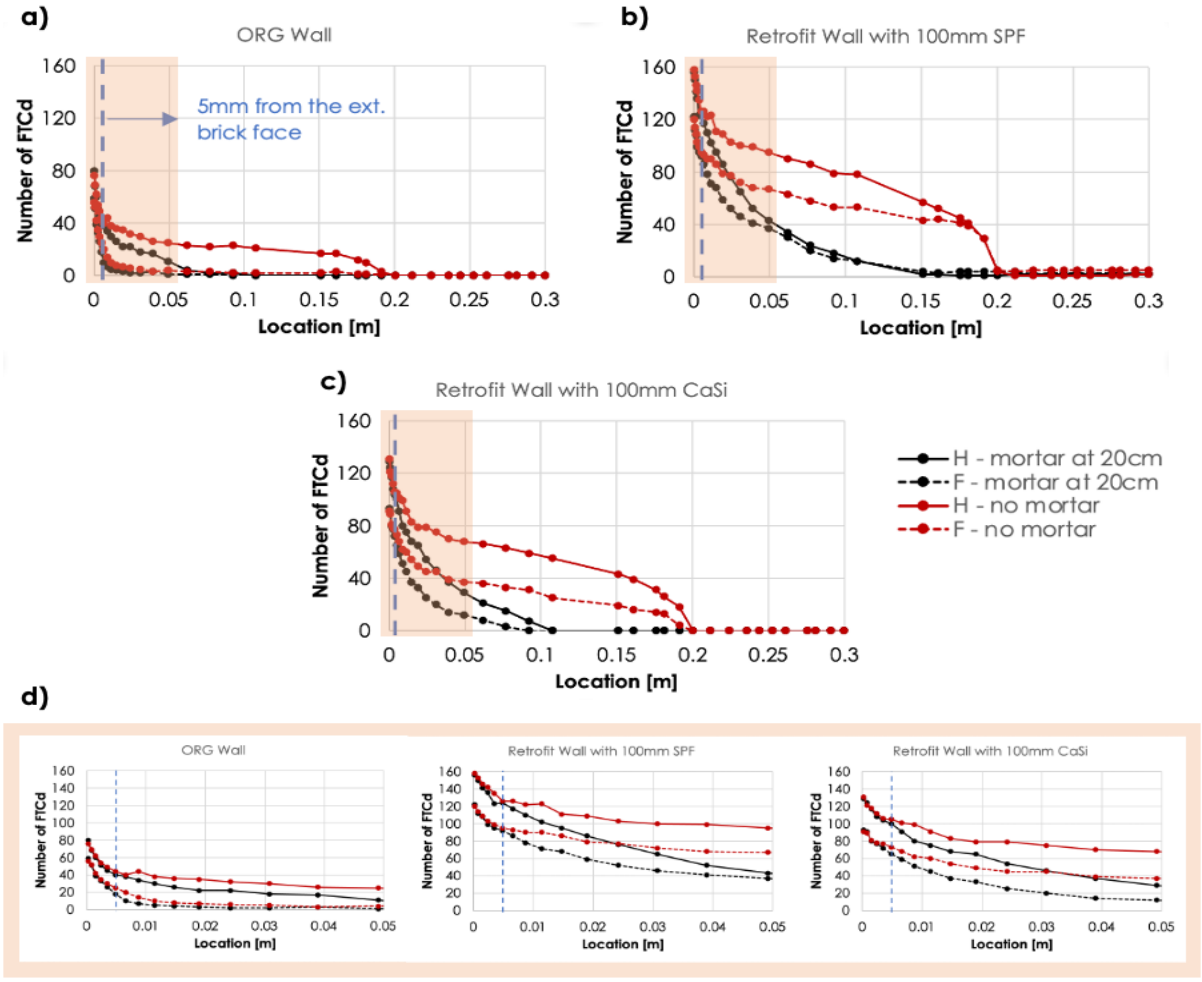

Figure 5-4. Comparison between two brick configurations: brick with mortar joints (black) and isotropic brick (red) using the total number of FTCd outputted at several points through the brick layer. The comparison was made for a) an ORG wall, b) a retrofit wall with 100mm SPF and c) a retrofit wall with 100mm CaSi. A close up of the results at the very first centimeters of the brick wall is shown in d).

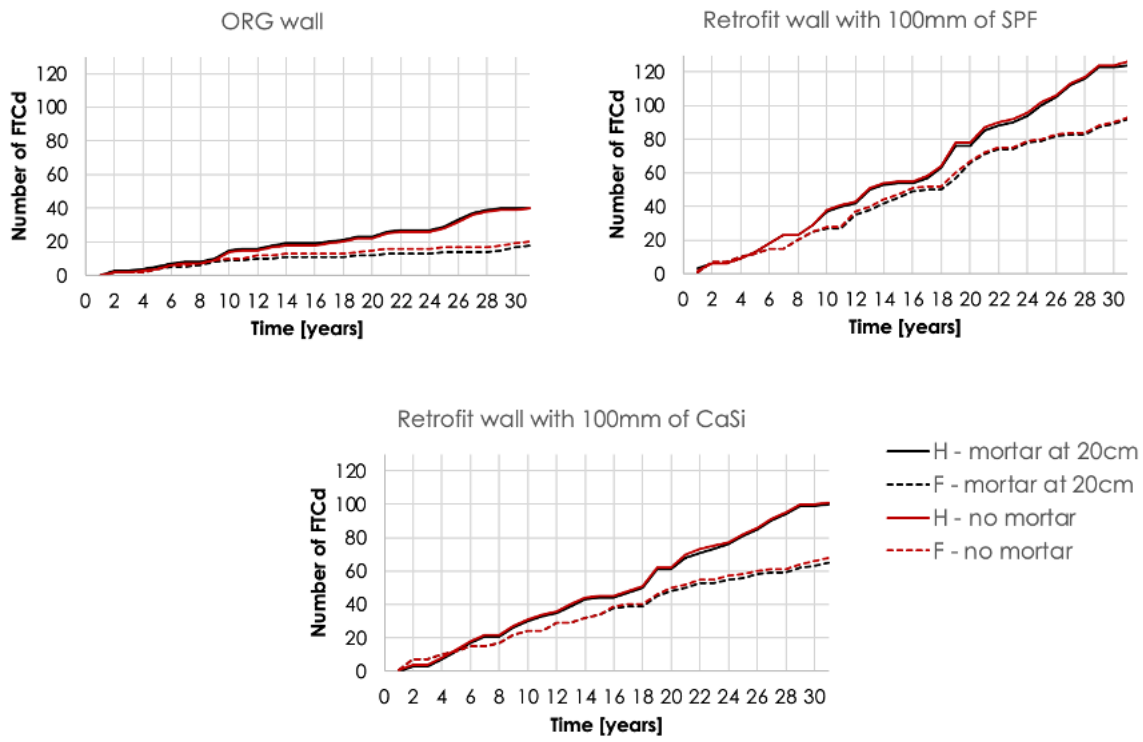

Figure 5-5. Comparison between two brick configurations: brick with mortar joints (black) and isotropic brick (red) using the number of FTCd outputted at 5mm from the exterior surface of the brick.

To further investigate the accuracy of the brick wall characterization, the impact of the location of the mortar application was compared between two scenarios: (1) when mortar is applied at 20 cm from the exterior surface of the brick (Figure 5-3b) and (2) when mortar is applied at 10 cm from the exterior surface of the brick (Figure 5-3c). A reference wall (ORG) without any insulation and a retrofitted wall with (SPF) were modelled. The number of critical freeze-thaw cycles were computed at the end of 31 years at 5mm depth and over several locations through the walls using both FTCd and FTCcrit. Scattered plots were used to compare the correlation between the influence of the mortar location on the severity of FT damage. The number of freeze-thaw cycles obtained when mortar was applied at 10 cm are given on the x-axis of the plot, and on the y-axis, are the values of the freeze-thaw cycles corresponding to when mortar was applied at 20 cm (Figure 5-6). The coefficient of determination R^2 was also computed for comparison. If the results obtained from the two scenarios are matching, all dots should fall on a straight line and R^2 should be 1. From Figure 5-6, it is very clear there is a strong correlation between the results, since $R^2 > 0.99$. This indicates that the mortar position does not influence the severity of FT damage risk at 5mm,

and therefore; moving forward, mortar is assumed to be applied at 20 cm from the exterior surface of the brick.

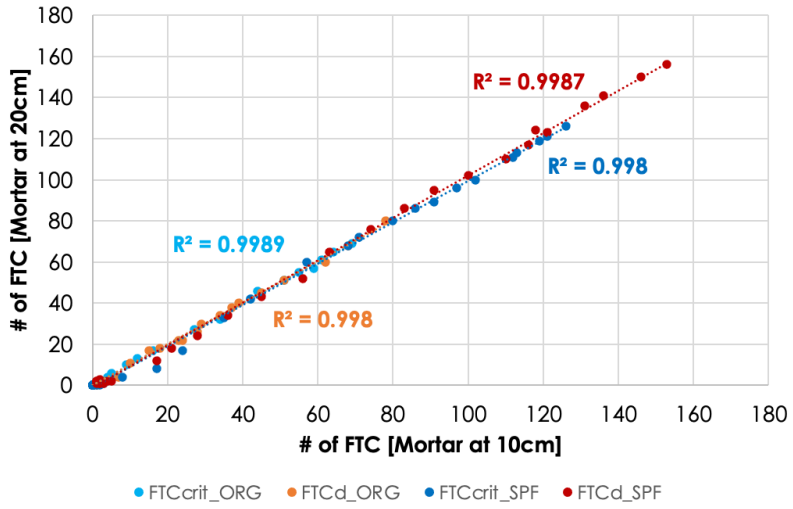

Figure 5-6. Correlation between the number of freeze-thaw cycles (FTC) when counting FTCcrit (blue) and FTCd (red) when mortar joint is applied at 20cm and at 10cm from the exterior surface of the brick – for an ORG wall and a retrofit wall with 100mm of SPF.

5.3.2. Impact of different climatic realizations

As mentioned earlier, the climatic input parameters can have a significant impact on the hygrothermal performance of building envelopes. For FT damage assessment, any alteration in the temperature, solar radiation, rainfall, and subsequently wind-driven rain, as well as the sequence of climatic events might influence the results.

The annual total number of FTCcrit and FTCd over 31-consecutive years were compared for four different climate realizations over a historical and future period and for three wall assemblies (ORG and retrofit walls using SPF and CaSi) facing 8 different orientations. FTCcrit and FTCd were outputted at 5mm from the exterior surface of the brick. Figure 5-7 shows the comparison using FTCcrit number for East facing walls. It can be seen that the mean and maximum annual total FTCcrit was mostly higher under Run#4 weather conditions for all three walls over future climates. Under historical period, the mean annual total FTCcrit has slightly higher values under Run#2 and Run#9 for ORG and retrofit walls, respectively, while Run#2 and Run#4 resulted in higher maximum annual total FTCcrit for ORG and retrofit wall, respectively. Similar results were observed for other wall orientations using annual total FTCd number. Given that the FT damage risk of internally insulated walls under future climates is of the interest and Run#4 climate

conditions present generally higher risks, the next simulations were carried out using climatic data generated under Run#4 for both historical and future periods.

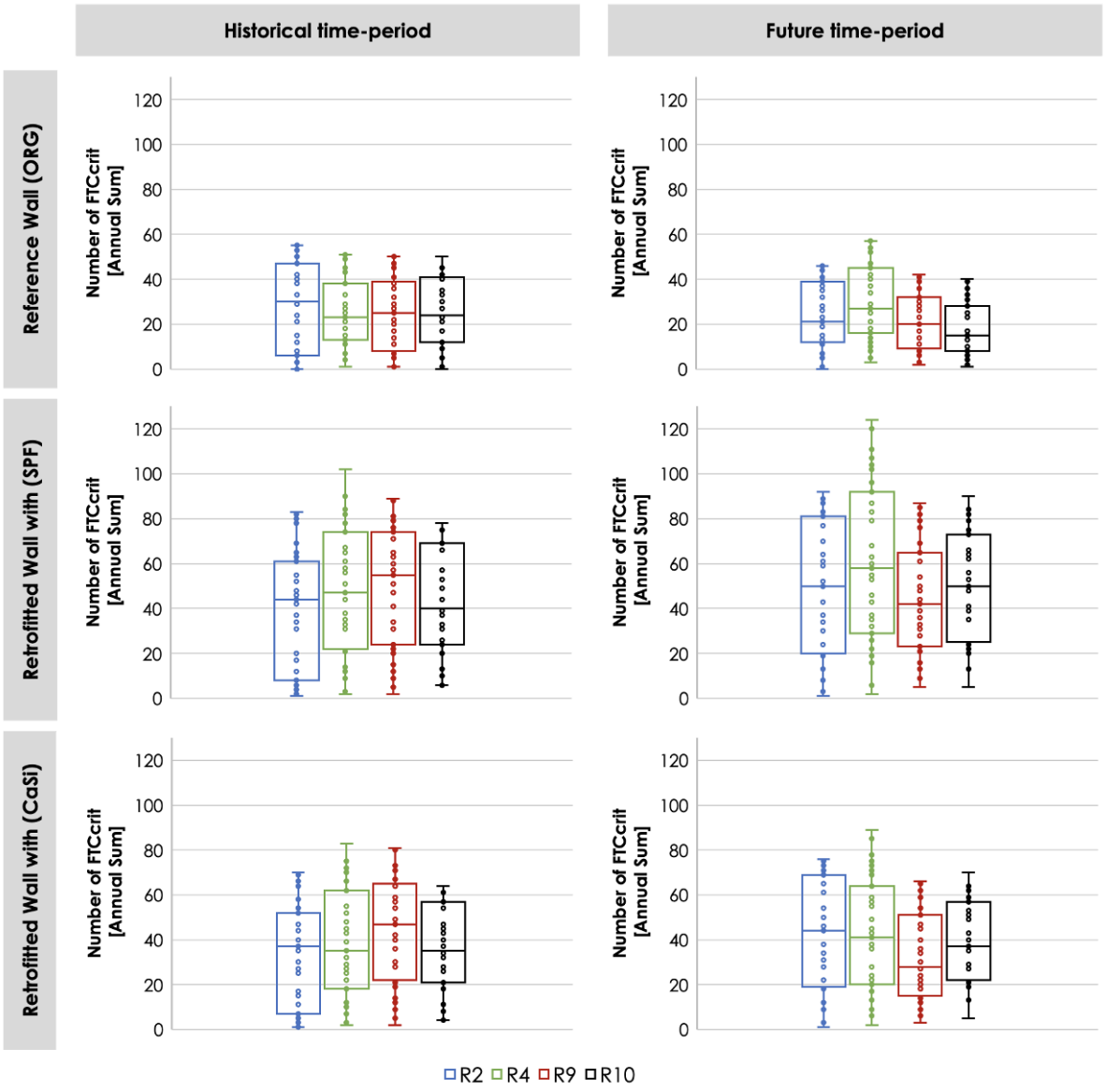

Figure 5-7. Comparison of the annual total number of FTCcrit between four climate realizations (R2, R4, R9 and R10) computed at 5mm from the exterior surface of the brick for a reference wall (ORG) and internally insulated walls with (SPF) and (CaSi). The walls are facing East under the historical and future climate of Ottawa.

5.3.3. Impact of different wall orientations

Figure 5-8 shows the impact of wall orientations on the estimated number of freeze-thaw cycles of old brick masonry walls located in Ottawa and modelled under historical and future climatic loads of Run 4 and Run 9. As mentioned earlier, Run 4 was selected because it presents the most

critical climatic conditions for the occurrence of FT damage over the future period, and Run 9 was used to explore the impact of wall orientations under different climatic conditions and confirm the results obtained with Run 4. The severity of FT damage is assessed based on total numbers of freeze-thaw cycles calculated over the 31-year period using both FTCd and FTCcrit at 5mm from the exterior surface of the brick.

When the number of FTCd is computed, results for the ORG wall show that walls facing North and North-East (NE) experienced the highest number of freeze-thaw cycles among all orientations under the historical time-period of Run 4. A reduced FT damage risk is predicted in the future for ORG walls for most orientations. For instance, it is estimated that the number of FTCd will decrease by half in the future on ORG walls, except for those facing the West, where an increase of 3 freeze-thaw cycles in total is expected. Moreover, although the risk to FT damage is expected to decrease in the future, walls facing North-East and North remain the orientations with the highest damage risk.

For the internally insulated walls with (SPF), the FT damage trend looks somehow similar to the ORG walls under both historical and future time-periods, but with an increased magnitude. It was also observed that facades facing East and North-East (NE) have the highest number of FTCd. And although a reduced risk to FT is predicted in the future for most wall orientations (with an important decrease for SE, South and SW facing walls), an increase of 4 FTCd in total is estimated for North facing walls.

Similar trends are found for both ORG and retrofitted walls when climate conditions of Run 9 were used, however with a reduced severity over the historical period, and the difference due to climate change is less significant.

However, when FTCcrit numbers are computed, results were different and the trend was not as consistent as those obtained using FTCd indicator: a) In general, FTCcrit predicted less freeze-thaw cycles for ORG and retrofitted walls (Run 4) and higher freeze-thaw cycles for (ORG wall) or similar number of freeze-thaw cycles (retrofitted wall) (Run 9) over the historical period , and b) higher freeze-thaw cycles on the North, NE and East orientations in the future, though a more significant drop in FTCcrit is most likely to happen on the South-facing facades. When FTCcrit is used, the FT damage risk is reduced in South-facing façade while increased on the North, NE and the East orientation.

FTCcrit and FTCd were also calculated at different locations (points of investigation) from the exterior surface of the brick, and similar trends were observed.

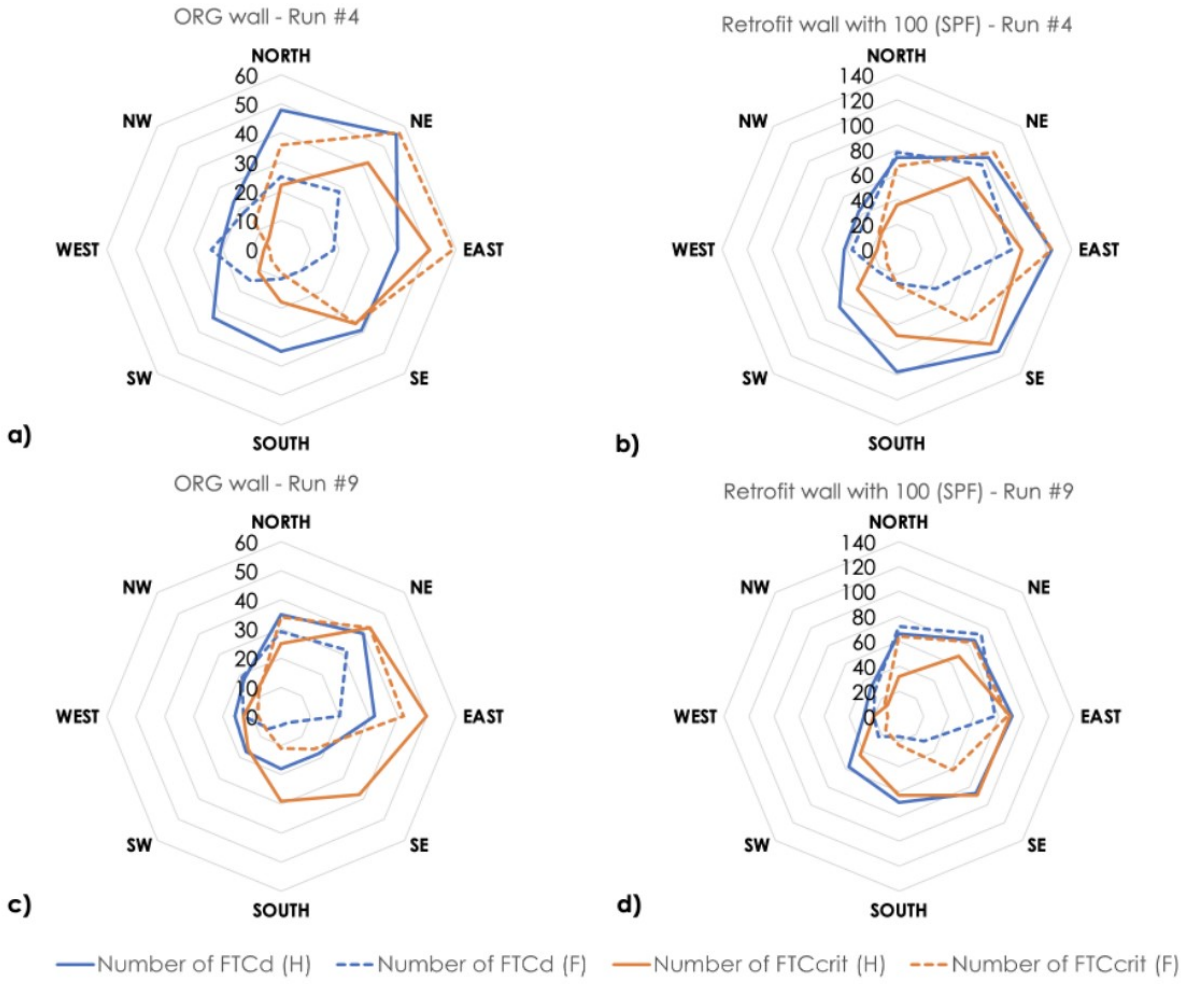

Figure 5-8. Total number of freeze-thaw cycles over the 31-year period using FTCd (blue) and FTCcrit (orange) for an ORG wall (a and c) and a retrofitted brick masonry wall with 100mm SPF (b and d), under the historical and future climate of Ottawa. The climate parameters were generated according to climate realizations: Run #4 and Run #9.

To conclude, it seems that the masonry walls facing East and North-East orientations will suffer from utmost FT damage related problems. Comparing the results with the climatic data under which these simulations were computed, the prevailing direction for wind-driven rain in Ottawa is South-West while the lowest temperatures occur at walls facing North. As shown in Figure 5-2, North facades receive the least amount of WDR, and the South-West façade receives the greatest amount of direct solar radiation and therefore longer hours of warmer temperatures. Whereas East-facing walls receive a significant amount of WDR (especially if observing the wind direction during rain hours and FT season only) and moderated solar radiation compared to South-West

facing walls. Thus, based on the results, the most exposed orientation with respect to the FT damage is considered East for Ottawa. And moving forward, for the selection of MRYs analysis, simulations will be performed for walls facing East.

5.3.4. Impact of rain deposition factor [Fd]

Figure 5-9 shows the impact of rain deposition factor (Fd) on the estimated number of freeze-thaw cycles on old brick masonry walls (original and retrofit) facing East and modelled under historical climate of Ottawa. The potential risk of freeze-thaw damage presented below is the yearly number of freeze-thaw cycles at 5mm depth from the brick exterior surface over 31 years continuous simulations, using FTCd. Similar trend is observed for FTCcrit.

In general, results showed an increase in the number of FTCd when the rain deposition factor increased. This is expected because the higher the Fd, the more severe is the wall exposure to WDR, and hence to moisture. The more moisture reaching the brick surface at freezing temperatures, the greater the risk of FT damage. For an ORG, a maximum of 1 FTCd per year was counted when Fd = 0.35 versus 8 FTCd at Fd = 1.0. The retrofitted walls with SPF have highest number of FTCd; a maximum of 5 cycles per year when Fd = 0.35 and 12 cycles per year at Fd = 1.0. Note that, the yearly number of FTCd did not vary much at lower rain deposition factors. For instance, the ORG wall experienced an increase of around 4 FTCd/year between Fd = 0.35 and 0.5, however, the maximum yearly FTCd number did not change for the retrofitted wall, but more FT events occurred when Fd = 0.5. To sum up, the application of interior insulation is safer when walls are protected from moisture sources and can be risky when walls are fully exposed to WDR. Therefore, moving forward, to reduce the number of simulations, all scenarios will be assumed at high exposure of rain with Fd = 1.0.

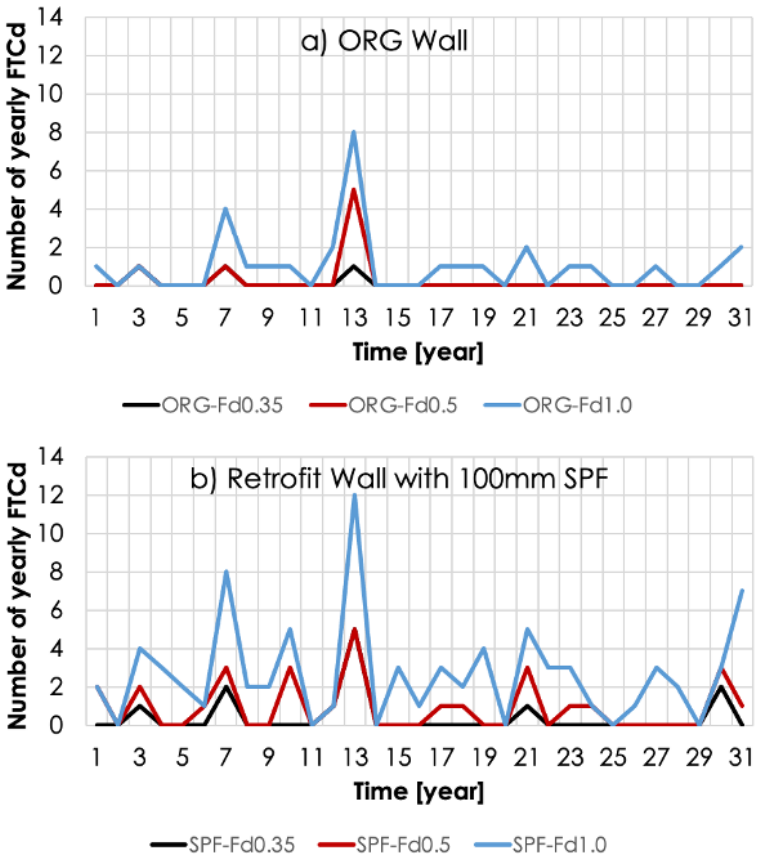

Figure 5-9. Number of yearly freeze-thaw cycles outputted from DELPHIN [FTCd] under different rain deposition factors (0.35, 0.5 and 1.0) for a) a reference wall (ORG) and b) a retrofitted wall with 100mm (SPF) interior insulation at 5mm depth from the exterior brick surface. Walls are assumed to be facing East.

5.3.5. Impact of different insulation systems

Figure 5-10 compares the impact of internal insulation on the FT damage risk of historic masonry walls under a changing climate. Two of the three types of insulation systems (SPF and CaSi) were compared to a reference wall (ORG) through a historical (1986-2016) and future (2062-2092) time-periods. All walls were assumed to include mortar joints at 20cm from the exterior surface of the brick and are facing East and receive an amount of WDR calculated with a deposition factor Fd = 1.0. The FT damage indicators (FTCd and FTCcrit) were computed yearly at 5mm from the exterior brick surface.

A general observation of the results indicates that adding interior insulation will increase the number of freeze-thaw cycles: both FTCd and FTCcrit increased when internal insulation is added. For instance, under a historical climate, an ORG wall received a maximum number of 5 FTCd per year, while yearly FTCd was a maximum of 13 and 10 for SPF and CaSi, respectively. Numbers

of FTCcrit were found slightly different: a maximum of 4, 11 and 7 yearly FTCcrit were recorded for an ORG, SPF and CaSi, respectively. Results also showed that years with the maximum number of cycles were different between the two FT damage indicators; however, the number of FT cycles were very close for both time-periods using the same FT damage indicator. In addition, results for different climate realizations and wall orientations followed a similar pattern but of different level. However, this paper only presents results for walls facing the East.

Different damage indicators predicted different responses under the future climate: counting the maximum yearly number of FTCd estimated a reduced FT risk by 4 to 5 FTCd; but a similar FT risk for FTCcrit in the future (the maximum yearly FTCcrit number was 11 for SPF wall and 7 for CaSi under historical and future years). However, the yearly average number was somehow consistent: it decreased by one cycle per year for FTCd and increased by one cycle per year for FTCcrit in the future. Despite this difference, the overall FT damage risk will increase when internal insulation is applied – the most critical case is when SPF is used.

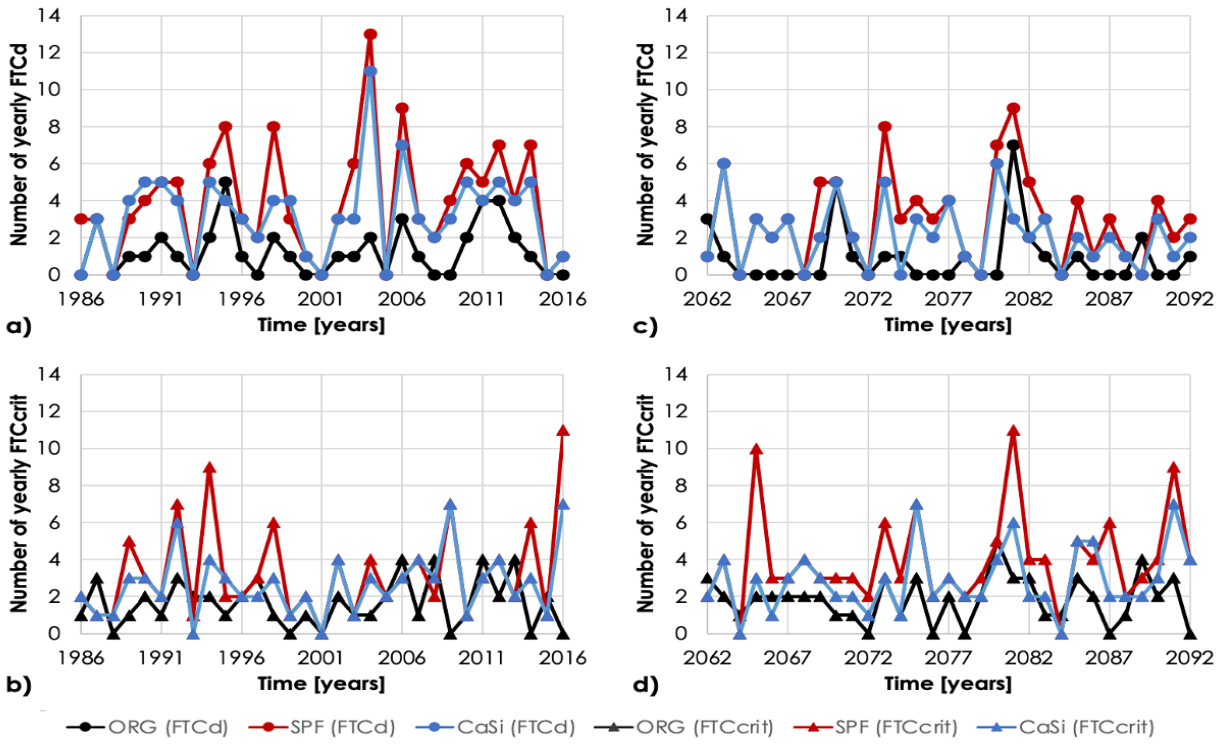

Figure 5-10. Comparison of the yearly number of freeze-thaw cycles between a reference wall (ORG) and two internally retrofitted walls (SPF and CaSi) facing East under historical (Fig. 10-a and b) and future (Fig.10-c and d) time-periods. Results were computed for two FT damage indicators: FTCd and FTCcrit.

5.3.6. Comparison between 31Y and single years

Following the methodology outlined in Section 5.1, the severity of FT damage of ORG and retrofit walls with 100mm of SPF are ranked and **Error! Reference source not found.** lists a summary o f the top four "single" years ranked in a descending order according to their FT damage severity based on annual total FTCd and FTCcrit numbers.

Results showed that the ranking of the years are different for the two types of wall assemblies. For instance, the top four years ranked to have the greatest number of FTCd for the ORG under a historical climate are: 1995, 2012, 2011, 2004 and 2006. However, for an internally retrofitted wall with 100mm SPF, the years are: 2004, 2006, 1998, 2012 and 2014. Besides, the top four future years with the highest number of FTCd are: 2063, 2091, 2070, and 2080 for (ORG) and 2081, 2080, 2073, and 2063 for (SPF) walls (Table 5-4).

Table 5-4. Summary of the top four "single" years ranked in a descending order according to their FT damage severity when using two simulation-based indices (FTCcrit and FTCd).

Simulation-based index	Climate	Wall type	Years ranking (descending order of the FT damage risk)			
			First	**Second**	**Third**	**Fourth**
FTCd	H	ORG	1995	**2012** 2011	**2004** **2006**	1987
		SPF	**2004**	**2006**	1998	**2012** 2014
	F	ORG	**2063**	2091	2070	**2080**
		SPF	**2081**	**2080**	**2073**	**2063**
FTCcrit	H	ORG	2014	1992	**2006** 2007 **2012**	2009
		SPF	2016	1994	2009	1992
	F	ORG	**2063** **2081**	**2065**	**2073** **2080** 2091	2067
		SPF	**2081**	**2065**	2091	2075

(H): Historical time-period; (F): Future time-period; (ORG): masonry wall in its original state (reference wall); (SPF): retrofit wall with extruded polystyrene insulation.

Moreover, the ranking of years was found different for different FT damage indicators. Only a few years were ranked equally when using the number of FTCcrit and FTCd. Those years are 2006 and 2063 for the reference wall (ORG) and 2081 for the retrofit wall (SPF). Other years were selected among the most severe ones but had different ranking with different FT damage indicator and different wall types (those years are marked in bold). For example, when counting the FTCd numbers, year "2004" was ranked the third for the (ORG) wall and the first for the (SPF) wall. Also, year "2080" was ranked the fourth for the (ORG) wall but the second for the (SPF) wall

when FTCd are counted. The same year was ranked third when FTCcrit is calculated for the (ORG) wall.

The ranking of "single" years helped to determine the severity of weather conditions of individual years on the FT damage risk of brick masonry constructions. One question to answer in this paper is whether one single year simulation can represent the FT damage risk obtained from simulation over the 31 consecutive years, thus, MRY selected based on single-year can assess the long-term FT damage for brick walls. To answer this question, we need to investigate whether the annual FT cycle of a particular year is influenced by the previous year's weather conditions, in other words, whether an accumulative effect of weather events exist for FT damage, like mold growth, which is influenced by the sequence of weather events. Therefore, the number of FT cycles obtained from single year simulation alone were compared to the number of FT cycles obtained for the same year but from the 31-year consecutive simulations (Figure 5-11). This analysis was done based on the yearly number of FTCd since more common years were found using this damage indicator.

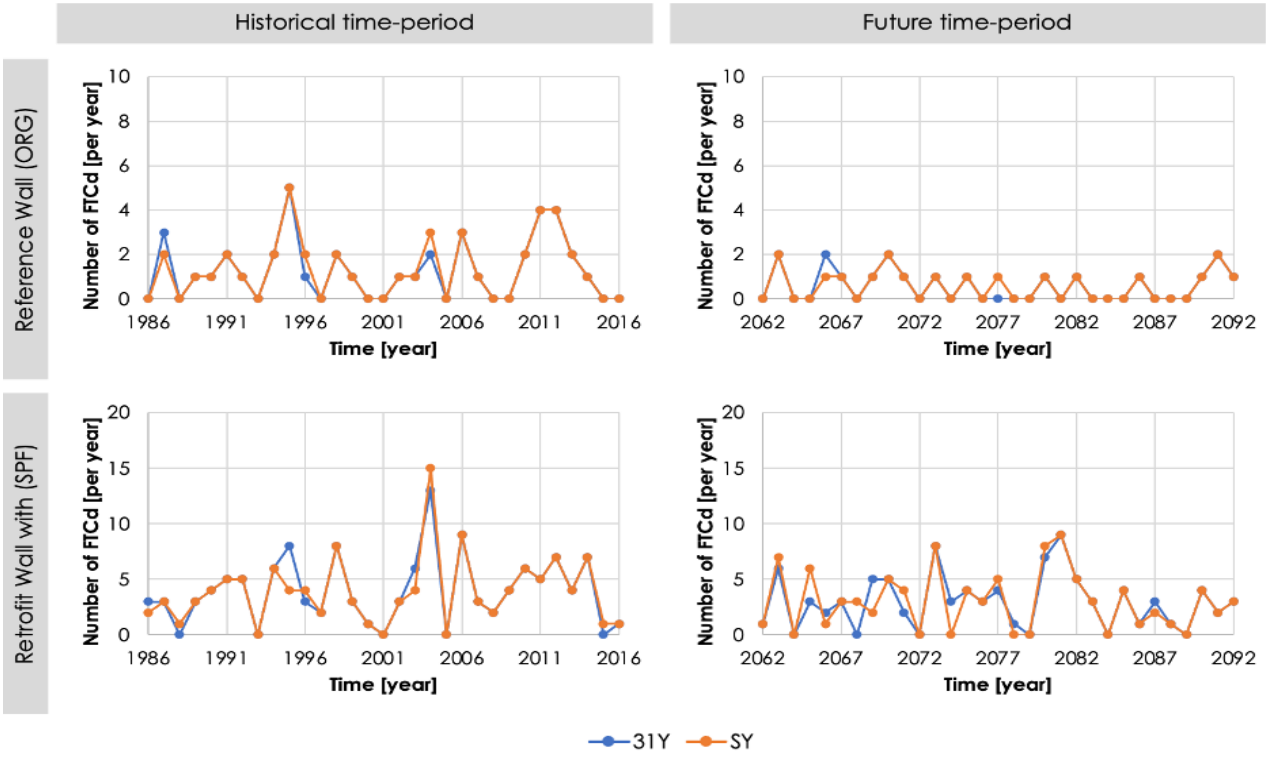

Figure 5-11. The total number of freeze-thaw cycles (FTCd) per year following consecutive simulations of 31-year period (31Y) in blue, and when each year is simulated alone as a single year (SY) in red. This comparison was done for an ORG wall and a retrofit wall with 100mm of SPF.

Table 5-5. The average and maximum yearly FTCd number and the total count of FT damage events obtained for an ORG wall and three internally insulated walls with 100mm of: SPF, CaSi and MY – under historical (H) and future (F) time-periods.

	ORG				SPF				CaSi				MW			
Time-period	H		F		H		F		H		F		H		F	
Sims	31Y	SY	31Y	SY	31Y	SY	31Y	SY	31Y	SY	31Y	SY	31Y	SY	31Y	SY
Average	1	1	0.5	0.5	4	4	3	3	3.2	3.2	2	2	3.5	3.5	2.5	2.5
Max.	5	5	2	2	13	15	9	9	9	11	6	6	28	26	7	7
No. of FT damage events	20	20	14	15	26	28	25	24	28	27	25	24	10	12	26	24

Table 5-6. Summary of the top four "single" years ranked in a descending order according to their FT damage severity for an ORG wall and three internally insulated walls: SPF, CaSi and MW.

Climate	Wall type	Ranking of the years (descending order of the FT damage risk)			
		First	**Second**	**Third**	**Fourth**
H	ORG	1995	2012 2011	**2004** **2006**	1987
	SPF	**2004**	**2006**	1998	2012 2014
	CaSi	**2004**	**2006**	2012 2014	1998
	MW	**2004**	**2006**	1998 2012 2014	1991 2010
F	ORG	**2063**	2091	2070	**2080**
	SPF	2081	**2080** 2073	**2063**	2065
	CaSi	**2063**	**2080**	2073	2065
	MW	2081	**2063** 2073 **2080**	2065	2070 2077

As shown in Figure 5-11, the yearly numbers of FTCd obtained through SY simulations are very similar to those obtained by the consecutive 31Y simulations. This is more evident for the ORG wall; however, the discrepancies found for the retrofitted wall were very minimal and for a few years. A closer analysis of these results indicated that the maximum yearly FTCd was 13 and 15, for 31Y and SY, respectively for a historical climate; whereas for the future period, the maximum reached 9 FTCd for both 31Y and SY simulations. In addition, the average number of yearly FTCd were identical for both 31Y and SY simulations: an average of 4 FTCd was obtained under the historical climate and an average of 3 FTCd was predicted under a changing climate (Table 5-5).

A further analysis comprised the evaluation of 31Y and SY simulation results for two additional insulated walls with CaSi and MW. Results obtained matched closely between 31Y and SY simulations. This implicates that freeze-thaw damage does not have the accumulative effect, and therefore single years' simulations (SY) could be used to select an MRY for each time-period.

To select a reliable simulation-based MRY for FT damage assessment, a severe year should be commonly found between the different wall assemblies. According to ASHRAE 160, this year should be the 93rd percentile year in severity, which corresponds to the second highest in a 30-year period. Following ASHRAE's requirement, the MRY should be 2006 for the historical period and 2080 for the future period (Table 5-6). These years were selected based on retrofitted walls ranking, rather than the ORG wall because the FT damage risks of retrofitted walls for future years is of importance and interest. Additionally, even though years 2006 and 2080 are not ranked second for the ORG walls, but they are found among the first four years in terms of FT damage severity. Also, comparing the selected MRYs with the second highest years ranked according to the ORG wall, the difference in their severity is minor. Comparing 2012 and 2006, the difference is only 2 FTCd per year. The difference between 2091 (ranked second highest for ORG) and 2080 (the selected MRY) was 1 FTCd per year (Figure 5-11).

Another approach to select simulation-based MRYs is to find the common worst year for all the constructions. This approach was suggested by (Geving, 1997; Rode, 1993; Sanders, 1996). Accordingly, the MRYs should be 2004 and 2080. These MRYs were also found in compliance with retrofitted walls of 50mm and 200mm insulations.

5.4. Conclusions

Selecting a moisture reference year (MRY) to assess freeze-thaw damage related problems is a challenging task. Previous studies have shown that climate-based indices do not lead to a reliable selection of MRY for the assessment of freeze-thaw damage risk of internally insulated historic masonry walls. To fill this gap, a methodology was developed in an attempt to select an MRY based on hygrothermal simulations and to verify whether it could be applied for as many scenarios as possible. Ottawa is chosen as an example. First, we identify the parameters that have the greatest influence on FT damage through parametric analysis. Then, simulations are performed for a continuous 31-year period and for each single year. A comparison of the results suggest that FT damage has no accumulative effect; and therefore, MRYs can be selected as the single year with

the 93rd percentile FT damage severity or the worst year commonly found between masonry walls pre and post retrofit. The application of MRYs was then verified for different insulation types and thicknesses. Results showed that simulation-based MRYs are construction and orientation dependent; however, they are reliable to use for retrofitting design decision making. In summary, the primary findings are as follows:

- A comparison between an isotropic brick and a heterogenous brick with mortar joints configurations showed that both configurations lead to a similar FT damage response at locations close to the external surface of the brick masonry. However, the use of an isotropic brick configuration in simulations results in higher FT damage severity within the brick, which highlights the importance of a more accurate representation of masonry walls.
- Comparing climate realizations based on their climatic parameters (e.g., the annual total amount of WDR, or the yearly average ambient temperature) is not accurate for assessing the risk to FT damage of masonry walls, because FT damage occurs at the concurrence of wetting and sub-zero temperature within the brick – which needs the hygrothermal conditions of the brick to identify. Therefore, based on a previous study, four out of the 15 climatic realizations that have the lowest error to the 90th percentile were selected for comparison. For Ottawa, the climate realization with the greatest impact on the FT damage risk of historic masonry structures (Run#4) was different than the one accounting for the highest amounts of WDR over both historical and future periods (Run#10).
- In contrast to most previous studies assuming the prevailing WDR direction as the most critical to consider when assessing the occurrence of FT-related damage, this study shows that the WDR direction during the frost season can better represent the orientation having the highest risk to FT damage. Although the prevailing WDR direction is south-south-west (SSW) for Ottawa, wall assemblies facing East were at a higher risk to FT damage given that for FT damage to occur, both the degree of wetting and temperature fluctuations above and below the freezing point are required. As such, when analyzing the most critical orientation for the risk to FT-damage, the combined effect needs to be evaluated accordingly, not simply the amount of WDR.
- The application of internal insulation will change the hygrothermal response of masonry walls, and thus, increase the risk of FT damage. This is expected, given that the insulation will prevent heat flow through the wall, that, in turn, makes the wall colder and more vulnerable to FT

damage during freezing season. Results also showed that it is riskier to use SPF than CaSi insulation – this too is expected – since CaSi has capillary active structure and lower vapour resistance factor (μ), in contrast to that of SPF, and fundamentally, CaSi wicks away any moisture accumulation from the surfaces to which the insulation has been applied.

- The two commonly used FT damage indicators, FTCd and FTCcrit do not provide consistent FT damage risk prediction for future climates although they have a strong correlation. Based on the FTCd, the FT damage risk will most likely decrease for historic masonry walls, prior and post-retrofit. However, FTCcrit predicted an increased FT damage risk mainly on walls facing North, NE and East, and a reduced risk on other orientations.
- The comparison shows that annual FT cycles obtained from 31-year consecutive simulation is very similar to single-year simulation, which indicates that yearly weather variation has little accumulative effect on annual FT cycles, therefore, single-year simulation results can be used to represent long-term performance for the MRY selection.
- The simulation-based MRYs are location, construction and orientation-dependent, therefore, to select an MRY suitable for the assessment of FT damage, a series of parameters must be investigated first to determine the most influential conditions on the risk to FT damage. The proposed approach in this paper for the selection of a simulation-based MRY proved to be applicable for retrofitting decision making.

Chapter 6. The Impact of Interior Insulation on Historic Masonry Buildings in Ottawa under Present and Future Climates

6.1. Introduction

The preservation of cultural values in historic buildings and the enhancement of their energy performance may initially appear to be conflicting. For instance, it is not always possible to apply thermal insulation to the exterior walls while preserving their facades. In such situations, internal insulation measures need to be explored, which are currently considered as the most challenging retrofit measure for historic buildings. Assessing the compatibility of insulation materials in respect to moisture retention within historic masonry structures and their impact on the long-term moisture performance of such structures, is a crucial element to consider when evaluating different insulation options. The literature indicates that the implementation of internal insulation to historic brick masonry walls in respect to changing climate conditions presents significant challenges and risks related to managing moisture and preserving structural integrity. It is therefore important to thoroughly evaluate the potential risks associated with moisture-related problems such as freeze-thaw damage of masonry structures.

In this chapter, recommendations are provided for enhancing the energy efficiency of older historic buildings whilst maintaining their moisture safety by examining methods for internal insulation. The primary aim was to explore the feasibility of insulating masonry walls of historical structures internally, without affecting their long-term durability, nor their cultural significance. To achieve this goal, the hygrothermal behavior of historic masonry walls is investigated before and after retrofitting using internal insulation, in response to both historical and future climate loads. The investigation includes various factors such as local climate conditions, building type, as well as brick and insulation materials properties.

Hygrothermal simulations for a 31-year period were performed to predict the risk of freeze-thaw damage to the masonry structures. The risk of freeze-thaw damage was evaluated by determining the number of freeze-thaw cycles using the FTCd indicator, as provided from the output of the DELPHIN simulation model. Solid masonry construction was widely used in the Ottawa region a hundred years ago. This method was commonly employed in the construction of farmhouses and numerous heritage buildings (“Solid Masonry,” 2022). Therefore, Ottawa was selected as the study

location to conduct a comprehensive analysis on the potential effects of climate change on the freeze-thaw damage of internally insulated brick masonry walls of older historic buildings. The simulations included hourly climatic parameters for both historical and future climate periods, allowing for a thorough evaluation of the effects of climate change on the risk to freeze-thaw damage in this Canadian location.

6.2. Methodology

6.2.1. Wall assemblies

The brick material was modelled for different configurations: a) full brick (20cm) followed by mortar joints, thereafter half a brick (10cm); b) three half-bricks (10cm each) with mortar joints in between, and c) Two full bricks (20cm each) with mortar joints in between. The geometry of the different wall assemblies is provided in Figure 6-1. Two historic brick materials were selected from the DELPHIN materials database, these included: Old Building Brick Persiusspeicher (referred to as Brick A), and Old Brick Dresden (referred to as Brick B). These two brick materials have been found to have similar properties to the exterior reclaimed bricks "ERUL" and "ERUH" found in Canada. These brick materials are considered typical and have average FT resistant properties, measured experimentally by Aldabibi (Aldabibi et al., 2022), with a critical degree of saturation (S_{crit}) of 55% and 45%, respectively, for Brick A and Brick B. As for the mortar, a historical mortar was selected from the DELPHIN material database. All material properties are listed in Table 3-3.

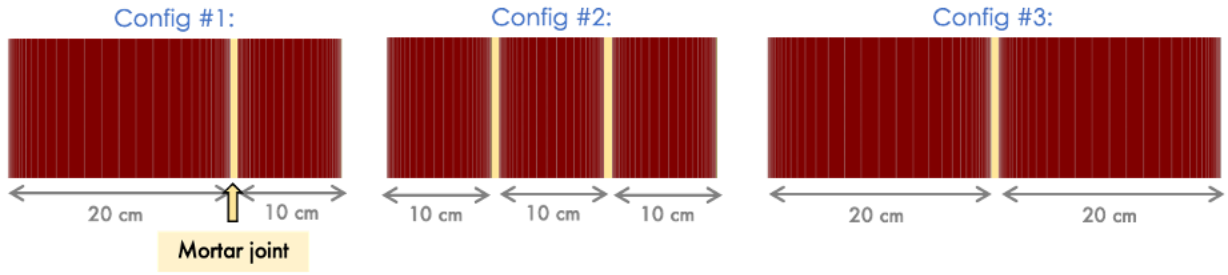

Figure 6-1. The brick material was modelled for different configurations: a) full brick (20cm) followed by mortar joints, then half a brick (10cm), b) three half-bricks (10cm each) with mortar joints in between, and c) Two full bricks (20cm each) with mortar joint.

6.2.2. Wall orientations

The orientation of masonry walls can significantly affect the exposure of the masonry wall to environmental loads, including wind-driven rain and solar radiation, thereby influencing the

potential for moisture accumulation and freeze-thaw damage. Hence it is of particular importance for building preservation practitioners when implementing insulation retrofit solutions to consider the effect of wall orientation on the risk to freeze-thaw damage of masonry walls.

By integrating the understanding of wall orientation into preservation plans, practitioners can tailor insulation solutions and mitigation strategies to address the specific hygrothermal loads posed by different orientations, ultimately safeguarding the long-term integrity of historic masonry in the face of evolving climate conditions. As such, this study was carried out for eight different orientations: North, North-East (NE), East, South-East (SE), South, South-West (SW), West and North-West (NW).

6.2.3. Boundary conditions

The indoor and outdoor boundary conditions have already been introduced in Section 3.4.3. However, in this chapter additional parameters have been included, such as building typology (building height, roof type, environmental exposure), wall orientation, and the resulting amount of WDR in respect to the different wall orientations. These are included to assess the potential risk of FT damage under a wide range of scenarios. The additional parameters are introduced in the sub-section below.

6.2.3.1. WIND-DRIVEN RAIN (WDR)

Similarly to that presented in previous chapters, the amount of WDR impinging on the building envelope was calculated according to the method given in ASHRAE 160 (ANSI/ASHRAE, 2021). However, in this Chapter different building heights were considered under different exposure categories and roof types (different deposition factors).

As such, in regard to building height, a low-rise (<≤ 10m) and a medium rise building (> 10m and <≤ 20m) were assumed under sheltered, medium, and severe exposures, having exposure factors (Fe) = 0.7, 1.0 and 1.4, respectively (Table 6-1). Different rain deposition factors (Fd) were also assumed for walls below a: steep-slope roof, for which Fd = 0.35; low-slope roof, Fd = 0.5 and; Fd = 1.0, for walls subject to rain runoff (Table 6-2).

Table 6-1. WDR exposure factor (F_E) adapted from (ANSI/ASHRAE, 2021).

Building height (m)	Type of exposure category		
	Severe	Medium	Sheltered
< 10	1.4	1.0	0.7
> 10 and ≤ 20	1.4	1.2	1.0

Table 6-2. WDR deposition factor (F_D) adapted from (ANSI/ASHRAE, 2021).

Deposition factors (F_D)	Roof type
0.35	Walls below a steep-slope roof
0.5	Walls below a low-slope roof
1.0	Walls subject to rain runoff

6.2.4. Performance indicators for assessing wall performance

The risk of freeze-thaw damage was computed using the number of critical freeze-thaw cycles obtained from DELPHIN (FTCd). The formation of ice in DELPHIN is taken into account by assuming the instantaneous equilibrium between the three phases (vapor, liquid, and ice), and by applying a freezing point depression whilst assuming that the pore space fills from the smallest to the largest pore and that ice crystalizes outside of the liquid phase (Nicolai et al., 2013; Sontag et al., 2013). The use of this model permits investigating whether the moisture content is sufficiently high to fill pores where water could freeze. In this paper, one FT cycle was counted when the ice volume rate (IVR) was lower than the minimum value of 0.55 and 0.45 (corresponding to the value for S_{crit} of the bricks as chosen in this paper). The ice volume rate or IVR is the ratio of the ice volume to the pore volume. According to the literature, even a few freeze-thaw cycles can trigger significant degradation of a brick masonry wall. Straube et al. (2010b) and Ueno et al. (2013b, 2013a) observed a degradation in samples, examined after 6 cycles, whereas in numerous other instances FT damage has been shown to occur after 20 to 30 cycles. van Aarle et al. (2015) proposed that damage occurs once the brick is subjected to 25–35 cycles of freezing and thawing. Thus, in referencing to (Choidis et al., 2023), the relation between the number of freeze-thaw cycles and the actual damage is presented in Table 6-3.

Table 6-3. Risk for mechanical damage of the masonry wall based on the number of freeze-thaw events – adapted from (Choidis et al., 2023).

Number of freeze-thaw cycles	Risk to mechanical damage
0	No damage
1 – 5	Damage possible
6 – 35	Damage likely
> 35	Observable damage

6.2.5. Simulation scenarios

The findings from the previous chapter (Chapter 5) suggested that simulation-based MRYs are dependent on the wall construction, as well as their location and orientation. However, in this chapter, a comprehensive analysis is provided of the potential impacts of climate change on FT damage to internally insulated historic brick walls. Accordingly, simulations were carried out over a continuous period of 31 years for each time-period. Only one climate projection was examined (i.e., Run #4), as previous findings, provided in previous chapters, have indicated that Run #4 represents the most severe scenario for the occurrence of FT damage (Sahyoun et al., 2024). Given, as well, the number of freeze-thaw cycles is cumulative, the results at the end of the simulation period were evaluated. The input parameters for the hygrothermal simulations are listed in Table 6-4, below.

Table 6-4. Input parameters for hygrothermal simulations.

Input Parameter	Variation	Description
Location	1	Ottawa
Time period	2	Historical (1986-2016) | Future (2062-2092)
Wall orientation	8	North (N), North-East (NE), East (E), South-East (SE), South (S), South-West (SW), West (W) and North-West (NW)
Rain deposition factor	3	0.35, 0.5 and 1.0
Rain exposure factor	3	0.7, 1.0 and 1.4
Brick types	3	Brick A (S_{crit} = 0.55), Brick B (S_{crit} = 0.45), and Brick C (S_{crit} = 0.8)
Brick thickness	3	300mm: One full brick (200mm) followed by mortar joints, then half a brick (100cm) | 300mm: Three half-bricks (100mm each) with mortar joints in between | 400mm: Two full bricks (200mm each) with mortar joints in between.
Internal insulation type	3	Spray Foam Polyurethane (SPF), Mineral Wool (MW), and Calcium Silicate (CaSi)
Insulation thicknesses	3	50mm, 100mm and 200 mm

6.3. Results and discussion

The risk to the occurrence of freeze-thaw damage of brick masonry walls is influenced by several factors that need to be carefully considered during construction and before any retrofit project. These factors include the material properties of the brick masonry, the presence of moisture, the rate of water absorption, the type of insulation used, and the environmental conditions to which the wall is exposed. Understanding how these factors interact and affect the resilience of masonry walls is essential for designing and building structures that can withstand freeze-thaw cycles without sustaining significant damage.

This section presents results on the impact of different insulation materials, the impact of different brick types of brick masonry and brick unit thickness, as well as the effect of wall orientation and exposure factors on the FT damage response of historic masonry wall assemblies before and after retrofit. By examining these factors through a parametric analysis, one can gain valuable insights into the specific parameters that play a significant role in minimizing the risk of freeze-thaw damage in brick masonry walls.

6.3.1. Impact of different insulation materials

In general, the projected risk to FT damage risk will most likely decrease in the future if no insulation is added to masonry walls having Brick A, with the exception of walls facing West – where the risk to FT damage is expected to slightly increase in the future (i.e., increase of 3FTCs) (Figure 6-2). However, adding even a small layer (i.e., < 50 mm) of insulation will increase the risk of FT damage for most façade orientations. Comparing the impact of insulation systems used to internally retrofit historic masonry walls, it was observed that the risk FT damage is highest when applying SPF insulation and is lowest when using CaSi. It is clearly shown in Figure 6-2, that uninsulated walls facing East will receive a total number of 20 freeze-thaw cycles in the future. The difference between this uninsulated wall (ORG_F) and when SPF insulation is added can vary between 60 and 77 FTCs depending on the insulation thickness applied. This difference is reduced when MW and CaSi insulations are applied to the retrofit and vary between 45 to 68 FTCs and 35 to 55 FTCs, respectively. Similar trends are predicted for most wall orientations, however, each with a different magnitude. For example, a West-facing wall would still experience an increased risk in FT damage when interior insulation is applied, but the difference is much less significant:

An increase of 9 to 12 FTCs, 5 to 10 FTCs, and 5 to 8 FTCs is expected for walls insulated with SPF, MW, and CaSi, respectively.

It is also important to note that the impact of both insulation type and thickness on the risk to FT damage of retrofit walls is more significant on those walls facing North, North-East, and East as compared to wall orientations of South-West, West and North-West, where the difference between retrofit strategies is minimal. It was also observed that insulating the latter facades will have little to almost no impact on the FT damage response of walls in the future. Figure 6-3 shows that the difference between non-insulated and internally insulated walls was found between 4 to 15 FTCs on West facing orientations. Whereas it is anticipated that the remaining orientations will receive a much higher number of FTCs, particularly those facing East and North-East, where minimum expected FTCs are of 30 for insulated walls using 50mm of CaSi, and a maximum of 77 FTCs for walls insulated using 200mm of SPF.

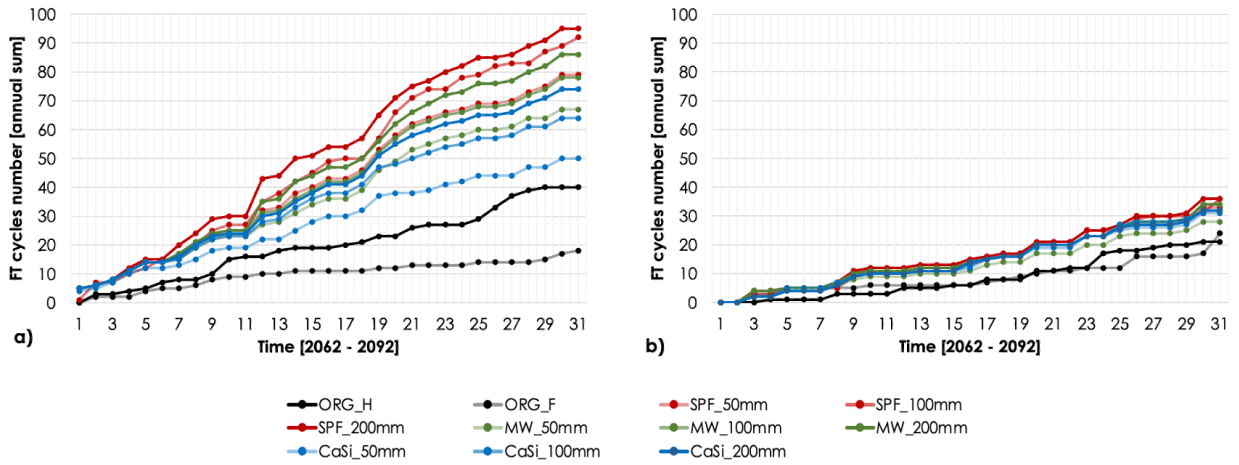

Figure 6-2. The Impact of different insulation types and thicknesses on the number of freeze-thaw cycles (FTCs) obtained on brick masonry walls (Brick A) facing a) East, and b) West orientations in the future (2062-2092).

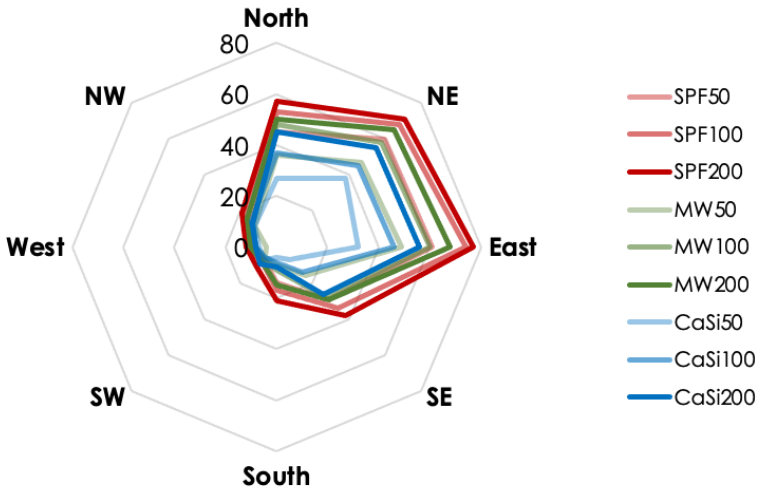

Figure 6-3. The difference of freeze-thaw cycles (FTCs) number between non-insulated walls and different internally insulation strategies on brick masonry walls (Brick A) facing 8 different orientations in the future (2062-2092).

6.3.2. Impact of different brick types

It is clear that masonry walls with Brick B will experience a higher number of freeze-thaw cycles than walls built with Brick A – both pre (Figure 6-4) and post-retrofit (Figure 6-5) – and under both historical and future time-periods. When walls are conserved in their original state (before any insulation is added), the risk to FT damage will most likely decrease for walls with Brick A under a changing climate. However, it is expected that walls with Brick B will experience an increased risk to freeze-thaw damage. It is also evident and common that both brick types will endure an increased amount of FT damage on their Northern and Eastern facades. Moreover, the difference of FTCs between these two wall types was less significant for walls facing West, North-West and North during the historical time-period. This difference increases significantly in the future (Figure 6-4).

When walls are internally insulated, the FT damage response of walls with either Brick A or Brick B increases in the future regardless of the type of insulation used. Figure 6-5 illustrates the difference in values of FTCs between retrofitted walls and walls in their original state in the future. This difference is calculated by subtracting the total number of FTCs obtained when walls are internally insulated from the total number of FTCs obtained prior to a retrofit ($\#FTCs_{\text{insulated walls}}$ - $\#FTCs_{ORG}$). This allows to understand the alteration of the initial state of masonry walls if internal insulation is applied. Results for both types of masonry walls show an increased potential for the occurrence of FT damage in the future; however, the damage differs in magnitude. It is evident

that masonry walls of Brick B will have a much more severe level of FT damage. For example, it is estimated that adding a 100mm SPF insulation will increase the number of FTCs on East facing walls by a maximum of 75 FTCs for walls of Brick A, and 220 FTCs for walls of Brick B. Although walls of Brick B will receive a greater number of FTCs; however, this number represents double the number of FTCs if walls are not insulated, as compared to five times the total number of FTCs for walls of Brick A. Moreover, walls with either brick types will experience a substantial risk to FT damage on their Northern and Eastern facades as compared to the walls facing the West orientation. South facing walls with Brick B will most likely have a high risk to FT damage. The type of insulation that induces the greatest amount of damage is SPF, followed by MW and finally CaSi, for which CaSi insulation has a much lower severity in FT damage when combined with walls having Brick B, as compared to the other two insulation systems (Figure 6-5).

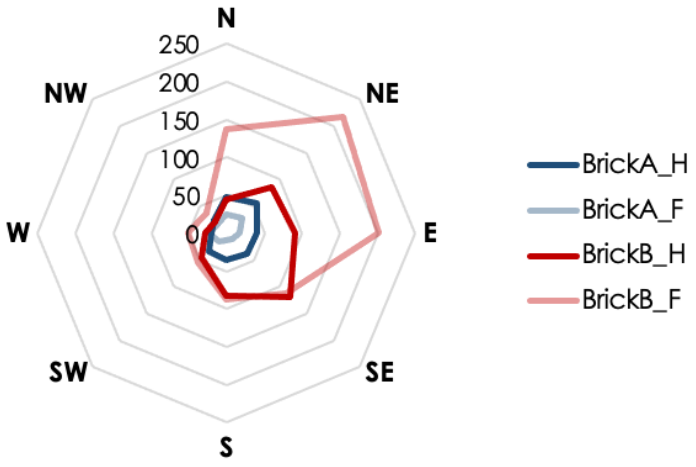

Figure 6-4. Numbers of (FTCs) obtained for two different masonry walls (before any insulation is added): Brick A (blue) and Brick B (red), after 31 years of simulations under historical (H) and future (F) time-periods.

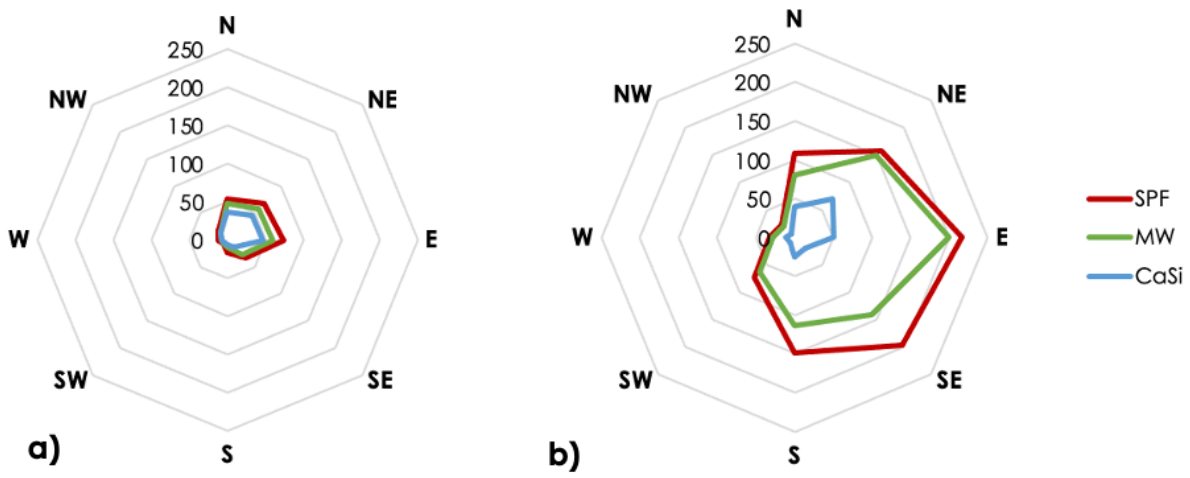

Figure 6-5. The difference in the number of (FTCs) between internally insulated walls (using 100mm of insulation) and original walls using two types of bricks: a) BrickA, and b) BrickB, obtained in the future (2062-2092).

6.3.3. Impact of brick masonry thickness

The impact of brick masonry thickness was investigated through the use of hygrothermal modelling to assess the response of historic masonry wall assemblies before and after retrofit. In Figure 6-6, the total number of FTCs obtained for uninsulated and insulated walls with 100mm incorporating SPF insulation is illustrated, showing both type of walls with different brick masonry assemblies of varying geometry and thicknesses: i) One full brick (20cm) followed by mortar joint, then half a brick (10cm) (in red), ii) Three half-bricks (10cm each), with mortar joints between bricks (in green), and iii) Two full bricks (20cm each) with mortar joints between bricks (in blue). Results show that under both historical and future climates, the brick masonry assemblies of varying geometry thicknesses did not have a major influence on the number of FTCs obtained for insulated walls facing different orientations. However, the difference was more significant for uninsulated walls facing North and East, where a 40cm thick masonry wall resulted in a higher number of freeze-thaw cycles than the two other scenarios. This could be explained given that thicker walls lead to prolonged moisture drying times due to delayed moisture dispersion within the structure of the wall, causing the moisture to accumulate at the exterior brick surface. The fact that no major differences were observed among different brick thicknesses when internal insulation is applied brings to attention the crucial role an internal insulation can play in managing moisture distribution within historic masonry walls. As such, if the addition of interior insulation is being considered for the retrofit of brick masonry walls, it is of particular importance to select an

insulation material that not only provides the necessary thermal benefits, but also helps regulate moisture levels within the masonry walls.

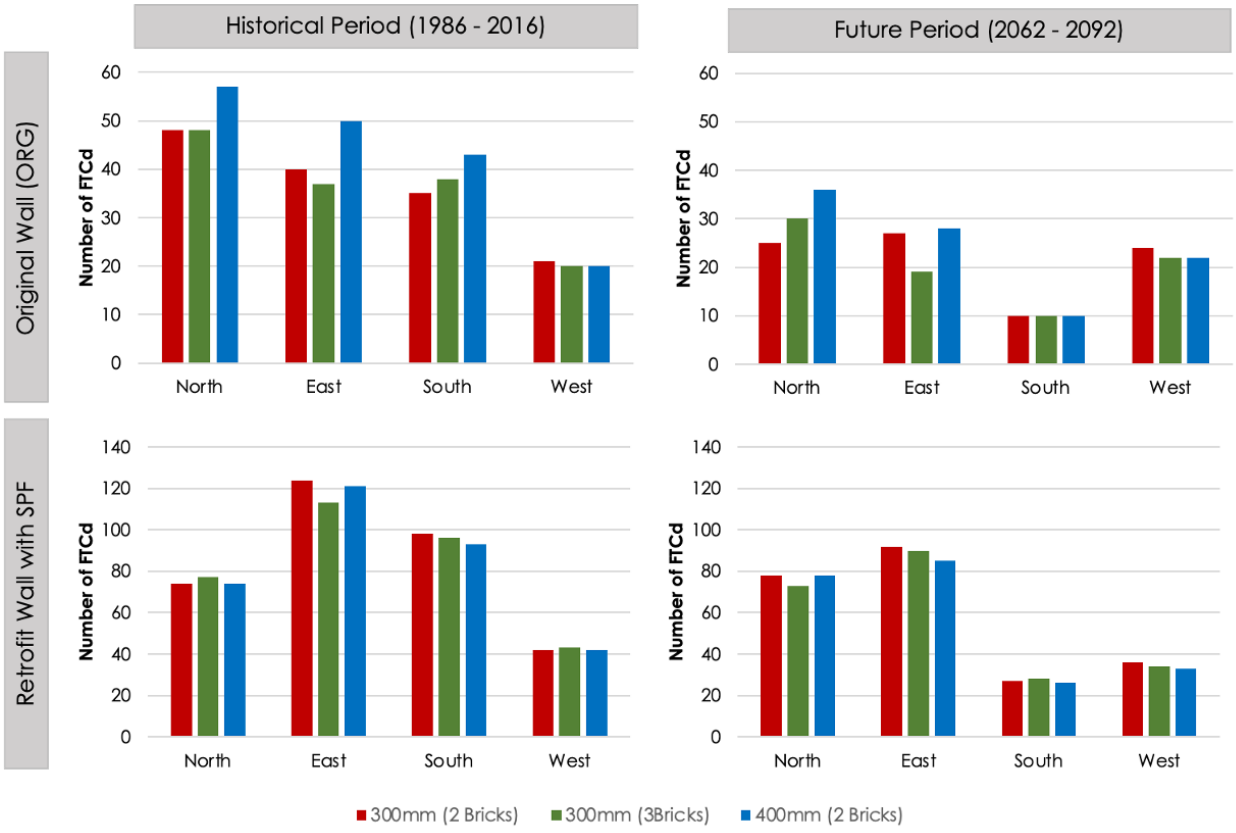

Figure 6-6. Total number of FTCs obtained for (ORG) and retrofit wall with 100mm (SPF) having different brick masonry geometry and thicknesses: i) one full brick (20cm) followed by mortar joints, then half a brick (10cm), ii) three half-bricks (10cm each) with mortar joints in between, and iii) Two full bricks (20cm each) with mortar joints in between.

6.3.4. Impact of different wall orientations and exposure factors

In Figure 6-7, the total number of FTCs for masonry walls with Brick A is presented in their original state (ORG), as obtained in the future following 31-years of continuous simulation. The walls face eight different directions and are subject to different wind-driven rain exposure and deposition factors. For ORG walls (before any insulation is added), it was obvious that at high exposure conditions (i.e., Fe = 1.4) and elevated rain deposition factors (i.e., Fd = 1.0), freeze-thaw damage will most likely occur on all walls facing any of the eight orientations. A more observable damage is predicted on the North and NE facing walls. Whereas at lower exposure conditions (i.e., Fe = 0.7 and Fd = 0.35), no damage is expected on walls facing South and SE, and only a possible damage is anticipated for all the remaining orientations. Results obtained at factor

values between the high and low extremes (i.e., when Fe = 1.0 and Fd = 0.5), showed that no FT damage will occur on walls facing SE, possible FT damage might occur on walls facing South and SW, whereas for all remaining orientations, FT damage is likely to occur. These results indicate that even without any retrofit measures, some of the historical masonry walls (i.e., those using brick having an "average" value for S_{crit}) in their original state are at risk of FT damage in the future.

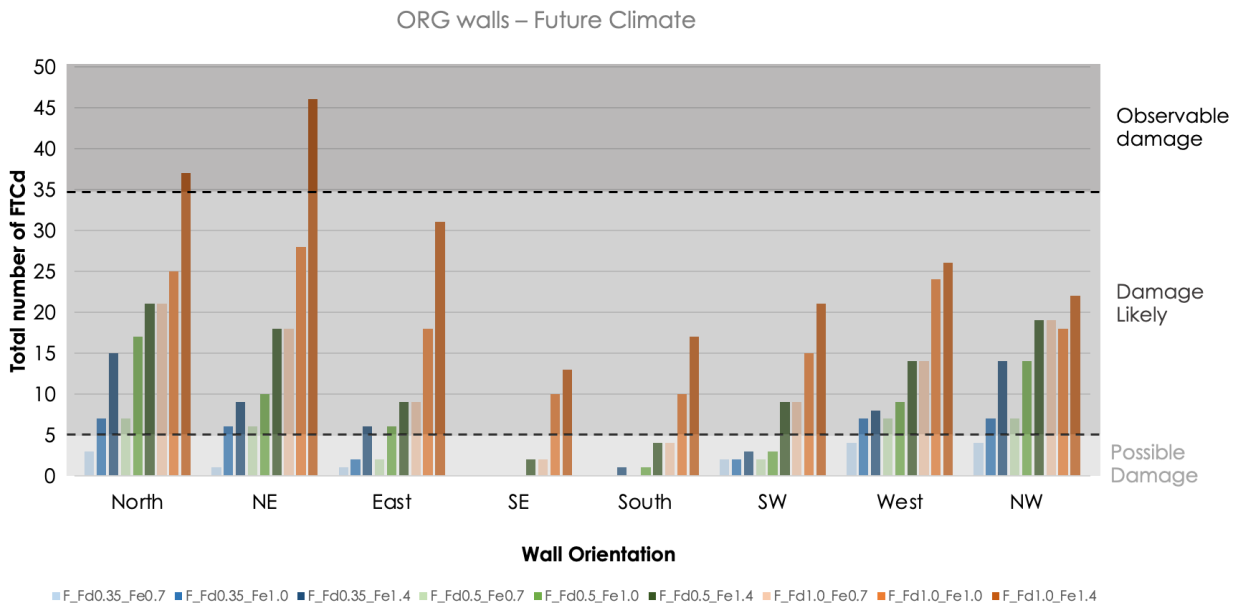

Figure 6-7. The total number of FTCs for ORG walls (Brick A) obtained in the future at different orientations and under different exposure and rain deposition factors.

Furthermore, the impact of different interior insulation systems and insulation thickness was assessed for different wall orientations and subjected to different exposure and rain deposition factors. This allows comparing the wall response to their initial conditions, understand whether the choice of a particular interior insulation is feasible for given scenarios, without damaging the existing structure. On the basis of this information, solutions to mitigate the potential FT damage for high-risk situations can then be determined. It was perhaps evident from a review of Figure 6-7 and Figure 6-8, that adding interior insulation will increase the risk to FT damage. It was also apparent that for situations of high rain deposition and exposure, all walls will most likely be subjected to damage likely or observable damage, regardless of the type, and level of insulation added. For all internally insulated walls, a 100mm of SPF will most likely lead to observable FT damage for high levels of exposure (i.e., Fe = 1.4 and Fd = 1.0). The risk is expected to be less for

South, SW, West and NW facing walls retrofit with 100mm of MW and CaSi insulation. Furthermore, under low exposure levels (i.e., Fe = 0.7 and Fd = 0.35), MW and CaSi were found safe to be applied on walls facing SE and South, whereas possible damage is expected for the remaining wall orientations.

A summary of the predicted mechanical FT damage for pre- and post-retrofit masonry walls under different rain deposition and exposure factors in the future was provided in Table 6-5. This includes the combination of the different types of insulation materials and their respective thicknesses, WDR exposure levels and the orientation of walls. It is clear that the more severe the exposure level, the higher the risk to FT damage. Also, although MW and CaSi are better insulation options for internally retrofit projects than SPF, they could also possibly cause damage for some type of buildings under medium and high WDR exposure.

Moreover, Figure 6-7, Figure 6-8 and Table 6-5 provide information on the occurrence of FT damage in the future at the end of 31 years. However, it was necessary to understand the time and duration over which FT damage is instigated. In Figure 6-9, the trendline for the number of freeze-thaw cycles number obtained in the future (2062-2092) is provided for brick walls in their original state (ORG) and when internally insulated. In this figure, walls are assumed facing North, and are subject to different rain deposition and exposure factors. The threshold value of 5 FTCs indicates the onset of likely damage (LD), and the threshold for the onset of observable damage (OD) is given as 35 FTCs. In general, results indicate that under low rain deposition and exposure factors (Figure 6-9-a and -b) possible FT damage (PD) is expected to occur starting at year 5, and year 25 for insulated and uninsulated walls, respectively. Likely FT damage (LD) is also expected to occur starting at year 12 when 100mm and 200mm of SPF is applied, and at year 20 for the remaining insulated walls (when Fd=0.35 and Fe=0.7). However, a LD will most likely start earlier (at year 8) for all insulated walls when Fd=0.35 and Fe=1.0, and as well, when Fd=0.5 and Fe=0.7. Moreover, the higher the rain deposition and exposure factors, the earlier the damage is predicted to occur. For instance, a possible occurrence of FT damage (PD) could start as early as year one, followed by a likely FT damage (LD) starting at years 4 to 5 for both insulated and non-insulated walls. It is also anticipated that an observable damage (OD) will most likely occur between years 14 and 20 for insulated walls, as compared to year 29 for uninsulated walls (Figure 6-9-f). Results for other walls orientation are summarized in Figure C3 – Figure C8 (Appendix C).

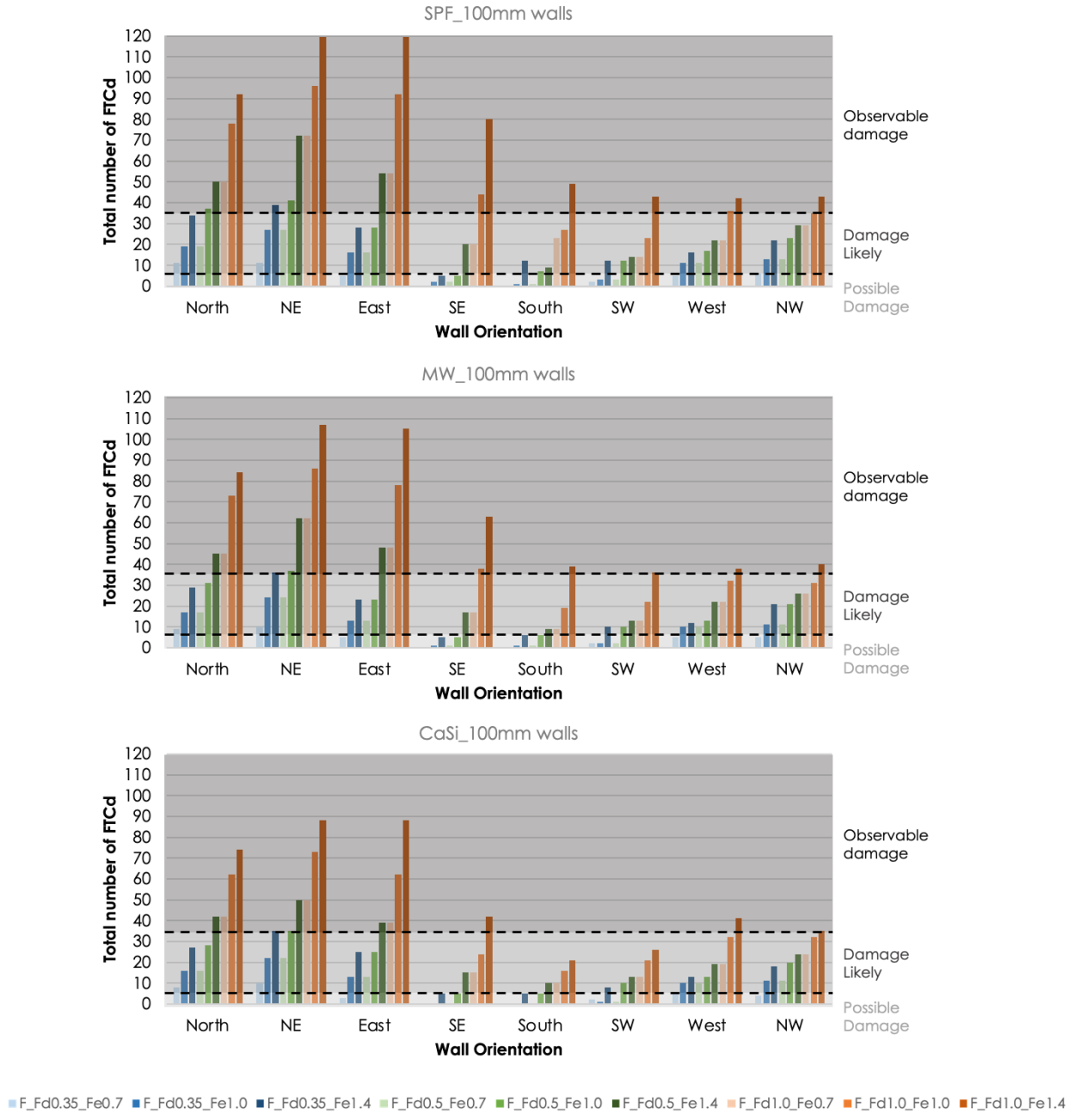

Figure 6-8. The total number of FTCs obtained under a future climate, for internally insulated masonry walls (of Brick A) with 100mm of a) SPF; b) MW; and c) CaSi at different orientations and under different exposure and rain deposition factors.

Table 6-5. Summary of the predicted mechanical FT damage for pre- and post-retrofit masonry walls under different rain deposition and exposure factors in the future.

Wall Type	Wall Orient.	Fd = 0.35; Fe = 0.7	Fd = 0.35; Fe = 1.0 & Fd = 0.5; Fe = 0.7	Fd = 0.35; Fe = 1.4 & Fd = 0.5; Fe = 1.0	Fd = 0.5; Fe = 1.4 & Fd = 1.0; Fe = 0.7	Fd = 1.0; Fe = 1.0	Fd = 1.0; Fe = 1.4
ORG	North	PD	LD	LD	LD	LD	OD
	NE	PD	LD	LD	LD	LD	OD
	East	PD	PD	LD	LD	LD	LD
	SE	ND	ND	ND	PD	LD	LD
	South	ND	ND	ND	PD	LD	LD
	SW	PD	PD	PD	LD	LD	LD
	West	PD	LD	LD	LD	LD	LD
	NW	PD	LD	LD	LD	LD	LD
SPF	North	LD	LD	LD (50-100mm) OD (200mm)	OD	OD	OD
	NE	LD	LD	OD	OD	OD	OD
	East	PD	LD	LD (50-100mm) OD (200mm)	OD	OD	OD
	SE	ND (50-100mm) PD (200mm)	PD	PD (50-100mm) LD (200mm)	LD	OD	OD
	South	ND (50-100mm) PD (200mm)	PD	LD	LD	LD (50-100mm) OD (200mm)	OD
	SW	PD	PD	LD	LD	LD	OD
	West	PD	LD	LD	LD	LD	OD
	NW	PD	LD	LD	LD	LD	OD
MW	North	LD	LD	LD	OD	OD	OD
	NE	LD	LD	LD (50-100mm) OD (200mm)	OD	OD	OD
	East	PD	LD	LD	OD	OD	OD
	SE	ND	ND (50mm) PD (100-200mm)	PD	LD	LD (50mm) OD (100-200mm)	OD
	South	ND	ND (50mm) PD (100-200mm)	PD	LD	LD	LD (50mm) OD (100-200mm)
	SW	PD	PD	LD	LD	LD	LD (50mm) OD (100-200mm)
	West	PD	LD	LD	LD	LD	OD
	NW	PD	LD	LD	LD	LD	OD
CaSi	North	LD	LD	LD	OD	OD	OD
	NE	LD	LD	LD	OD	OD	OD
	East	PD	LD	LD	OD	OD	OD
	SE	ND	ND (50-100mm) PD (200mm)	PD	LD	LD	LD (50mm) OD (100-200mm)
	South	ND	ND (50-100mm) PD (200mm)	PD	LD	LD	LD
	SW	PD	PD	LD	LD	LD	LD
	West	PD	LD	LD	LD	LD	LD (50mm) OD (100-200mm)
	NW	PD	LD	LD	LD	LD	LD (50mm) OD (100-200mm)

ND: No Damage (0 FTC); **PD**: Possible Damage (1 – 5 FTCs); **LD**: Likely Damage (6 – 35 FTCs); and **OD**: Observable Damage (> 35 FTCs)

Colors indicates the severity of the mechanical FT damage; where green is used for a (ND) scenario, lighter gradient of orange is used for (PD) and (LD) scenarios and the darker orange for (OD) situations.

It was also noticed that the type of insulation and the insulation thickness have no significant impact on the possible damage and the likely start times for FT damage. For instance, all internally insulated walls could be subjected to a possible FT damage or a likely FT damage at around the same time (i.e., possible damage is predicted as early as the first year and a likely damage could occur anytime between 3 to 8 years in the future). However, the effect from the use of insulation was more significant at that time of an observable FT damage event. For example, observable FT damage is predicted to occur between years 22 to 24, 25 to 30, and 27 to 30 when SPF, MW and CaSi insulations are used, respectively (Figure 6-9-d). This difference becomes even greater with the increased levels of exposure (Figure 6-9-e and Figure 6-9-f).

In addition, an overall analysis of the findings indicated that the influence of insulation type and insulation thickness is minimal at low exposure levels. It becomes more significant at high levels of exposure (i.e., higher levels of Fd > 0.5 and Fe > 0.7), as expected, due to an increased amount of WDR making the walls more wet, and therefore, resulting in longer drying times as compared to that which occurs for low exposure scenarios.

A consistent pattern of FTCs was also noted across various thicknesses of insulation. However, with greater insulation thickness, an earlier occurrence of FT damage was observed. This aligns with expectations, given that thicker insulation results in an exterior surface of the brick wall having reduced temperatures, leading to protracted moisture drying times due to a delayed distribution of moisture throughout the wall.

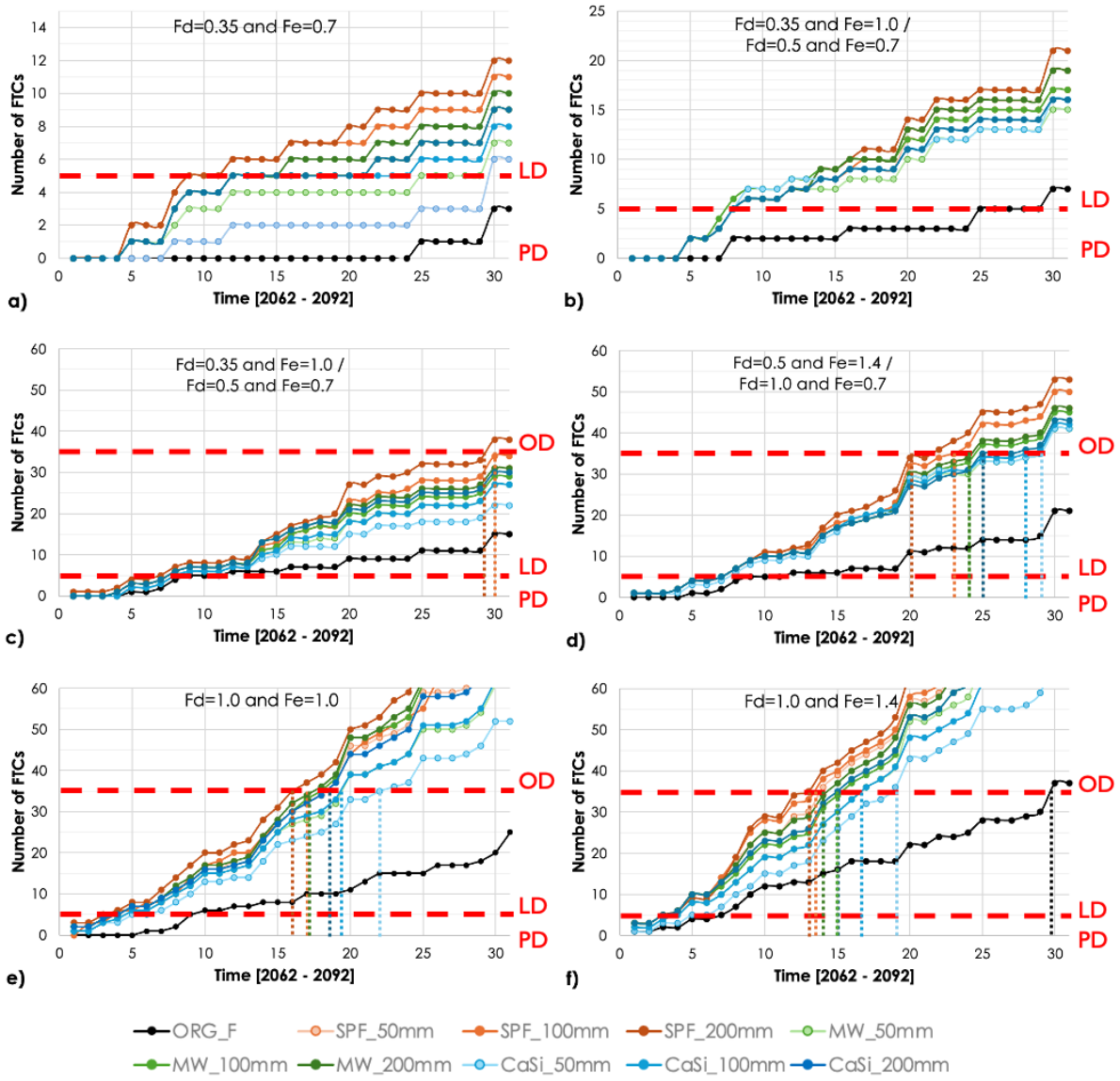

Figure 6-9. The freeze-thaw cycles number obtained in the future (2062-2092) for brick walls in their original state (ORG) and when internally insulated. Walls are facing North and are subject to different rain deposition and exposure factors.

6.3.5. Discussion and potential solutions

Based on the findings presented in previous sections, it is evident that adding internal insulation will increase the risk to FT damage of historic masonry walls. However, it is still possible to insulate heritage masonry structures internally without compromising their durability in the future. In Table 6-6, a summary is provided of the predicted mechanical FT damage and the applicability of interior insulation under the different parameters discussed in this study. It is useful to note that this study was mainly conducted using an average brick type (i.e., having average frost resistant

properties), and therefore, it is not recommended that these buildings be internally insulated if they are exposed to high levels of WDR (i.e., when walls are not sheltered, and walls are subject to rain runoff). Moreover, several scenarios were shown where interior insulation could be safely applied, and conversely, when caution was needed.

Table 6-6. The predicted mechanical FT damage and the applicability of interior insulation

		Internal insulation is applicable	**Careful application of internal insulation**	**Internal insulation is not recommended**
Freeze-thaw damage		No visible damage (ND)	Possible or likely damage (PD and LD)	Visible damage/ Observable damage (OD)
Exposure to rain and typology of existing walls (Fd and Fe)	Fd=0.35 & Fe=0.7	- All walls facing South and SE.	- Walls facing West, SW and NW: PD after 17 years. - Walls facing North, NE and East: PD could occur in 5 years and LD is expected earlier when 200mm of SPF insulation is used.	
	Fd=0.35 & Fe=1.0; Fd=0.5 & Fe=0.7	- Walls insulated with MW and CaSi facing South and SE.	- Walls with SPF insulation facing South and SE: PD starting after 12 years. - Walls facing West and NW: PD occurring between 7 to 16 years, and LD might occur after 20 years on average. - Walls facing North, NE and East: PD and LD occurring as early as the 5th and the 8th year.	
	Fd=0.35 & Fe=1.4; Fd=0.5 & Fe=1.0		- Most walls except NE and East: PD starting between 1 to 12 years, and LD occurring between 7 to 20 years. - Walls facing North, NE and East: PD and LD occurring as early as the 4th and the 8th year.	- Walls with SPF and MW facing NE: OD occurring between the 24th and the 29th year in the future.
	Fd=0.5 & Fe=1.4; Fd=1.0 & Fe=0.7		- Walls facing South, SE, SW, West and NW: PD starting at 3-5 years, and LD starting between 6 – 15 years. -Walls facing North, NE and East: PD occurring as early as the first year and LD between 3 to 7 years in the future.	- All walls facing North, NE and East are at risk of OD, starting as early as 14 years in the future when SPF is applied.
	Fd=1.0 & Fe=1.0		- All walls facing South, SW, West and NW: PD starting at 3 years, followed by LD.	- Walls facing North, NE, East and SE are at risk of OD starting at 12 years in the future.
	Fd=1.0 & Fe=1.4		-Walls facing South, SW, West and NW	All walls will possibly experience OD in the future: - Uninsulated walls facing North and NE will experience OD in 25 years in the future. - Walls facing North, NE, East and SE: OD starting at 10 years.

Since the main factors influencing the onset of FT damage are the temperature fluctuation above and below freezing point, the moisture load, and the frost resistance of the brick masonry material, one should think of ways to reduce the impact of these factors. While it is almost impossible to change/modify the climatic conditions to which historic buildings are exposed, one should think about other alternatives to mitigate the effect of climate change while preserving these buildings for the future generations. One way to reduce the severe exposure to WDR is the installation of overhang or physical elements to protect the building envelopes at risk to FT damage. However, this option may not be feasible and prohibited due to cultural and architectural conservation purposes. Therefore, one potential solution could be the improvement of the brick masonry units and their replacement with better frost resistive bricks. Since no brick material with high frost resistant properties was tested, we have used the same Old Building Brick Persiusspeicher (Brick A) with the same properties, but only modified its critical saturation degree (from S_{crit} = 55% to S_{crit} = 80%). Simulations were performed for different wall orientations and under high WDR exposure levels using different insulation types and thicknesses. Results in Figure 6-10 compares the freeze-thaw cycle numbers (FTCs) between an average brick (S_{crit}=55%) and frost-resistant brick (S_{crit}=80%) under the future climate of Ottawa. Walls were assumed to be facing East. It is obvious that the critical saturation degree property of the brick has a major influence on its FT damage response. For instance, using a better brick material quality (S_{crit}=80%) resulted in zero FTC number; and it was the case regardless of the insulation system used, wall orientation and WDR amount to which historic structures are exposed. It is therefore safe to suggest the replacement of brick masonry units (mainly those under high exposure of WDR) for internal insulation retrofit projects if the budget allows it.

Based on the findings of this study, we suggest the preliminary decision-making guideline below for internal insulation retrofit projects (Figure 6-11). The procedure includes situations where: i) insulation is safe to be applied on the interior wythe of historic brick walls, ii) internal insulation could be applied with caution, and iii) internal insulation is not recommended. It also includes solutions to situations where interior insulation is regarded as critical. The recommendation is based on FTC analysis, and interstitial condensation wasn't part of the evaluation criteria.

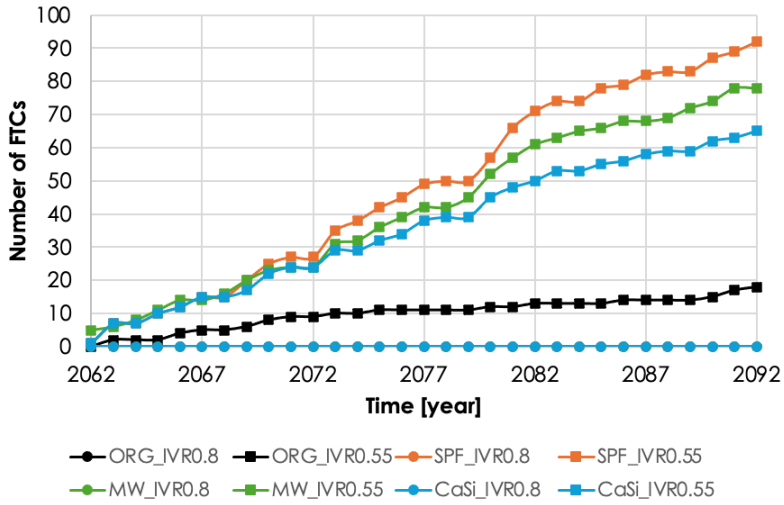

Figure 6-10. A comparison of values for freeze-thaw cycling (FTCs) between an average brick (S_{crit}=55%) and frost-resistant brick (S_{crit}=80%) under future climate loads of Ottawa. Walls are assumed to be facing East and subjected to high exposure levels.

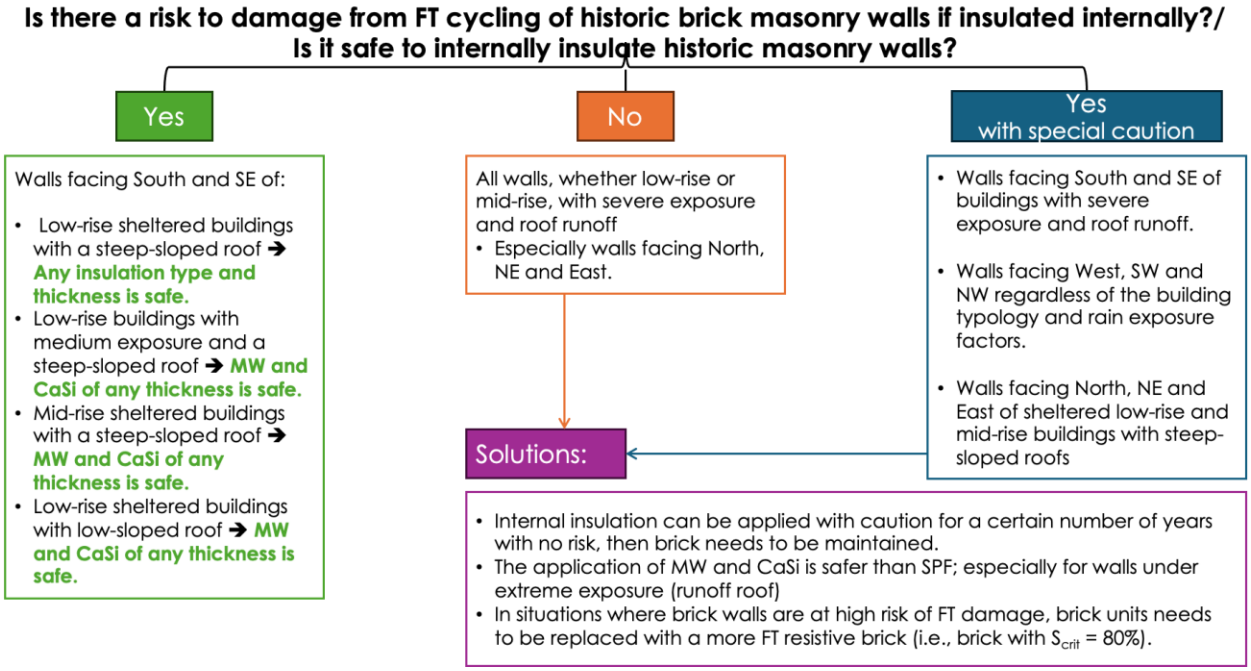

Figure 6-11. Preliminary decision-making procedure for internal insulation retrofit projects for historic brick masonry walls.

6.4. Conclusions

This study aims to develop a preliminary decision guideline to improve the energy performance of historic buildings through inspecting internal insulation measures. The goal was mainly to investigate whether it is possible to internally insulate historic masonry walls without compromising their cultural identity and durability for the years to come. To address this objective, this chapter investigated the hygrothermal response of historic masonry walls, prior to and post-retrofit under Ottawa's changing climate. The study involves many parameters related to the climatic conditions of the chosen location, the building typology and the material properties of brick and insulation materials. At first, this study compares the performance of two brick masonry units of average frost resistance value (tested in Canada) and then compared their response to a better frost resistant brick. Three different configurations of the brick masonry were modelled: i) one full brick (20cm) followed by mortar joints, then half a brick (10cm), ii) three half-bricks (10cm each) with mortar joints in between, and iii) Two full bricks (20cm each) with mortar joints in between. Three insulation systems of different types and thicknesses were considered. And wall assemblies were assumed to face eight cardinal orientations and exposed to different levels of WDR. The main findings of this study could be summarized as follow:

- Adding interior insulation to historic brick walls can have a significant impact on their durability. Selecting the appropriate insulation solution requires an understanding of the hygrothermal characteristics of both the materials within the current wall and potential insulation systems. This study showed that for the same insulation material the higher the thermal resistance of the insulation added, the higher the potential FT damage risk. And while there are some situations where any insulation types and thicknesses are safe to be applied, more scenarios include carefulness or prohibition over applying any insulation. It was also found that applying MW and CaSi results in lower FT cycles compared to using SPF.
- One of the major factors affecting the occurrence of FT damage is the quality of the existing brick units. Before considering any retrofit measure, it is important to assess the hygrothermal response of masonry walls in their original state under current and future climate conditions. It is also vital to compare internal insulation strategies to the original state of the walls in order to evaluate the risk incurred when insulation is applied. This study showed that different brick types can have a significant influence not only on the durability of the wall assemblies; but

also, on the anticipated pattern of FT damage in the future. For example, a brick with higher frost resistance properties (Brick A) is likely to have lower risk of damage from freezing and thawing in the future. Conversely, it was expected that a less resistant brick (Brick B) will face an increased risk. Besides, the modelling and thickness of the brick masonry did not have a major influence on the number of FTCs obtained for insulated walls facing different orientations.

- The orientation towards which wall assemblies are facing have a great impact on the amount of WDR impinging on these structures, and therefore, integrating the understanding of wall orientation into preservation plans can inform the selection of suitable insulation materials to effectively manage moisture movement and minimize the risk of freeze-thaw damage. In general, walls facing North, NE and East will have a higher risk of FT damage, while walls facing towards the South, SE and West have a reduced risk.
- Other factors contributing to the alteration of the amount of WDR is the building typology, its roof and its immediate surrounding. Under different exposure levels and scenarios, uninsulated and insulated masonry walls responded very differently. When walls are protected and sheltered, interior insulation could be applied in certain situations. However, when walls are under high levels of WDR exposure, cautions in applying interior insulation are required.

Based on the parametric analysis, this study presents an initial decision-making procedure for internal insulation retrofit projects. It also suggests some solutions in situations where high level of caution is required. To ensure the long-term preservation of historic brick walls, it is crucial to consider the replacement of brick masonry units with those that possess enhanced durability and resistance to freeze-thaw cycles. By replacing the existing brick masonry units with more resilient alternatives, the structural integrity of the walls can be significantly improved. Selecting the appropriate replacement brick masonry units involves careful consideration of their hygrothermal properties and ability to withstand the effects of freeze-thaw cycles. It is therefore essential to choose units that exhibit low water absorption and resistance to frost action. These properties will help prevent moisture penetration, reduce the potential risk for damage caused by freezing and thawing, and ensure the continued stability of the brick walls.

Another factor that should be part of the decision-making and preservation plan of brick masonry structures – that has not been covered through this study – is the crucial role that mortar joints play

to maintain the rigidity and durability of masonry structures. Future work should include a proactive preservation and maintenance strategy to ensure the continued integrity and longevity of historic brick walls. Regular inspections and maintenance activities such as repointing mortar joints, repairing damaged bricks, and addressing any signs of deterioration are vital to prevent and mitigate the impact of environmental factors, including freeze-thaw cycles. In conclusion, a holistic approach that encompasses insulation material selection, replacement of brick masonry units, and proactive preservation and maintenance strategies is essential for safeguarding the integrity and longevity of historic brick walls. In this study, Ottawa is selected as a case study. The methodology and framework developed in this study can be applied to other geographical locations and will be integrated into upcoming research.

Chapter 7. Contributions, Conclusions and Future Work

7.1. Contributions

This research was intended as an investigation of the potential for internally insulating historic brick masonry walls without compromising their long-term strength and structural integrity in response to varying future climatic conditions. In order to meet this primary goal, hygrothermal simulations were necessary to assess the existing condition of the walls and their performance subsequent to the implementation of internal insulation. Considering the investment of time and resources in conducting long-term simulations, as well as the benefit of choosing a single moisture reference year to accurately represent the climate over an extended period and assess the impact on building materials over time, initially, as part of this study, the effectiveness of current climate-based indices was assessed to identify a suitable MRY for evaluating freeze-thaw damage risk to masonry walls. However, when it was shown that the methods for selecting climate-based MRYs were not useful to adequately represent the actual performance of brick masonry walls, an alternative method to select MRYs was then sought, based on hygrothermal simulations of specific types of brick masonry construction. A parametric analysis was also developed in this study to permit evaluating the potential risk to FT damage associated with the application of internal insulation using a combination of climatic factors, moisture load, and as well, material properties. The contributions include:

- A review of publications available for the conservation, rehabilitation, and restoration of historic buildings in North America – with a particular consideration given to historic buildings of masonry construction.
- An evaluation of existing climate indices to assess the risk to freeze-thaw damage of internally insulated masonry walls.
- A parametric analysis to identify the parameters that have the greatest influence on freeze-thaw damage.
- A methodology developed for the selection of MRYs based on the results derived from hygrothermal simulations of multiple scenarios with a variation of parameters, including, material properties, moisture loads, and climate conditions.

- The verification of the application of simulation-based MRYs for different insulation types and thicknesses. These MRYs are wall assembly construction and orientation dependent; however, they are reliable for use in decision making for the design of brick masonry wall retrofit.
- An evaluation of the freeze-thaw damage response pattern under current and future climate loads.
- A preliminary decision guideline to improve the energy performance of historic buildings while maintaining the moisture safety of bricks with internal insulation.
- Solutions proposed for instances where the application of internal insulation is at high risk to the historic masonry structures.

7.2. Conclusions

Adding interior insulation to historic brick walls can have a significant impact on their durability. The choice of insulation material is crucial in ensuring the preservation of the brick walls over time. It is of importance to consider the hygrothermal properties of the insulation material to prevent any adverse effects on the historic structure.

7.2.1. Conclusions regarding existing climate-based indices

- The correlation between climate-based indices and response-based indices is weak, indicating that solely using climate-based indices does not accurately reflect the freeze-thaw damage risk of brick masonry wall assemblies.
- The rankings derived from climate-based indices showed a stronger correlation with the FTDR index ranking, but the findings were not consistent and differed across various climate scenarios.
- Different simulation-based indicators can result in different year rankings for each time period, leading to a differing choice of MRY. Furthermore, the highest overall correlation was observed between IFTC and FTCd. The relationship between the FTDR index and other response-based indicators was mostly weak; however, it displayed a stronger correlation with FTCd and IFTC than MWI.

7.2.2. Conclusions regarding simulation-based indices in assessing the long-term response of masonry walls

- A comparison between masonry configurations that included an isotropic brick and a heterogeneous brick with mortar joints revealed that both configurations produced similar responses in respect to FT damage near the outer surface of the brick masonry. However, utilizing an isotropic brick configuration in simulations resulted in greater severity of FT damage within the bricks, emphasizing the need for a more precise representation of masonry walls.
- Comparing observations based on climatic factors, such as the total yearly amount of WDR or the annual mean ambient temperature, is not suitable for evaluating the risk to FT damage of masonry walls. This is because FT damage occurs when both wetting within the brick coincides with the occurrence of sub-zero temperatures, in such situations assessing of the hygrothermal conditions specific to the brick masonry are required to determine whether FT damage has occurred.
- Contrary to the majority of earlier research, which focused on the prevailing WDR direction as the primary orientation when assessing FT-related damage of masonry walls, in this study it was revealed that the WDR direction during the frost season may provide a more accurate representation of the orientation posing the greatest risk of FT damage. As such, when analyzing the most critical orientation for the risk to FT-damage, the combined effect of temperature fluctuations and WDR direction needs to be evaluated accordingly – not simply the amount of WDR.
- The two frequently employed indicators of FT damage, FTCd and FTCcrit, do not offer consistent predictions for future climate-related FT damage despite their significant correlation.
- The annual FT cycles derived from a 31-year continuous simulation closely resemble those from a single-year simulation. This suggests that yearly variations in weather have a limited cumulative effect on annual FT cycles, thereby implying that results from a single-year simulation can effectively represent long-term performance for MRY selection.
- The MRYs selected based on simulation are influenced by location, construction, and orientation. Therefore, before choosing a MRY for assessing FT damage, it is important to examine a range of parameters to identify the most significant factors affecting the risk of

FT damage. The method suggested in this study for selecting a simulation-based MRY has been shown to be suitable for making decisions regarding retrofitting.

7.2.3. Conclusions regarding the impact of interior insulation on the durability of historic masonry walls

- Adding insulation to older brick masonry walls can greatly affect their longevity. Choosing the right insulation involves understanding the moisture and heat properties of both the existing wall materials and insulation systems as may be potentially used in their retrofit. In this study, it was demonstrated that higher R-values of insulation increased the risk of future damage. Whereas certain situations allow for a safe application of any type or thickness of insulation, in many cases the application of insulation to the masonry wall must be approached with caution or ought to be prohibited altogether. It was also concluded, based on the results of this research, that applying mineral wool and calcium silicate is more reliable choice as compared to that of using spray polyurethane foam as insulation for a retrofit application.
- It was also shown, from the results of this research that various types of brick masonry can significantly affect not only the durability of wall assemblies but also anticipated patterns in FT damage over time. Furthermore, both brick type and masonry thickness did not have a significant impact on the number of FTCs observed for insulated walls facing different orientations.
- The direction in which wall assemblies were positioned significantly affected the amount of WDR they receive. Therefore, incorporating knowledge of wall orientation into preservation plans can help in selecting appropriate insulation materials to effectively control moisture movement and reduce the likelihood of freeze-thaw damage. Results from this study consistently indicated that buildings located in Ottawa and having walls oriented towards North, NE, and East were more susceptible to FT damage. Conversely, walls facing South, SE, and West generally carried a lower risk.
- Other elements that impact the variation in the quantity of WDR include the type of building, the building roof, and the building's immediate environment. Uninsulated and insulated masonry walls exhibited distinct responses under various exposure levels and conditions. Interior insulation may be suitable for protected and sheltered walls in specific

cases; however, the use of interior insulation is not advisable for walls exposed to high levels of WDR (i.e. unprotected walls, with roof runoff, and facing towards critical WDR orientations).

- This study offers an initial procedure for making decisions regarding internal insulation retrofit projects. It also suggests specific approaches for situations that demand careful considerations, where masonry wall assemblies are more prone to FT damage. To ensure the long-term preservation of historic brick masonry walls, it is essential to contemplate replacing brick masonry units with more durable and resistant options that can withstand freeze-thaw cycles. Substituting the current brick masonry units with stronger alternatives can greatly enhance the structural integrity of the walls. The selection of suitable replacement brick masonry units requires careful assessment of their hygrothermal properties and ability to endure the effects of freeze-thaw cycling. Therefore, it is crucial to opt for brick units having low water absorption and resistance to frost action. These characteristics will help prevent moisture from seeping in and minimize the risk of damage from freezing and thawing, thereby ensuring the continued structural integrity of the brick masonry walls.

7.3. Future work

Future efforts should focus on implementing a proactive plan for preserving and maintaining historic brick walls to maintain their structural integrity over time. A critical aspect is to conduct regular inspections and maintenance tasks, such as repairing mortar joints, replacing damaged bricks, and addressing signs of deterioration, in order to prevent and minimize the effects of environmental factors such as freeze-thaw cycling. Overall, it is essential to adopt a comprehensive approach that includes selecting appropriate insulation materials, replacing brick masonry units when necessary, and employing proactive preservation and maintenance methods to ensure the sustainability of historic brick walls. Given the susceptibility of historic brick walls to freeze-thaw cycling, environmental considerations should play a significant role in the preservation and maintenance plan. Measures to minimize the impact of moisture movement, such as appropriate drainage systems and protective coatings, should be evaluated and implemented as part of the overall preservation strategy.

As well conducting on-site measurements to validate the freeze-thaw damage indicators is a crucial step in assessing the condition of historic brick walls. Gathering quantitative data from on-site measurements would enable undertaking a comprehensive analysis of the freeze-thaw damage indicators. Documenting the measurements and details of observations provides a foundation for informed decision-making regarding the preservation and maintenance of historic brick walls. Besides, interstitial condensation should be considered in tandem with FT damage analysis.

It is important to note that Conclusions drawn from simulations conducted over the future period until 2092 are based on material properties known as of today, which are assumed to remain constant over this timeframe. However, it is possible that these material properties could degrade over time, and the impact of such aging effects requires further investigation. And while FT cycles may serve as a useful basis for comparative studies, examining the relationship between these cycles and the real-world degradation of historic masonry walls, both in their original state and when internally insulated, could provide valuable insights.

This thesis used Ottawa as an example to address the research questions. The methodology and framework developed in this thesis can be applied to other geographical locations. Future research should concentrate on examining the most effective approaches for upgrading historic masonry walls in different urban areas across Canada.

List of publications

Journal papers:

1) Sahyoun, S., Ge, H. and Lacasse, M.A. (2024). The impact of interior insulation on historic masonry buildings in Ottawa under a present and a future climate. (submitted and under peer review to the Journal of Building and Environment).

2) Sahyoun, S., Ge, H., and Lacasse, M. A. (2024). Selection of moisture reference year for freeze thaw damage assessment of historic masonry walls under future climate: A simulation-based approach. *Building and Environment,* 111308.

3) Sahyoun, S., Ge, H., Lacasse, M. A., and Defo, M. (2021). Reliability of existing climate indices in assessing the freeze-thaw damage risk of internally insulated masonry walls. *Buildings,* 11(10), 482.

Conference papers:

1) Sahyoun, Sahar; Lin Wang, Hua Ge, Maurice Defo and Michael Lacasse. 2020. "Durability of internally insulated historical solid masonry under future climates: A stochastic approach." *XV International Conference on Durability of Building Materials and Components*.

2) Sahyoun, Sahar; Hua Ge, Chetan Aggarwal, Maurice Defo and Travis Moore. 2020. "Effect of selected moisture reference year on the durability assessment of wall assemblies under future climates." *XV International Conference on Durability of Building Materials and Components*.

3) Defo, Maurice; Michael Lacasse, Sahar Sahyoun and Travis Moore. 2019. "Impacts of Wind-Driven Rain Calculation Methods on the Moisture Performance of Wood-frame Walls." *2019 Buildings XIV International Conference*. https://www.techstreet.com/standards/impacts-of-wind-driven-rain-calculation-methods-on-the-moisture-performance-of-wood-frame-walls?product_id=2095295#jumps

4) Sahyoun, Sahar; Hua Ge, Maurice Defo and Michael Lacasse. 2019. “Evaluating the potential of freeze-thaw damage in internally insulated masonry under climate change using different models.” *Central European Symposium on Building Physics.* MATEC Web of Conferences 282. https://doi.org/10.1051/matecconf/201928202081
5) Lacasse, Michael; Travis Moore, Maurice Defo, Abhishek Gaur, Abdelaziz Laouadi and Sahar Sahyoun. 2018. “A guideline for design for durability of building envelopes”. *Proceedings of the CIB / NRC Symposium*.

Reports:

1) Sahyoun, S., Ge, H. and Lacasse, M.A. (2021). “Best Practices to Improve the Thermal Energy Performance of Heritage Buildings: A Literature Review”. (Submitted for publication), Technical Report (2023-12-12), A1-015802.3 (NRCC-CONST-xxxxxE), National Research Council of Canada, Construction, 35 p;

2) Sahyoun, S., Defo, M. and Lacasse, M. A. (2019). “Assessing the climate resilience of buildings to the effects of hygrothermal loads: Impacts of wind-driven rain calculation methods on the moisture performance of walls.” Technical Report (2019-04-30), CRB-CPI-Y3-R14 (NRCC-CONST-56360E), National Research Council of Canada, Construction, 56 p; https://doi.org/10.4224/40001822

3) Maurice Defo, Sahar Sahyoun and Michael A. Lacasse (2019), “Impacts of indoor conditions calculation methods on the moisture performance of wood-frame walls”, Technical Report (2019-04-30), (NRCC-CONST-56517E), National Research Council of Canada, Construction, 30 p; https://doi.org/10.4224/40002686

4) Lacasse, M., Defo, M., Gaur, A., Moore, T. and Sahyoun, S. (2018). “Approach for assessing the climate resilience of buildings to the effects of hygrothermal loads.”, Technical Report (2018-06-30), CRB-CPI-Y2-R18 (NRCC-CONST-56269E), National Research Council of Canada, Construction, 44 p; https://doi.org/10.4224/23003982

References

Aldabibi, M.A., Nokken, M.R., Ge, H., 2022. Effect of Adding Thermal Insulation on Frost Damage of Masonry Walls. Presented at the The 5th Conference on Building Energy and Environment, Montreal, Canada.

Aldabibi, M.A., Nokken, M.R., Ge, H., 2020. Improving Frost Durability Prediction based on Relationship between Pore Structure and Water Absorption. Presented at the the XV International Conference on Durability of Building Materials and Components (DBMC 2020).

ANSI/ASHRAE, 2021. Criteria for Moisture-Control Design Analysis in Buildings. (ANSI/ASHRAE Standard 160-2021). American Society of Heating, Refrigerating and Air-Conditioning Engineers, Inc, Atlanta, GE, USA.

ANSI/ASHRAE, 2019. ANSI/ASHRAE Guideline 34-2019. Energy Guideline for Historic Buildings.

ANSI/ASHRAE, 2016. Criteria for Moisture Control Design Analysis in Buildings; American Society of Heating, Refrigerating and Air-Conditioning Engineers, Inc. Atlanta, GE, USA.

ASHRAE, 2010. Environmental weather loads for hygro- thermal analysis and design of buildings. (No. RP-1325). American Society of Heating, Refrigerating and Air- Conditioning Engineers, Inc, Atlanta.

ASHRAE, 2009. ASHRAE Handbook: Fundamentals; ASHRAE.

ASTM, 2007. ASTM Standard C67-07a, Standard Test Methods for Sampling and Testing Brick and Structural Clay Tile.

Berezkin, Y., Urick, M., 2013. Modern Polyurethanes: Overview of Structure Property Relationship., in: Olymers for Personal Care and Cosmetics., Chapter 4. ACS Publications, pp. 65–81.

Bharadwaj-Somaskandan, S., Krishnamurthi, B., Sergeeva, T.A., Shutov, F., 2003. Macro- and Microfillers as Reinforcing Agents for Polyurethane Elastomers. Macro- and Microfillers as Reinforcing Agents for Polyurethane Elastomers. https://doi.org/10.1177/009524403035397

Blumberga, A., Freimanis, R., Blumberga, D., Veidenbergs, I., Hansen, E., Hansen, T.K., Du, G., Stöcker, E., Sontag, H., Freudenberg, P., Janssen, H., Roels, S., di Giuseppe, E., D'Orazio, M., Gianangeli, A., Quagliarini, E., Møller, E.B., Capener, C.M., Lång, L., Johansson, P.,

Lasvaux, S., Giorgi, M., Favre, D., Padey, P., Wagner, G., 2020. Written guidelines for decision making concerning the possible use of internal insulation in historic buildings.

Blumberga, A., Kašs, K., Kamendere, E., Žogla, G., Kamenders, A., Blumberga, D., Grāvelsiņš, A., 2019. Robust Internal Thermal Insulation of Historic Buildings - State of the art on historic building insulation materials and retrofit strategies. (No. D1.2). RIBuild Deliverable.

Bottino-Leone, D., Larcher, M., Herrera-Avellanosa, D., Haas, F., Troi, A., 2019. Evaluation of natural-based internal insulation systems in historic buildings through a holistic approach. Energy 181, 521–531.

Cabrera, P., Samuelson, H., Kurth, M., 2019. Simulating Mold Risks under Future Climate Conditions. Presented at the Building Simulation 2019, Rome, Italy, pp. 1530–1538. https://doi.org/10.26868/25222708.2019.211130

Canada's Historic Places, 2010. Standards and Guidelines for the Conservation of Historic Places in Canada – Second Edition.

Canada's Historic Places, 2007. Durability & Energy Efficiency. Heritage and Conservation Brief.

Canada's Historic Places, 2003. Standards and Guidelines for the Conservation of Historic Places in Canada – First Edition.

Choidis, P., Coelho, G.B.A., Kraniotis, D., 2023. Assessment of frost damage risk in a historic masonry wall due to climate change. Advances in Geosciences 58, 157–175. https://doi.org/10.5194/adgeo-58-157-2023

CMHC, 2011. Near Net Zero – Energy Retrofits for Houses. CMHC, Vancouver.

CMHC, 2004. Renovating for Energy Savings: Case Studies [WWW Document]. URL http://www.cmhc-schl.gc.ca/en/co/grho/reensa/index.cfm

Cornick, S., Djebbar, R., Alan Dalgliesh, W., 2003. Selecting moisture reference years using a Moisture Index approach. Building and Environment 38, 1367–1379. https://doi.org/10.1016/S0360-1323(03)00139-2

CSA, 2006. CSA Standard A82-0, Fired Masonry Brick Made from Clay or Shale.

CSN EN 12371, 2010. Natural stone test methods-Determination of frost resistance.

Delgado, J.M., Barreira, E., Ramos, N.M., De Freitas, V.P., 2012. Hygrothermal numerical simulation tools applied to building physics. Springer Science & Business Media.

Djebbar, R., van Reenen, D., Kumaran, M.K., 2001. Indoor and Outdoor Weather Analysis Tool for Hygrothermal Modelling., in: Proceedings of the Eighth Conference on Building Sciences and Technology - Solutions to Moisture Problems in Building Enclosures. Presented at the the Eighth Conference on Building Sciences and Technology, Toronto, Ontario, pp. 140–157.

EN ISO 6946, 2017. Building Components and Building Elements—Thermal Resistance and Thermal Transmittance—Calculation Methods (Standard). National Standards Authority of Ireland, Dublin, Ireland.

EN ISO 15927-3, 2009. Hygrothermal Performance of Buildings—Calculation and Presentation of Climatic Data Part 3: Calculation of a Driving Rain Index for Vertical Surfaces from Hourly Wind and Rain Data.

Environment and Climate Change Canada (ECCC), 2018. Memorandum of Understanding between National Research Council and Environment and Climate Change Canada. Government of Canada, Ottawa, Ontario.

Environment and Climate Change Canada (ECCC), 2016. Pan-Canadian Framework on Clean Growth and Climate Change: Canada's Plan to Address Climate Change and Grow the Economy.

Fagerlund, G., 1977. The critical degree of saturation method of assessing the freeze/thaw resistance of concrete. Mat. Constr. 10, 217–229. https://doi.org/10.1007/BF02478693

Fagerlund, G., 1973. Critical degrees of saturation at freezing of porous and brittle materials. Lund University.

Fan, D., 2014. Greening a Heritage Building. City of Vancouver.

Fraley, C., Raftery, A.E., 2002. Model-based Clustering, Discriminant Analysis and Density Estimation. Journal of the American Statistical Association 97, 611–631.

Fraley, C., Raftery, A.E., Murphy, T.B., Scrucca, L., 2012. mclust Version 4 for R: Normal Mixture Modeling for Model-Based Clustering, Classification, and Density Estimation. (Technical Report).

Freudenberg, P., Ørsager, M., Lasvaux, S., de Place Hansen, E.J., 2019. Monitoring Data Basis of European Case Studies for Sound Performance Evaluation of Internal Insulation Systems Under Different Realistic Boundary Conditions. (No. 3). RIBuild Deliverable D.

Gaur, A., Lacasse, M., Armstrong, M., 2019. Climate Data to Undertake Hygrothermal and Whole Building Simulations Under Projected Climate Change Influences for 11 Canadian Cities. Data 4, 72. https://doi.org/10.3390/data4020072

Geving, S., 1997. Moisture Design of Building Constructions: Hygrothermal Analysis Using Simulation Models. Norwegian University of Science and Technology, Norway.

Grossi, C.M., Brimblecombe, P., Harris, I., 2007. Predicting long term freeze–thaw risks on Europe built heritage and archaeological sites in a changing climate. Science of the Total Environment 377, 273–281.

Grunewald, J., 1997. Diffusiver und konvektiver Stoff- und Energietransport in kapillarporösen Baustoffen. (PhD Thesis). Technischen Universitat Dresden, Germany.

Grunewald, J., Nicolai, A., 2006. Effekte der Luftströmung auf das Hygrothermische Verhalten von Leichten Umfassungskonstruktionen., in: Erste Deutsch-Österreichische IBPSA-Konferenz. Presented at the IBPSA 2006, Technische Universität München, Germany.

Hagentoft, C.E., Harderup, E., 1996. Climatic influences on the building envelope using the Π factor., EA-Annex 24 Hamtie Task 2, Environmental Conditions.

Haupl, P., Fechner, H., Petzold, H., 2004. Interior retrofit of masonry wall to reduce energy and eliminate moisture damage: comparison of modeling and field performance., in: The Thermal Performance of the Exterior Envelopes of Buildings IX. Clearwater Beach, FL.

Haupl, P., Jurk, K., Petzold, H., 2003. Inside thermal insulation for historical facades., in: The 2nd International Conference on Building Physics, Antwerpen. AA Balkema Publishers, Antwerpen, Belgium, pp. 463–469.

Health Canada, 2011. Dampness, Mould and Indoor Air. Government of Canada.

Hensley, J.E., Aguilar, A., 2012. Improving energy efficiency in historic buildings. Government Printing Office.

Hukka, A., Viitanen, H., 1999. A mathematical model of mould growth on wooden material. Wood Science and Technology 33, 475–485.

Incropera, F.P., DeWitt, D.P., Bergman, T.L., 2015. Fundamentals of heat and mass transfer.

IPCC, 2022. Climate Change 2022: Impacts, Adaptation and Vulnerability. Contribution of Working Group II to the Sixth Assessment Report of the Intergovernmental Panel on Climate Change [H.-O. Pörtner, D.C. Roberts, M. Tignor, E.S. Poloczanska, K.

Mintenbeck, A. Alegría, M. Craig, S. Langsdorf, S. Löschke, V. Möller, A. Okem, B. Rama (eds.)]. Cambridge University Press, Cambridge, UK and New York, NY, USA.

IPCC, 2014. Climate Change 2014: Synthesis Report. Contribution of Working Groups I, II and III to the Fifth Assessment Report of the Intergovernmental Panel on Climate Change [Core Writing Team, R.K. Pachauri and L.A. Meyer (eds.)]. Intergovernmental Panel on Climate Change, Geneva, Switzerland.

Jandl, H.W., 1988. Rehabilitating Interiors in Historic Buildings. Technical Preservation Services, National Park Service, US Department of the Interior.

Janssen, H., Freudenberg, P., Tijskens, A., Hou, T., 2019. Robust Internal Thermal Insulation of Historic Buildings - Basic probabilistic analysis of hygrothermal performance of interior insulation.

Janssens, K., Feng, C., Marincioni, V., Van Den Bossche, N., 2024. Comparison of different frost models with hygrothermal simulations to better understand frost damage in porous building materials. Building and Environment 225. https://doi.org/10.1016/j.buildenv.2024.111399

Jelle, B.P., 2011. Traditional, state-of-the-art and future thermal building insulation materials and solutions – Properties, requirements and possibilities. Energy and Buildings. 43, 2549–2563.

Johansson, P., 2014. Determination of the critical moisture level for mould growth on building materials. (Ph.D. dissertation). Lund University.

Johansson, P., Bok, G., Ekstrand-Tobin, A., 2013a. The effect of cyclic moisture and temperature on mould growth on wood compared to steady state conditions. Building and Environment 65, 178–184.

Johansson, P., Lång, L., Capener, C.M., Møller, E.B., Quagliarini, E., D'Orazio, M., Gianangeli, A., Janssen, H., Feng, C., Langmans, J., Feldt Jensen, N., de Place Hansen, E.J., Peuhkuri, R.H., Hansen, T.K., 2019. Threshold values for failure, linked to types of building structures and failure modes.

Johansson, P., Time, B., Geving, S., Jelle, B.P., Kalagasidis, A.S., Hagentoft, C.E., 2013b. Interior insulation retrofit of a brick wall using vacuum insulation panels: design of a laboratory study to determine the hygrothermal effect on existing structure and wooden beam ends., in: Thermal Performance of the Exterior Envelopes of Whole Buildings XII International Conference. Clearwater Beach, FL, USA.

Kalamees, T., Vinha, J., 2004. Estonian Climate Analysis for Selecting Moisture Reference Years for Hygrothermal Calculations. Journal of Thermal Envelope and Building Science 27, 199–220. https://doi.org/10.1177/1097196304038839

Khudaverdian, D., 2005. Performance Evaluation of Retrofitted Solid Masonry Exterior Walls. Canada Mortgage and Housing Corporation, Ottawa - Ontario.

Klõšeiko, P., Arumägi, E., Kalamees, T., 2015. Hygrothermal performance of internally insulated brick wall in cold climate: A case study in a historical school building. Journal of Building Physics, 38, 444–464.

Kočí, J., Maděra, J., Černý, R., 2014. Generation of a critical weather year for hygrothermal simulations using partial weather data sets. Building and Environment 76, 54–61.

Kočí, J., Maděra, J., Keppert, M., Černý, R., 2017. Damage functions for the cold regions and their applications in hygrothermal simulations of different types of building structures. Cold Regions Science and Technology 135, 1–7. https://doi.org/10.1016/j.coldregions.2016.12.004

Kralj, B., Pande, G.N., Middleton, J., 1991. On the mechanics of frost damage to brick masonry. Computers & Structures 41, 53–66. https://doi.org/10.1016/0045-7949(91)90155-F

Lacasse, M.A., 2019. An overview of durability and climate change of building components. Canadian Journal of Civil Engineering 46, v–viii.

Langmans, J., Nicolai, A., Klein, R., Grunewald, J., Roels, S., 2011. Numerical Simulation of Building Components - Towards an Efficient Implementation of Air Convection in HAM-models. Presented at the 9th Nordic Symposium on Building Physics.

Li, R., 2005. Mould growth on building materials and the effects of borate-based preservatives. (Doctoral dissertation). University of British Columbia.

Lisø, K.R., Kvande, T., Hygen, H.O., Thue, J.V., Harstveit, K., 2007. A frost decay exposure index for porous, mineral building materials. Building and Environment 42, 3547–3555. https://doi.org/10.1016/j.buildenv.2006.10.022

Liu, J.S., 2013. Analysis of the Development and Application of Rigid Polyurethane Foam Material. Applied Mechanics and Materials 380–384, 4319–4322. https://doi.org/10.4028/www.scientific.net/amm.380-384.4319

Maage, M., 1984. Frost resistance and pore size distribution in bricks. Matériaux et Construction 17, 345–350.

Masson, P., 2015. Housing Research Report: Retrofitting Solid Masonry Residential Buildings. Canada Mortgage and Housing Corporation (CMHC).

Maurenbrecher, A.H.P., Shirtliffe, C.J., Rousseau, M.Z., Saïd, M.N.A., 1998. Monitoring the hygrothermal performance of a masonry wall with and without thermal insulation. Presented at the the 8th Canadian Masonry Symposium, Jasper, Alberta.

Mensinga, P., 2009. Determining the critical degree of saturation of brick using frost dilatometry . (Master's thesis). University of Waterloo.

Möller, E.B., Esad, A., Blumberga, A., Ekstrand-Tobin, A., de Place Hansen, E.J., Ståhl, F., Finken, G.R., Janssen, H., Grunewald, J., Freudenberg, P., Lasvaux, S., Jørgensen, S.B., Tvedebrink, T., 2018. Report on the material properties.

Moore, T.V., Lacasse, M.A., Wells, J., Kayll, D., Lee, I., Pratt, K., Becker, J., Bartko, M., Saragosa, J., 2022. Insulating Heritage Mass Masonry Buildings from the Interior: A Best Practice Guide to Mitigate Risk of Freeze-Thaw Damage (No. A1- 015802.1). National Research Council Canada (NRC).

Morelli, M., Scheffler, G.A., Nielsen, T.R., 2010. Internal insulation of masonry walls with wooden floor beams in northern humid climate., in: Thermal Performance of the Exterior Envelopes of Whole Buildings XI (U.S. Department of Energy, Oak Ridge National Laboratory). ASHRAE., Atlanta, GA, pp. 89–100.

Mukhopadhyaya, P., Kumaran, K., Nofal, M., Tariku, F., Van Reenen, D., 2005. Assessment of building retrofit options using hygrothermal analysis tool. Presented at the The proceedings of the 7th symposium on building physics in the Nordic countries., pp. 1139–1146.

Musunuru, S., Pettit, B., 2015. Measure Guideline: Deep Energy Enclosure Retrofit for Interior Insulation of Masonry Walls. Building Science Corporation, Westford, MA.

National Building Code of Canada (NBC)., 2020. National Building Code of Canada.

Natural Resources Canada., 2007. From impacts to adaptation: Canada in a changing climate. Government of Canada, Ottawa - Ontario.

Nelson, F., Outcalt, S.I., 1987. A computational method for prediction and regionalization of permafrost. Arctic and Alpine Research 19, 279–288.

Nicolai, A., 2007. Modeling and Numerical Simulation of Salt Transport and Phase Transitions in Unsaturated Porous Building Materials. Syracuse University.

Nicolai, A., Fechner, H., Vogelsang, S., Sontag, L., Paepcke, A., Grunewald, J., 2013a. DELPHIN 5.8 Model Reference.

Nicolai, A., Fechner, H., Vogelsang, S., Sontag, L., Paepcke, A., Grunewald, J., 2013b. DELPHIN 5.8 Model Reference.

Nielsen, A., Möller, E.B., Rasmussen, T.V., 2012. Use of sensitivity analysis to evaluate hygrothermal conditions in solid brick walls with interior insulation., in: The 5th International Building Physics Conference (IBPC)—NSB 2011. Kyoto, Japan, pp. 377–384.

Nijland, T.G., Adan, O.C.G., van Hees, R.P.J., van Etten, B.D., 2009. Evaluation of the effects of expected climate change on the durability of building materials with suggestions for adaptation. HERON 54, 37–48.

Ochs, F., 2010. Modelling Large-Scale Thermal Energy Stores. (Ph.D. Thesis). University of Stuttgart.

Odgaard, T., Bjarløv, S.P., Rode, C., 2018. Interior insulation–Experimental investigation of hygrothermal conditions and damage evaluation of solid masonry façades in a listed building. Building and Environment 129, 1–14.

Pachauri, R.K., Meyer, L.A., 2013. Climate Change 2014: Synthesis Report. Contribution of Working Groups I, II and III to the Fifth Assessment Report of the Intergovernmental Panel on Climate Change. Geneva, Switzerland.

Parks Canada, 2010. Standards and Guidelines for the Conservation of Historic Places in Canada: A Federal, Provincial and Teritorial Collaboration, Second Edition. (No. Catalogue number R62-343/2010E-PDF (ISBN 978-1-100-15953-9)).

Parks Canada, 2009. A Guide to Working with the Federal Heritage Buildings Review Office. (Guide). The Federal Heritage Buildings Review Office (FHBRO), Ottawa, Ontario.

Powers, T.C., Helmuth, R.A., 1953. THEORY OF VOLUME CHANGES IN HARDENED PORTLAND-CEMENT PASTE DURING FREEZING.

Region of Waterloo, 2013a. Practical Conservation Guide for Heritage Properties – Insulation.

Region of Waterloo, 2013b. Practical Conservation Guide for Heritage Properties – Masonry.

RIBuild, 2015. RIBuild (Robust Internal Thermal Insulation of Historic Buildings) [WWW Document]. URL https://ribuild.eu/

RIBuild, n.d. RIBuild - Guideline for selecting an internal insulation system. [WWW Document]. URL https://www.ribuild.eu/research-insulationsystems

Ritchie, T., 1960. Early brick masonry along the St. Lawrence in Ontario. Journal of the Royal Architectural Institute of Canada 37, 115–122.

Rode, C., 1993. Reference years for moisture calculations (Report T2- DK-93/02, International Energy Agency, Energy Conservation in Buildings and Community Systems Program, Annex 24 Heat, Air and Moisture Transfer in Insulated Envelope Parts (HAMTIE)). Denmark.

Sahyoun, S., Ge, H., 2020. Best Practices to Improve the Thermal Energy Performance of Heritage Buildings: A Literature Review.

Sahyoun, S., Ge, H., Aggarwal, C., Defo, M., Moore, T., 2020. Effect of Selected Moisture Reference Year on the Durability Assessment of Wall Assemblies under Future Climates. Presented at the the XV International Conference on Durability of Building Materials and Components, Barcelona, Spain.

Salonvaara, M., Sedlbauer, K., Holm, A., Pazera, M., 2010. Effect of selected weather year for hygrothermal analyses., in: Proceedings of Thermal Performance of the Exterior Envelopes of Whole Buildings XI. Presented at the thermal performance of the exterior envelopes of whole buildings XI., American Society of Heating, Refrigerating and Air-Conditioning Engineers, Inc, Atlanta.

Sanders, C., 1996. Environmental Conditions: Final Report Task 2. (International Energy Agency, Energy Conservation in Buildings and Community Systems Program, Annex 24 Heat, Air and Moisture Transfer in Insulated Envelope Parts (HAMTIE).). Laboratorium Bouwfysica, K.U.-Leuven, Belgium., Leuven, Belgium.

Scheffler, G., 2011. Hygric performance of internal insulation with lightweight autoclaved aerated concrete., in: 5th International Conference on Autoclaved Aerated Concrete, Bydgoszcz. pp. 323–335.

Scheffler, G.A., 2008. Validation of hygrothermal material modelling under consideration of the hysteresis of moisture storage. (Ph.D. thesis). Dresden University of Technology, Faculty of Civil Engineering, Institute of Building Climatology.

Scheffler, G.A., Grunewald, J., 2003. Material development and optimisation supported by numerical simulation for capillary-active inside insulation material., in: The 2nd

International Conference on Building Physics, Antwerpen. AA Balkema Publishers, pp. 77–85.

Sedlbauer, K., Künzel, H.M., 2000. Frost Damage of Masonry Walls—A Hygrothermal Analysis by Computer Simulations. Journal of Thermal Envelope and Building Science 23, 277–281. https://doi.org/10.1177/174425910002300309

Sehizadeh, A., Ge, H., 2016. Impact of future climates on the durability of typical residential wall assemblies retrofitted to the PassiveHaus for the Eastern Canada region. Building and Environment 97, 111–125.

Sontag, L., Nicolai, A., Vogelsang, S., 2013a. Validierung der Solverimplementierung des Hygrothermischen Simulationsprogramms DELPHIN [WWW Document]. Bauklimatik-Dresden. URL http://www.bauklimatik-dresden.de/delphin/benchmarks/hamstad.php (accessed 8.24.21).

Sontag, L., Nicolai, A., Vogelsang, S., 2013b. Validierung der Solverimplementierung des Hygrothermischen Simulationsprogramms DELPHIN. [WWW Document]. URL http://www.bauklimatik-dresden.de/delphin/benchmarks/hamstad.php (accessed 8.24.21).

Stopp, H., Strangeld, P., Fechner, H., 2001. The hygrothermal performance of external walls with inside insulation., in: The Thermal Performance of the Exterior Envelopes of Buildings VIII. Clearwater Beach, FL.

Straube, J., Mensinga, P., Schumacher, C., 2010a. Assessing the Freeze-Thaw Resistance of Clay Brick for Interior Insulation Retrofit Projects. Presented at the the XI International Conference Thermal Performance of the Exterior Envelopes of Whole Buildings, Clearwater, FL, USA.

Straube, J., Schumacher, C., 2007. Interior insulation retrofits of load-bearing masonry walls in cold climates. Journal of Green Building 2, 42–50. https://doi.org/10.3992/jgb.2.2.42

Straube, J., Schumacher, C., 2006. Assessing the Durability Impacts of Energy Efficient Enclosure Upgrades Using Hygrothermal Modeling. Journal of the International Association for Science and Technology of Building Maintenance and Monuments Preservation 2.

Straube, J., Schumacher, C., Mensinga, P., 2010b. Assessing the freeze-thaw resistance of clay brick for interior insulation retrofit projects. Presented at the XI International Conference Thermal Performance of the Exterior Envelopes of Whole Buildings, Clearwater, FL, USA, pp. 5–9.

Straube, J., Schumacher, C., Ueno, K., 2011. Internal insulation of masonry walls: final measure guideline. Prepared for US Department of Energy, Office of Energy Efficiency and Renewable Energy.

Straube, J., Ueno, K., Schumacher, C., 2012. Measure Guideline: Internal Insulation of Masonry Walls (No. No. DOE/GO-102012-3523). National Renewable Energy Lab. (NREL): Golden, Golden, CO, USA.

Toman, J., Vimmrova, A., Cerny, R., 2009. Long-term on-site assessment of hygrothermal performance of interior thermal insulation system without water vapour barrier. Energy and Buildings 41, 51–55.

Ueno, K., 2015. Technology Solutions Case Study: Retrofit Measures for Embedded Wood Members in Insulated Mass Masonry Walls. Building Science Corporation.

Ueno, K., Straube, J., Van Straaten, R., 2013a. Field monitoring and simulation of a historic mass masonry building retrofitted with interior insulation. Presented at the Thermal Performance of the Exterior Envelopes of Whole Buildings XII International Conference.

Ueno, K., Van Straaten, R., Schumacher, C., 2013b. Interior Insulation of Mass Masonry Walls: Joist Monitoring, Material Test Optimization, Salt Effects (No. Building America Report-1307). Building Science Corporation.

van Aarle, M., Schellen, H., van Schijndel, J., 2015. Hygro Thermal Simulation to Predict the Risk of Frost Damage in Masonry; Effects of Climate Change. Energy Procedia 78, 2536–2541. https://doi.org/10.1016/j.egypro.2015.11.268

Van Straaten, R., 2014. Improving access to the frost dilatometry methodology for assessing brick masonry freeze thaw degradation risk. Presented at the Canadian Conference on Building Science and Technology.

Vancouver Heritage Foundation, 2012. Conserving Heritage Buildings in Green and Growing Vancouver.

Vandemeulebroucke, I., Calle, K., Caluwaerts, S., De Kock, T., Van Den Bossche, N., 2019. Does historic construction suffer or benefit from the urban heat island effect in Ghent and global warming across Europe? Canadian Journal of Civil Engineering 46, 1032–1042.

Vandemeulebroucke, I., Defo, M., Lacasse, M.A., Caluwaerts, S., Van Den Bossche, N., 2021. Canadian initial-condition climate ensemble: Hygrothermal simulation on wood-stud and

retrofitted historical masonry. Building and Environment 187, 107318. https://doi.org/10.1016/j.buildenv.2020.107318

Vereecken, E., Roels, S., 2016. Capillary active interior insulation systems for wall retrofitting: a more nuanced story. International Journal of Architectural Heritage. 10, 558–569.

Vereecken, E., Roels, S., 2011. A numerical study of the hygrothermal performance of capillary active interior insulation systems., in: The 9th Nordic Symposium on Building Physics (NSB 2011). Department of Civil Engineering, Tampere University of Technology, Tampere, pp. 365–372.

Viitanen, H., Ojanen, T., 2007. Improved model to predict mold growth in building materials., in: Thermal Performance of the Exterior Envelopes of Whole Buildings X–Proceedings CD. pp. 2–7.

Viitanen, H., Ritschkoff, A., 1991. Mould growth in pine and spruce sapwood in relation to air humidity and temperature. (No. 221). Department of Forest Products, The Swedish University of Agricultural Sciences, Uppsala.

Walder, J., Hallet, B., 1985. A theoretical model of the fracture of rock during freezing. Geological Society of America Bulletin 96, 336–346.

Walker, R., Pavía, S., 2015. Thermal performance of a selection of insulation materials suitable for historic buildings. Building and Environment 155–165.

Wardeh, G., Perrin, B., 2008. Freezing–thawing phenomena in fired clay materials and consequences on their durability. Construction and Building Materials 22, 820–828. https://doi.org/10.1016/j.conbuildmat.2007.01.004

Weeks, K.D., Grimmer, A.E., 1995. The Secretary of the Interior's Standards for the Treatment of Historic Properties: With Guidelines for Preserving, Rehabilitating, Restoring & Reconstructing Historic Buildings. Government Printing Office.

Weeks, K.D., Jandl, W.H., 1996. The Secretary of the Interior's Standards for the Treatment of Historic Properties: A Philosophical and Ethical Framework for Making Treatment Decisions.

Wilkinson, J., DeRose, D., Straube, J., Sullivan, B., 2009. Measuring the impact of interior insulation on masonry walls in a cold climate. Journal of Building Enclosure Design 97–110.

Williams, B., Richman, R., 2017. Laboratory dilatometry and field test to assess durability of masonry. Journal of Building Physics 40, 425–443.

WMO, 2017. WMO Guidelines on the Calculation of Climate Normals (No. WMO-No. 1203). World Meteorologial Organization, Geneva, Switzerland.

Xu, J., Zhang, J., Grunewald, J., Zhao, J., Plagge, R., Ouali, A., Allard, F., 2009. A Study on the Similarities between Water Vapor and VOC Diffusion in Porous Media by a Dual Chamber Method. Clean 37, 444–453.

Zhao, J., Plagge, R., Grunewald, J., 2011. Performance assessment of interior insulations by stochastic method., in: The 9th Nordic Symposium on Building Physics (NSB 2011). Department of Civil Engineering, Tampere University of Technology, Tampere, pp. 465–472.

Zhou, X., Derome, D., Carmeliet, J., 2017. Hygrothermal modeling and evaluation of freeze-thaw damage risk of masonry walls retrofitted with internal insulation. Building and Environment 125, 285–298. https://doi.org/10.1016/j.buildenv.2017.08.001

Zhou, X., Derome, D., Carmeliet, J., 2016a. A new procedure for selecting moisture reference years for hygrothermal simulations: A new procedure for selecting moisture reference years for hygrothermal simulations. Bauphysik 38, 361–365. https://doi.org/10.1002/bapi.201610042

Zhou, X., Derome, D., Carmeliet, J., 2016b. Robust moisture reference year methodology for hygrothermal simulations. Building and Environment 110, 23–35. https://doi.org/10.1016/j.buildenv.2016.09.021

Appendices

Appendix A – Results of Chapter 4

Number of matching years

All years:

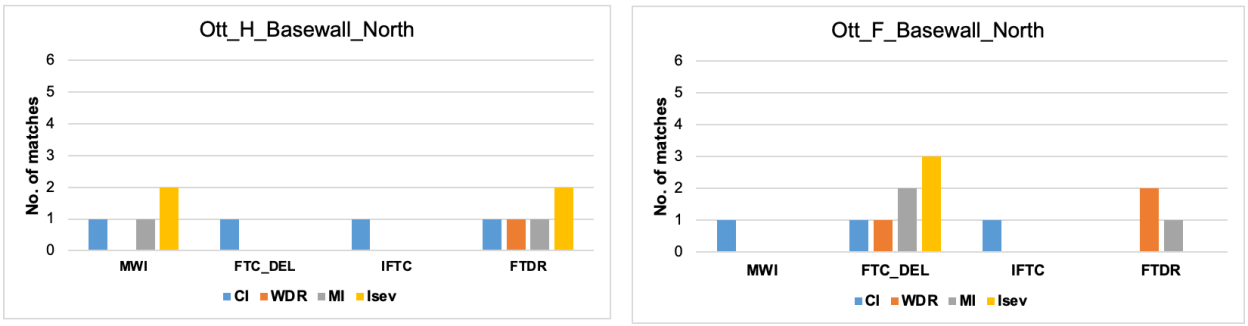

First 3 years:

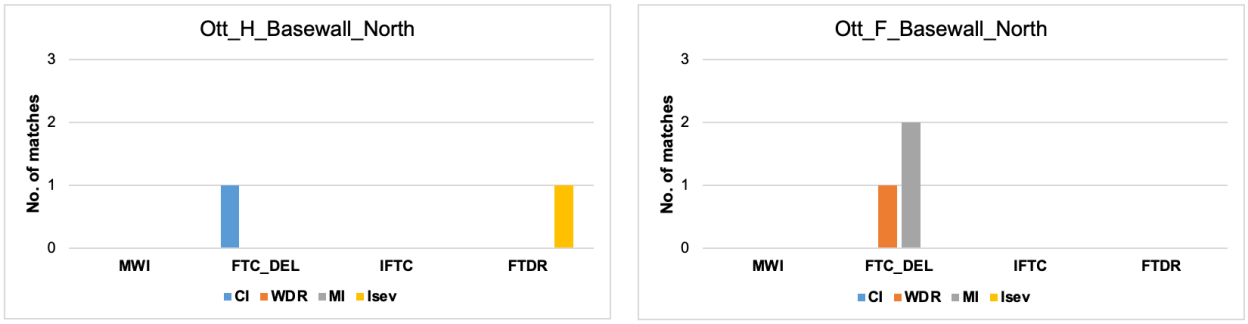

FIG – A1. Number of matching years between climate-based indices (legend) and the response-based indices (x-axis) for a base wall (brick wall in its original state) facing North orientation under historical and future climate in Ottawa.

All years:

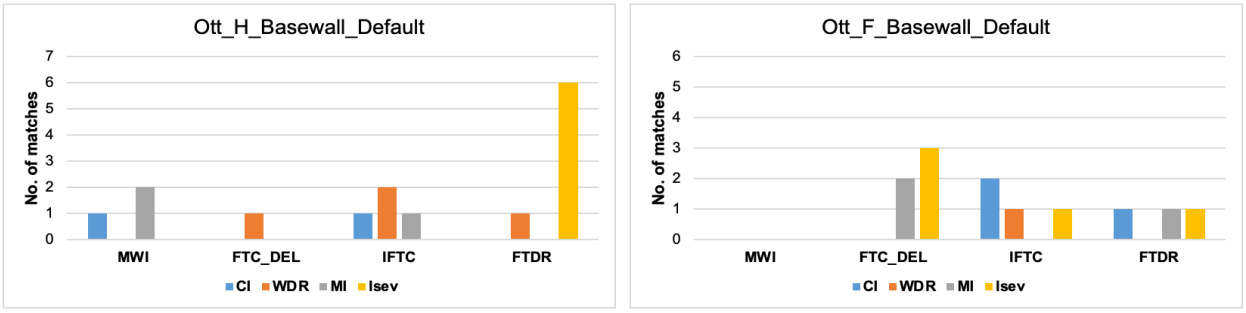

First 3 years:

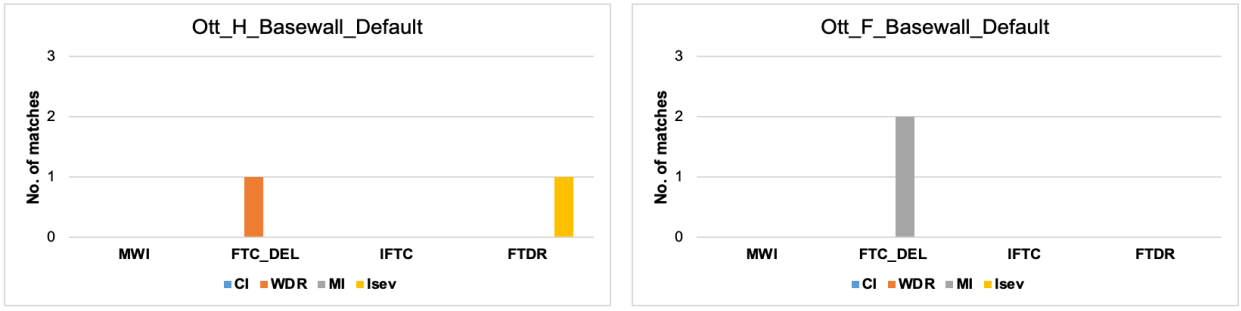

FIG – A2. Number of matching years between climate-based indices (legend) and the response-based indices (x-axis) for a base wall (brick wall in its original state) facing prevailing WDR orientation under historical and future climate in Ottawa.

All years:

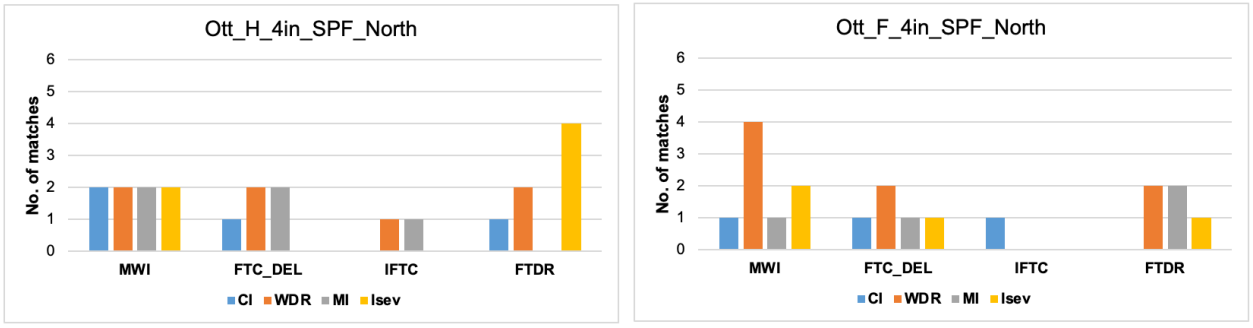

First 3 years:

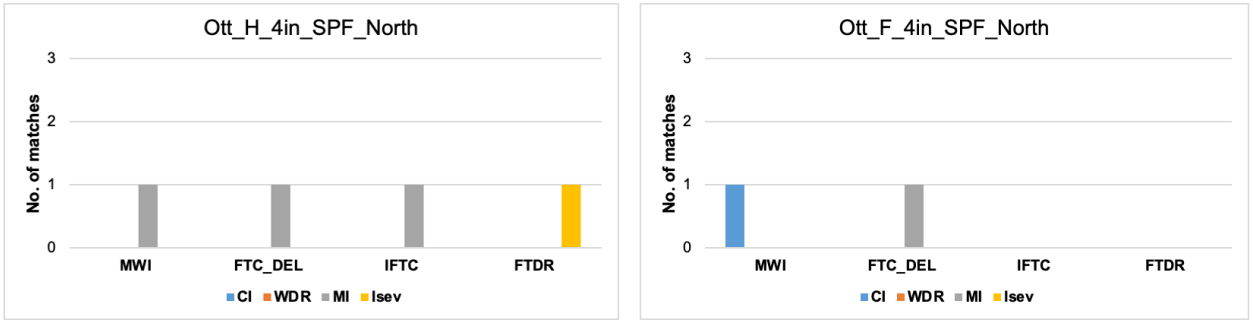

FIG – A3. Number of matching years between climate-based indices (legend) and the response-based indices (x-axis) for a retrofit wall (with 100mm of SPF insulation) facing North under historical and future climate in Ottawa.

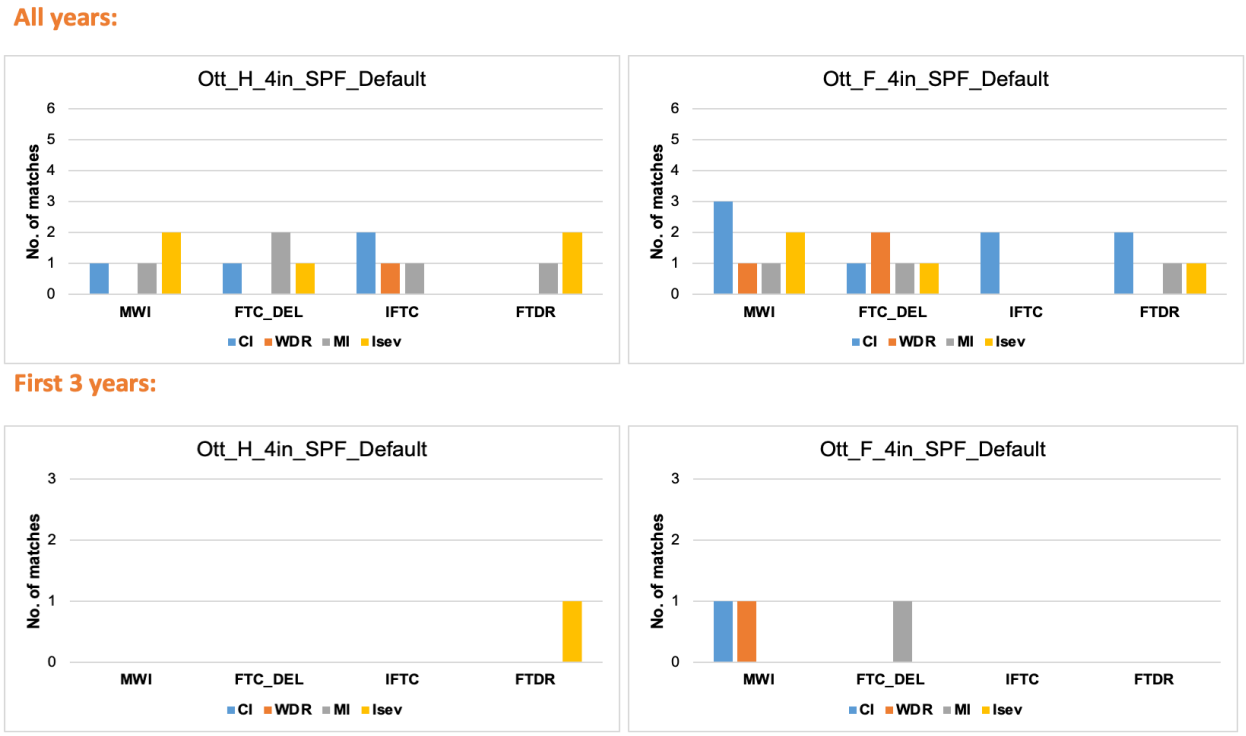

FIG – A4. Number of matching years between climate-based indices (legend) and the response-based indices (x-axis) for a retrofit wall (with 100mm of SPF insulation) facing prevailing WDR orientation under historical and future climate in Ottawa.

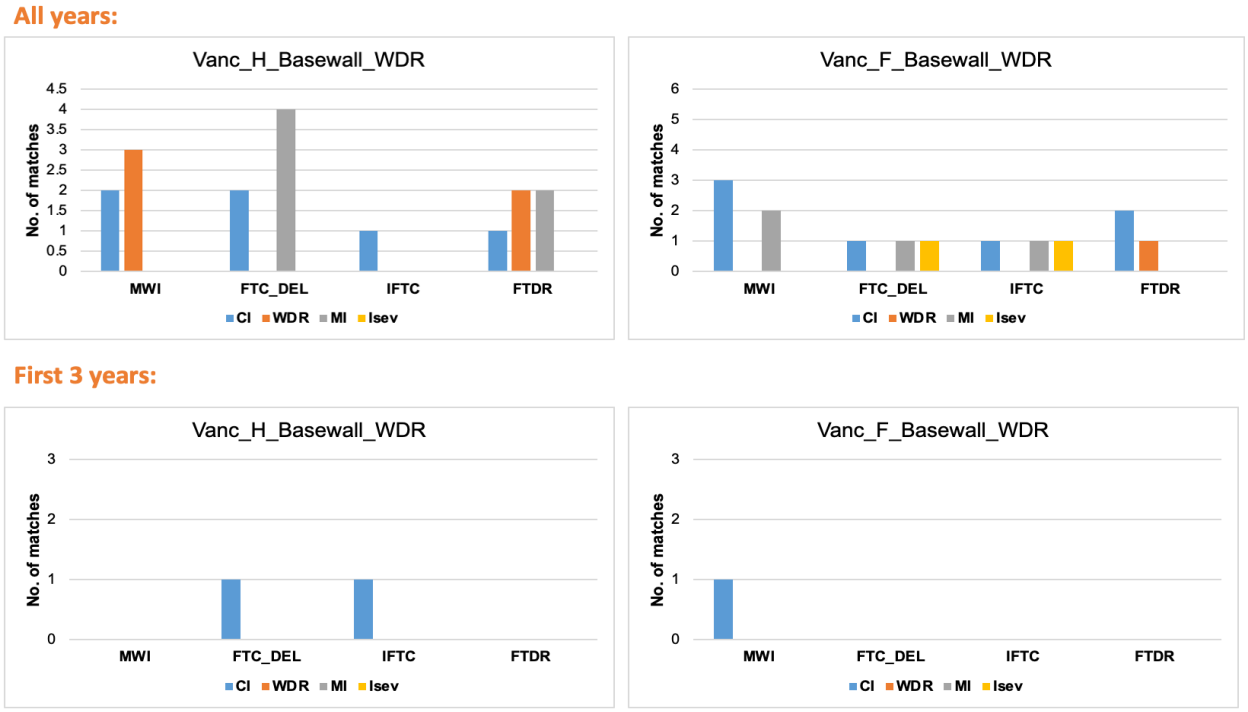

FIG – A5. Number of matching years between climate-based indices (legend) and the response-based indices (x-axis) for a base wall (brick wall in its original state) facing prevailing WDR orientation under historical and future climate in Vancouver.

All years:

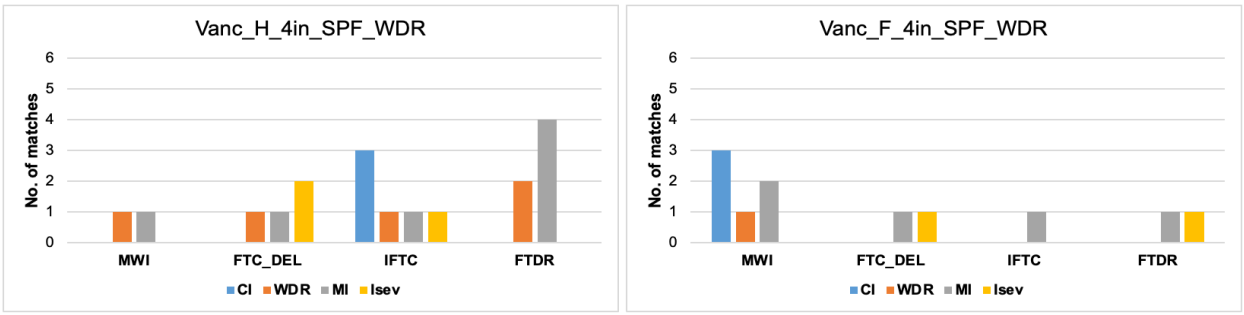

First 3 years:

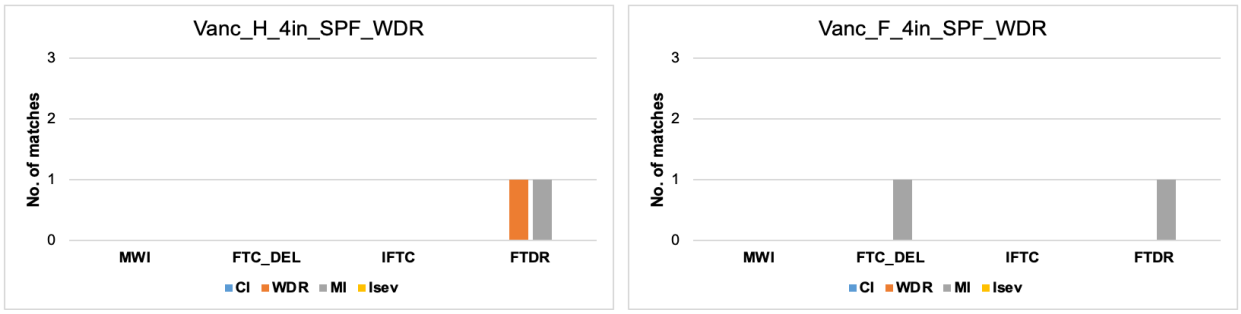

FIG – A6. Number of matching years between climate-based indices (legend) and the response-based indices (x-axis) for a retrofit wall (with 100mm of SPF insulation) facing prevailing WDR orientation under historical and future climate in Vancouver.

Scatter plots

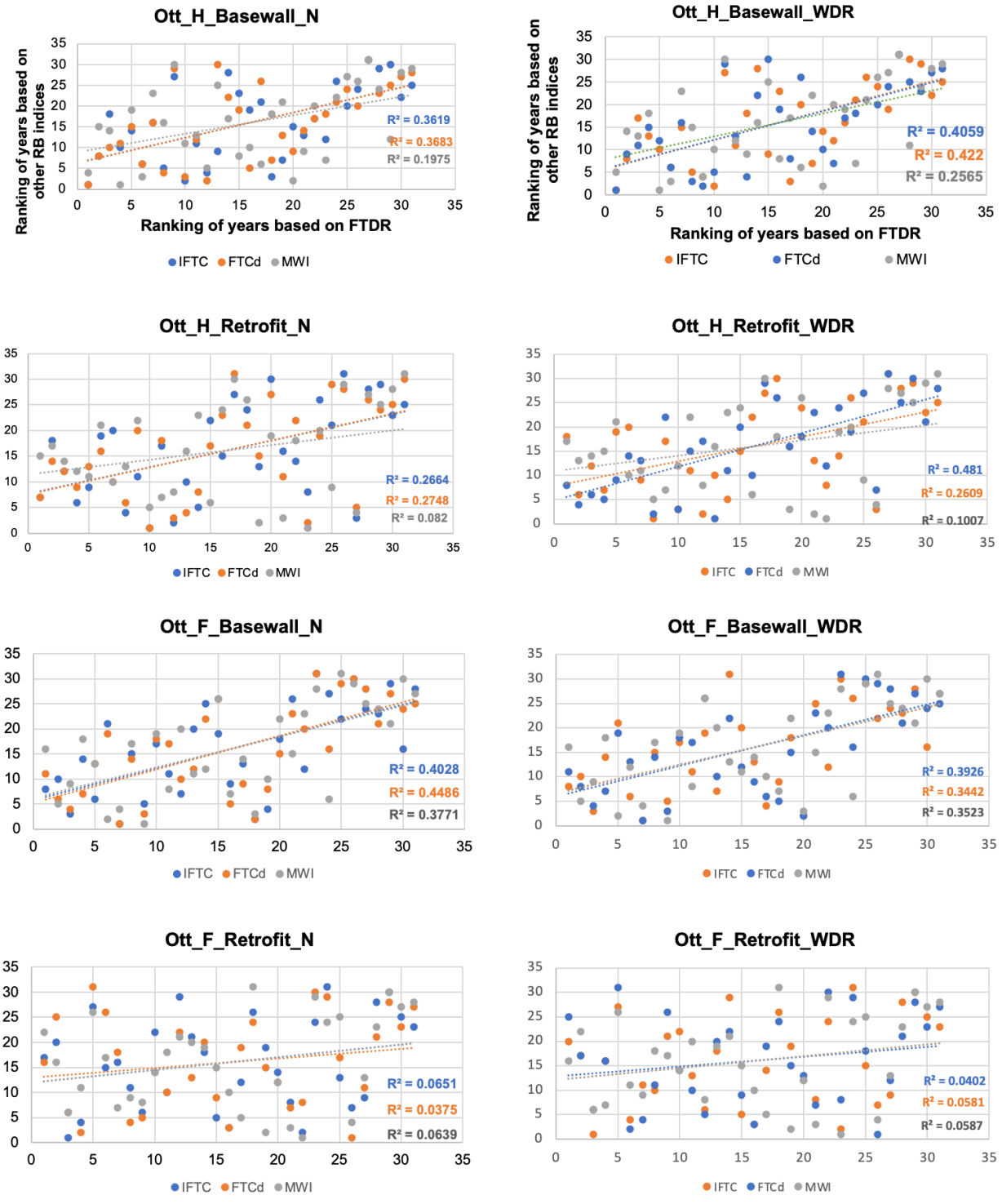

FIG – A7. Correlation between FTDR values based on the actual ranking and other response-based indices values—for a reference wall (Basewall) and a retrofit wall under historical and future periods. Walls are facing North and the prevailing WDR orientation in Ottawa.

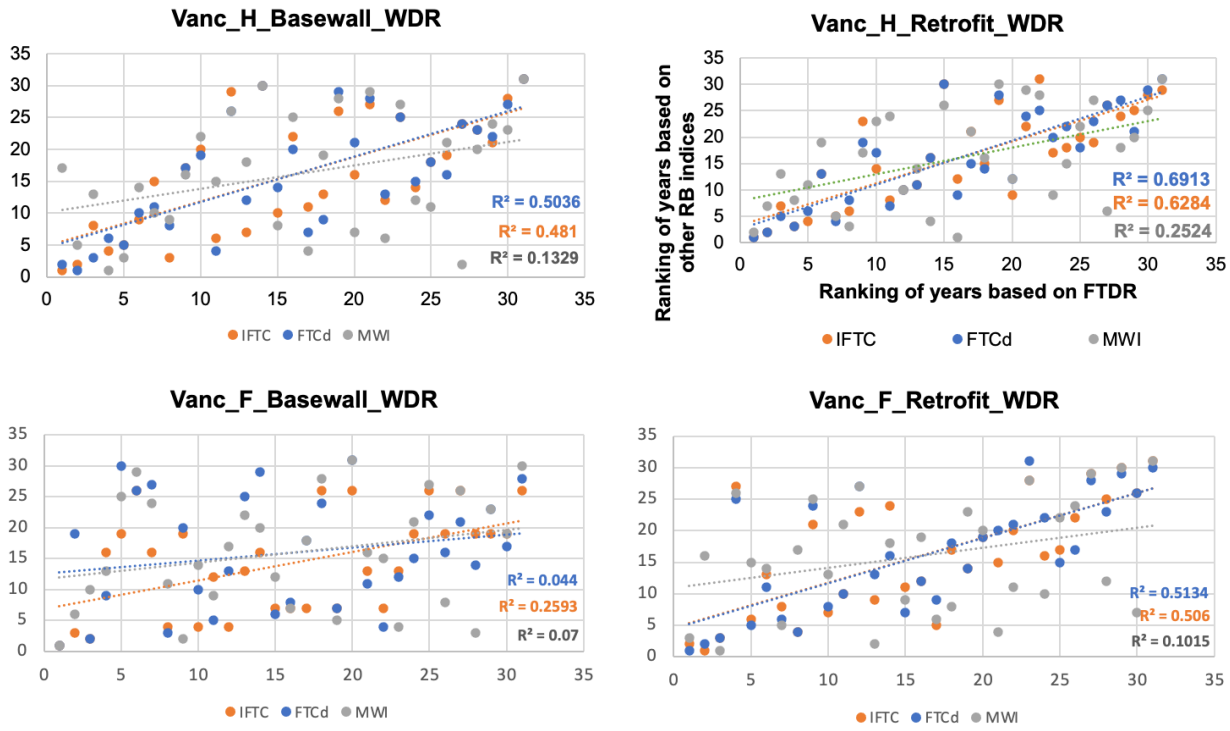

FIG – A8. Correlation between FTDR values based on the actual ranking and other response-based indices values—for a reference wall (Basewall) and a retrofit wall under historical and future periods. Walls are facing the prevailing WDR orientation in Vancouver.

Appendix B – Results of Chapter 5

Impact of different brick modeling configuration

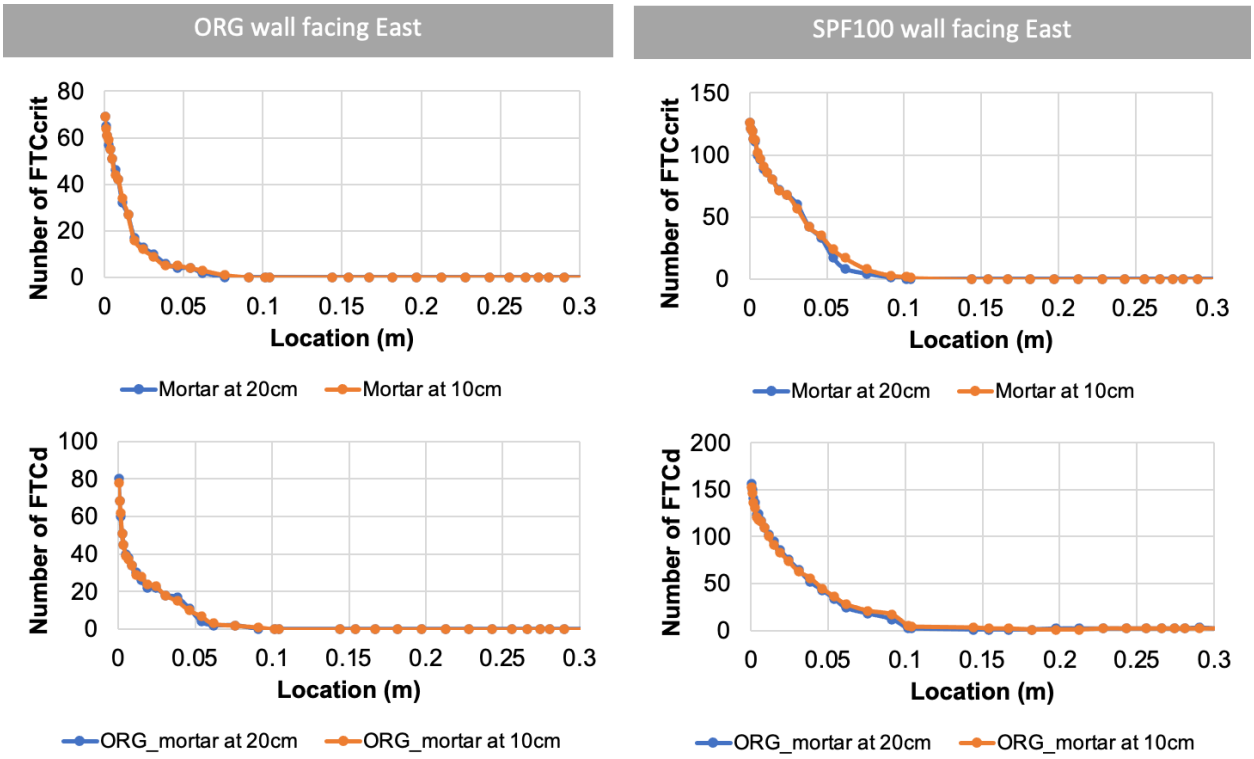

FIG – B1. Comparison between two brick configurations: brick with mortar joint applied at 20cm (blue) and at 10cm (red) from the exterior surface of the brick, using the total number of FTCcrit and FTCd outputted at several points through the brick layer – for an ORG wall and a retrofit wall with 100mm of SPF.

Comparison between 31Y and single years (SY)

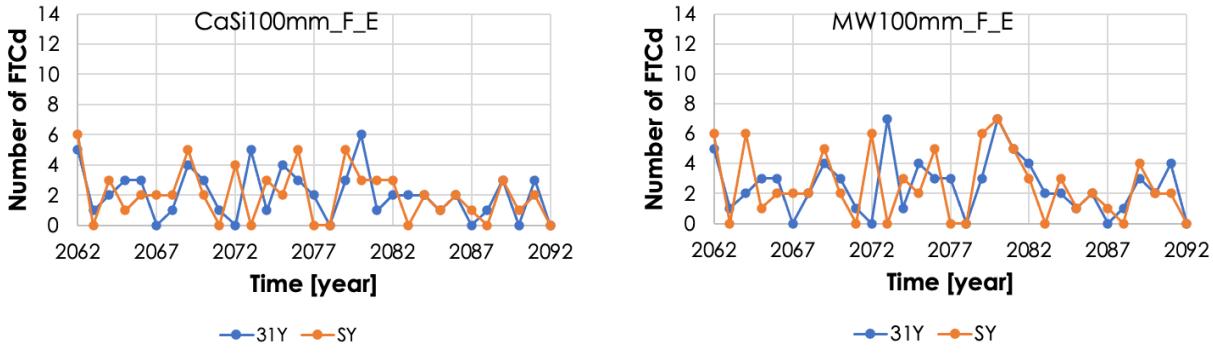

FIG – B1. The total number of freeze-thaw cycles (FTCd) per year following consecutive simulations of 31-year period (31Y) in blue, and when each year is simulated alone as a single year (SY) in red. This comparison was done for retrofit walls with 100mm of CaSi (left) and 100mm of MW (right).

Appendix C – Results of Chapter 6

Impact of different insulation materials

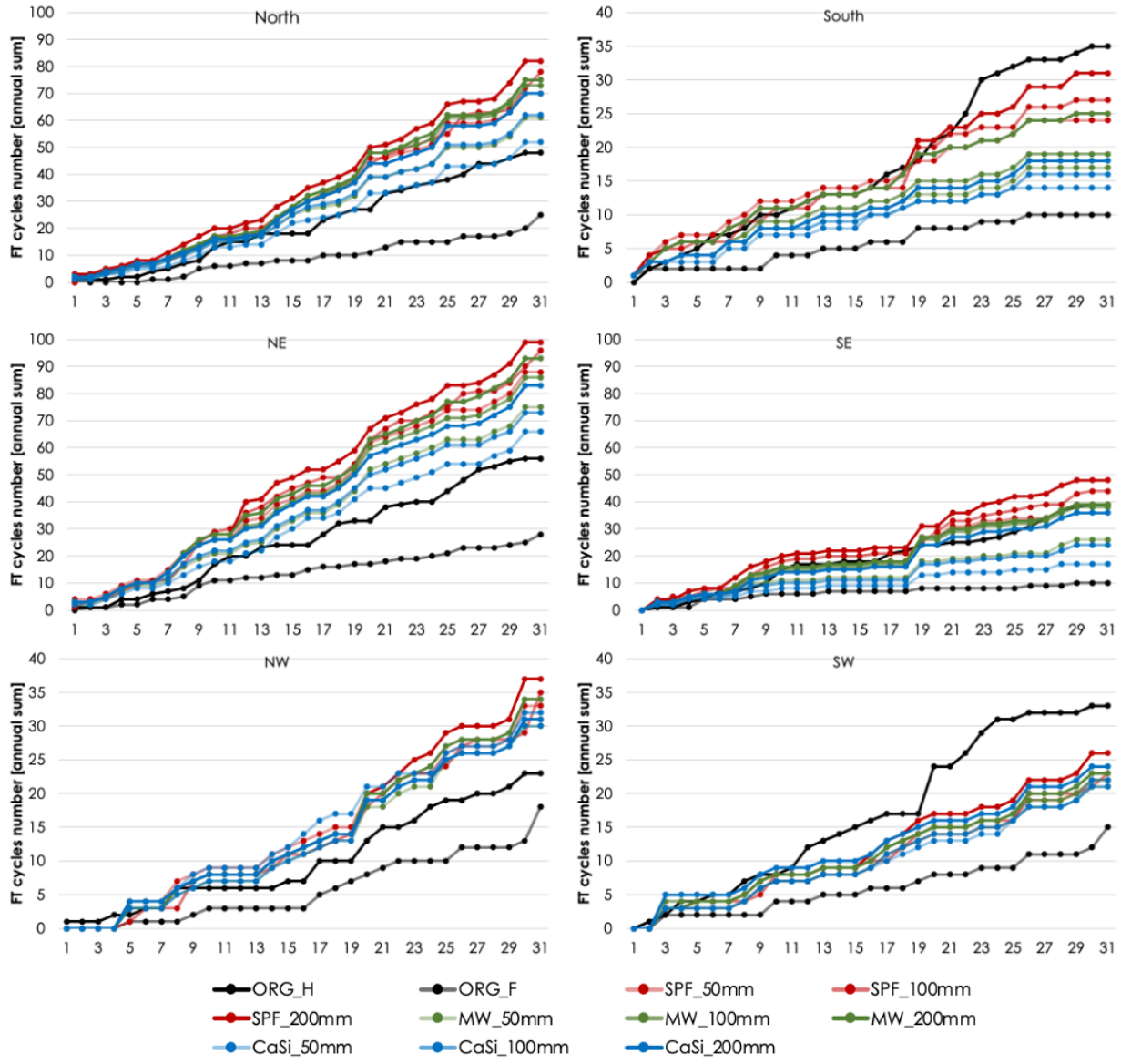

FIG – C1. The Impact of different insulation types and thicknesses on the number of freeze-thaw cycles (FTCs) obtained on brick masonry walls (Brick A) facing different orientations in the future.

Impact of brick masonry thickness

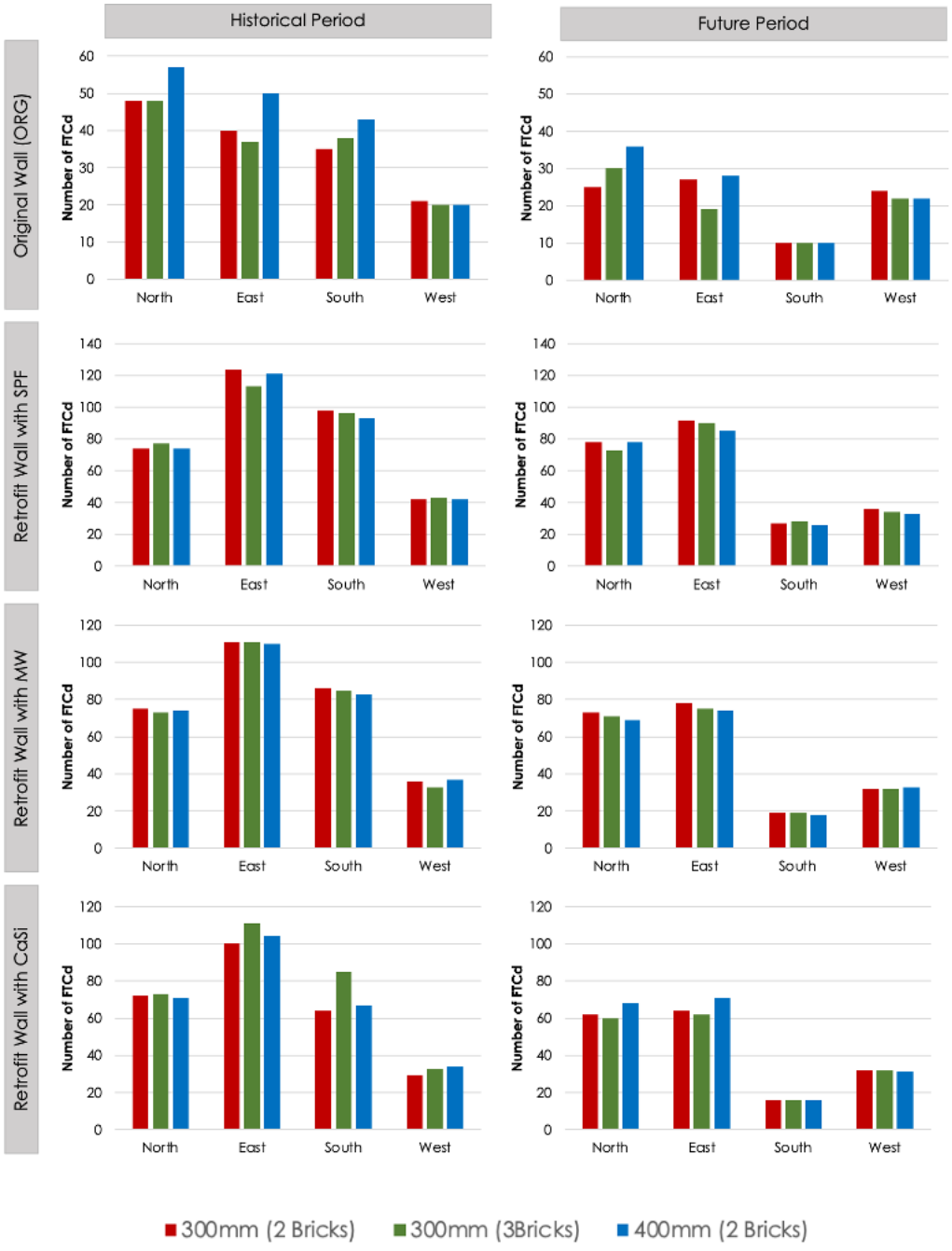

FIG – C2. Total number of FTCs obtained for different brick masonry geometry and thicknesses: i) one full brick (20cm) followed by mortar joints, then half a brick (10cm), ii) three half-bricks (10cm each) with mortar joints in between, and iii) Two full bricks (20cm each) with mortar joints in between.

Impact of different wall orientations and exposure factors

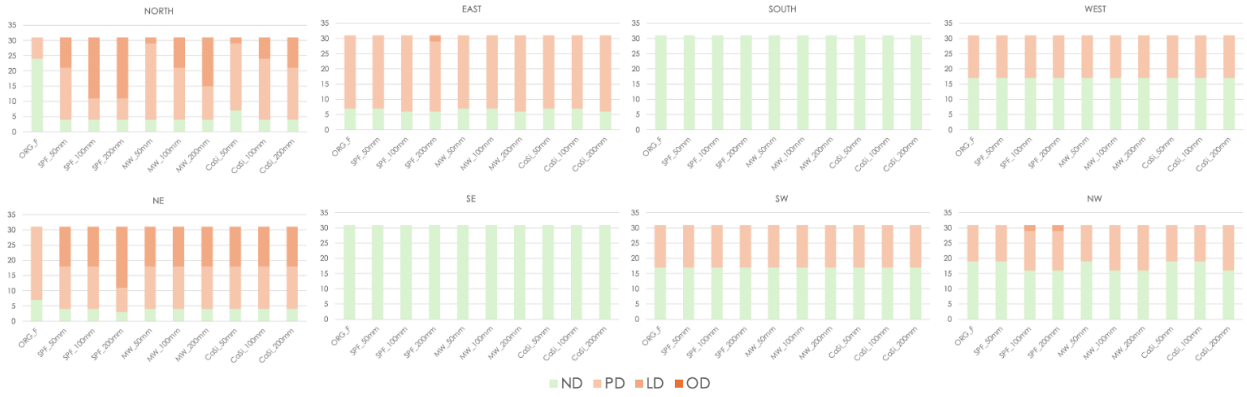

FIG – C3. The predicted mechanical FT damage for pre- and post-retrofit masonry walls – F_E=0.7 and F_D=0.35

FIG – C4. The predicted mechanical FT damage for pre- and post-retrofit masonry walls – F_E=1.0 and F_D=0.35; F_E=0.7 and F_D=0.5.

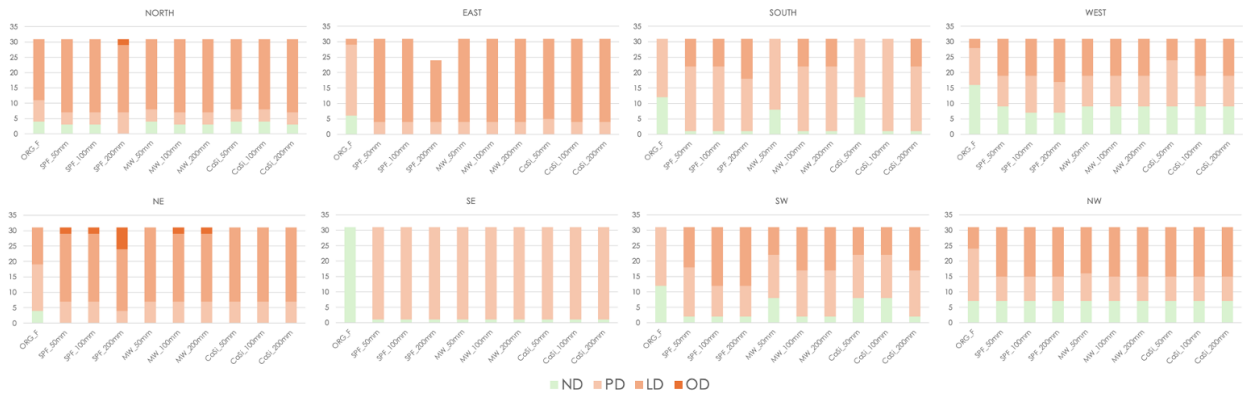

FIG – C5. The predicted mechanical FT damage for pre- and post-retrofit masonry walls – F_E=1.4 and F_D=0.35; F_E=1.0 and F_D=0.5.

FIG – C6. The predicted mechanical FT damage for pre- and post-retrofit masonry walls – F_E=1.4 and F_D=0.5; F_E=0.7 and F_D=1.0.

FIG – C7. The predicted mechanical FT damage for pre- and post-retrofit masonry walls – F_E=1.0 and F_D=1.0.

FIG – C8. The predicted mechanical FT damage for pre- and post-retrofit masonry walls – F_E=1.4 and F_D=1.0.

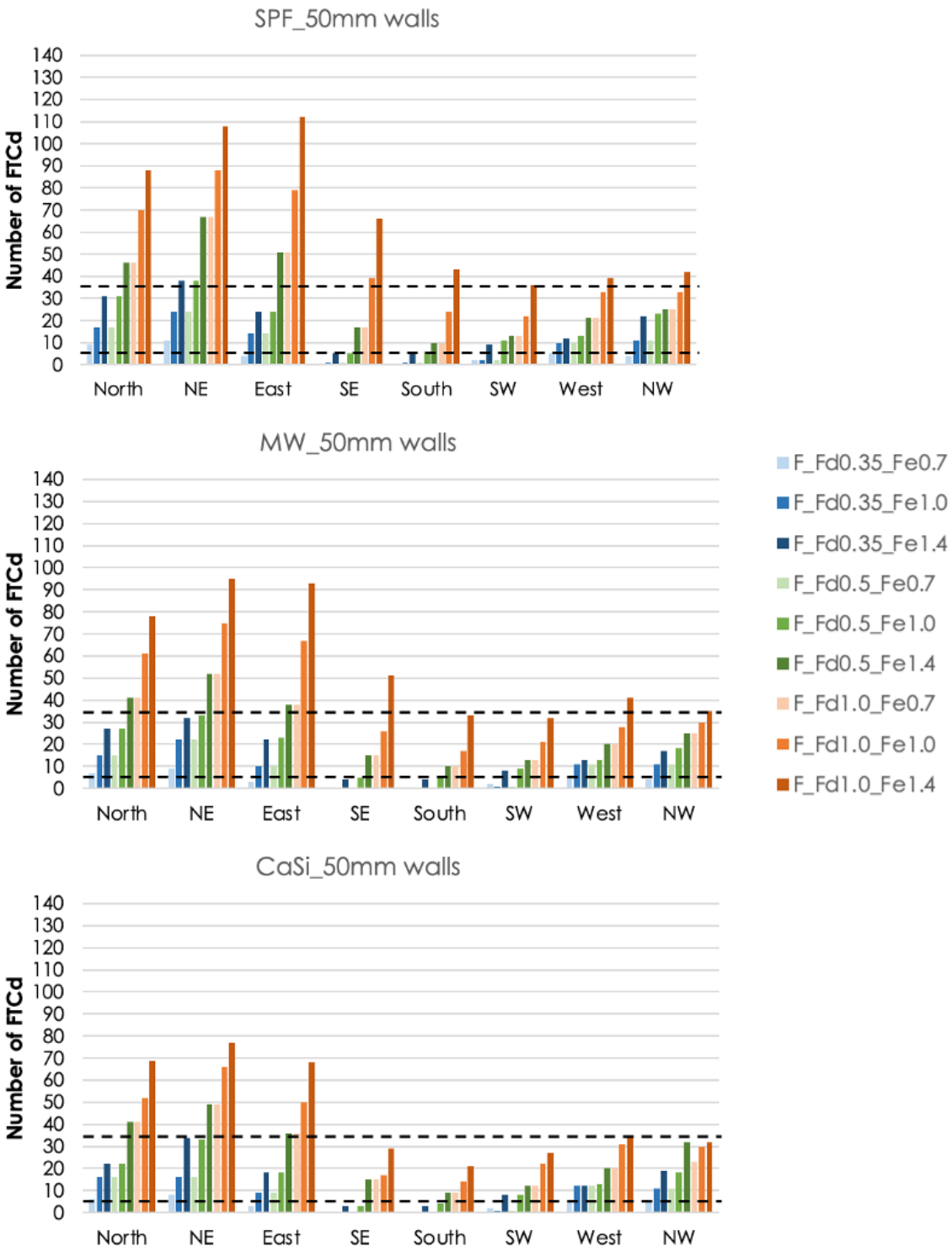

FIG – C9. The total number of FTCs obtained under a future climate, for internally insulated masonry walls (of Brick A) with 50mm of a) SPF; b) MW; and c) CaSi at different orientations and under different exposure and rain deposition factors.

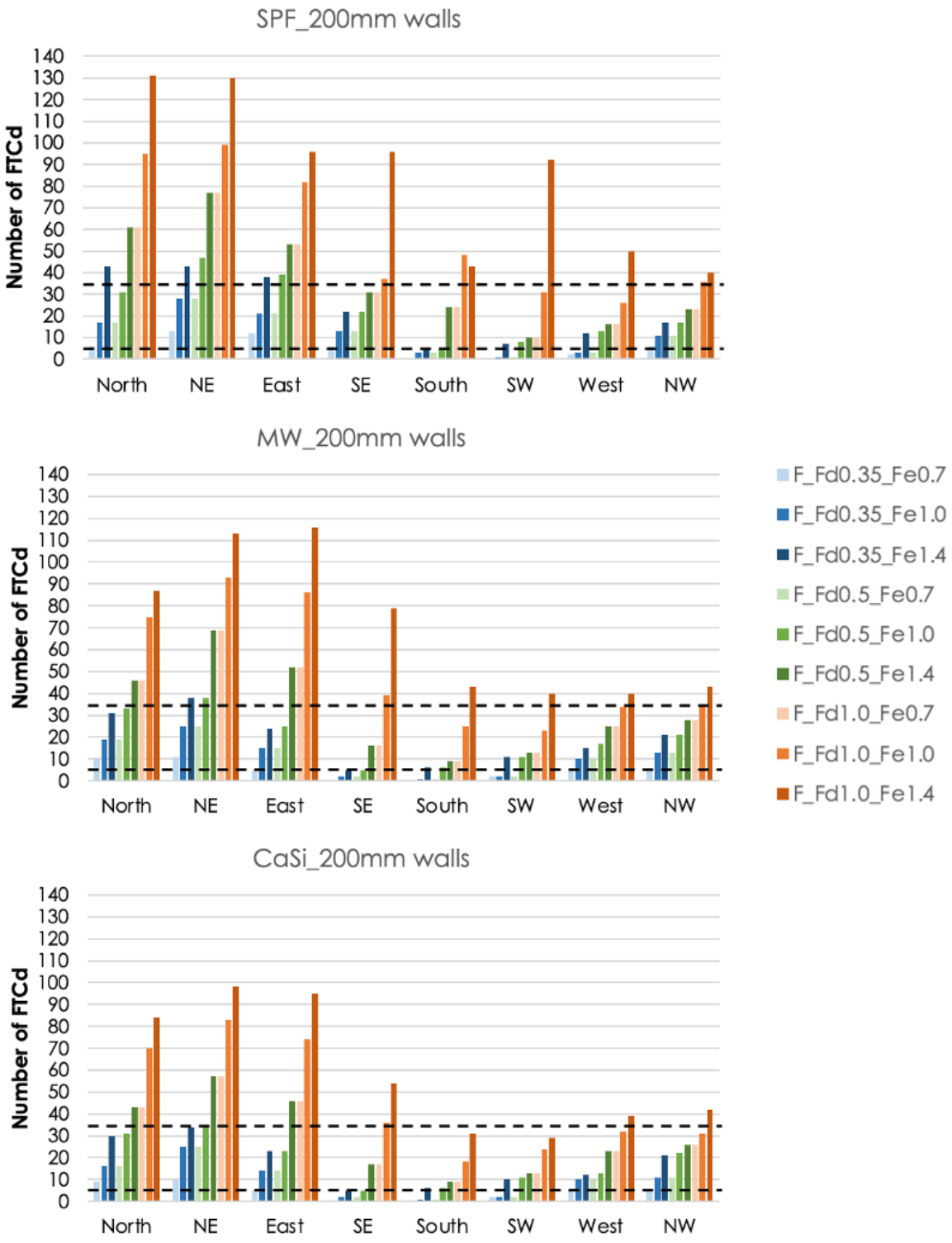

FIG – C10. The total number of FTCs obtained under a future climate, for internally insulated masonry walls (of Brick A) with 50mm of a) SPF; b) MW; and c) CaSi at different orientations and under different exposure and rain deposition factors.

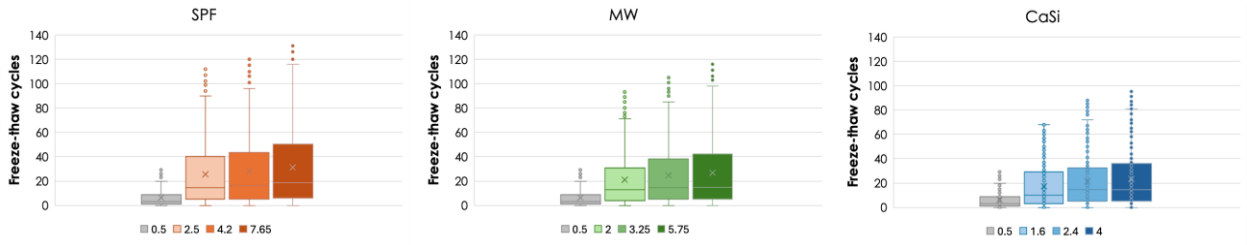

FIG – C11. The cumulative range of FTC obtained under all exposure scenarios using different insulation systems. The legend indicates the R-value of the internally insulated walls.

Appendix D – Published Papers